

Critical evaluation of vertical high resolution methods for determining hydraulic conductivity

Dissertation

der Mathematisch-Naturwissenschaftlichen Fakultät
der Eberhard Karls Universität Tübingen
zur Erlangung des Grades eines
Doktors der Naturwissenschaften
(Dr. rer. nat.)

vorgelegt von
Dipl.-Geol. Thomas Vienken
aus Neuss

Tübingen
2010

Tag der mündlichen Qualifikation:

24. 02. 2011

Dekan:

Prof. Dr. Wolfgang Rosenstiel

1. Berichterstatter:

Prof. Dr. Peter Grathwohl

2. Berichterstatter:

Dr. Peter Dietrich, UFZ Leipzig

Abstract

Environmental site investigations aim at delineating surface near (hydro-) stratigraphic units and their characterization. Knowledge about the spatial distribution of hydraulic conductivity (K) is the prerequisite for understand flow and fluid transport processes. Soil sampling and laboratory analysis of soil samples as well as the use of Direct Push (DP) technology are commonly applied methods for high resolution vertical characterization of sedimentary deposits.

The objective of this thesis is to provide a critical evaluation of these methods regarding their ability to reflect the structure of a complex sedimentary aquifer and their ability to predict K . Extensive field testing was conducted at different test site with focus of the field work at highly heterogeneous aquifer at the Bitterfeld test site.

Evaluation of methods to determine K from grain size analyses are based on the analyses of soil samples and multi level slug tests. Differences on calculated K between the different commonly applied formulas to calculate K were observed. Nevertheless, a high correlation was found between calculated and in situ measured K for most of the applied formulas. However, uncertainties that are associated with the (semi-) empirical nature of this method, heterogeneity of samples, and insufficient porosity estimates were identified to reduce the reliability of calculated K .

DP tools and sensor probes proved to be a reliable and efficient alternative for characterizing complex sedimentary systems in this thesis. Despite resolution differences, all of the applied methods captured the main aquifer structure. Results show that it is possible to describe the aquifer hydraulic structure on less than a meter scale by combining DP slug test data and continuous DP profiling data. However, the appropriate tool has to be chosen and parameter relations are site specific. Correlation between of high resolution DP profiling and grain size data on a centimeter scale was not possible due the small scale soil variability at the Bitterfeld test site.

Zusammenfassung

Die Erfassung und Charakterisierung oberflächennaher (hydro-)stratigraphischer Einheiten ist die Grundlage jeder umweltgeologischen Untergrunderkundung. Die Erfassung der räumlichen Verteilung der hydraulischen Leitfähigkeit (K) ist die Voraussetzung für Strömungs- und Transportmodellierungen. Bodenprobenahme und Laboruntersuchung sowie der Einsatz von Direct Push (DP) Verfahren sind häufig angewandte Methoden zur vertikal hochauflösenden Untergrunderkundung.

Das Ziel dieser Arbeit besteht in der kritischen Evaluierung dieser Methoden hinsichtlich ihrer Eignung zur Erfassung komplexer sedimentärer Ablagerungen und der Ermittlung von K . Der Hauptteil der Geländearbeiten konzentrierte sich auf die stark heterogenen Ablagerungen am Standort Bitterfeld.

Die Auswertung von Bodenproben und Multilevel Slug Tests bildet die Grundlage für die Evaluierung von Methoden zur Berechnung von K aus Siebanalysen. Unterschiede zwischen den errechneten K -Werten ergaben sich dabei in Abhängigkeit der benutzten Verfahren. Nichtsdestotrotz konnte eine gute Korrelation zwischen gemessen und errechneten K -Werten für den Großteil der getesteten Verfahren nachgewiesen werden. Der (semi-) empirische Charakter, Heterogenität der Proben, Messungenauigkeit und ungeeignete Porositätsschätzungen verringern jedoch die Aussagekraft dieser Methoden.

Die Ergebnisse dieser Arbeit zeigen, dass DP Anwendungen und Sensorsonden eine zuverlässige und effiziente Alternative zur Untergrunderkundung komplexer sedimentärer Systeme darstellen. Trotz unterschiedlicher räumlicher Auflösungsvermögen konnten alle getesteten Methoden die sedimentäre Schichtenfolge in Bitterfeld erfassen. Diese Arbeit zeigt, dass die Kombination von DP Slug Test Daten und hochauflösenden DP Profilen eine hydraulische Charakterisierung von Grundwasserleitern mit einer Auflösung von unter einem Meter ermöglicht. Allerdings müssen die geeigneten DP Methoden gewählt werden und die ermittelten Parameter-Beziehungen sind nur lokal gültig. Aufgrund der starken Heterogenität der Ablagerungen in Bitterfeld ist eine Korrelation zwischen Siebdaten und hochauflösenden DP Daten im Zentimeterbereich nicht möglich.

Index

Index	1
List of figures.....	4
List of tables.....	6
List of symbols.....	8
List of Greek symbols.....	11
List of abbreviations	12
1 Introduction.....	13
1.1 Motivation and objective	13
1.2 Field sites	15
1.2.1 Bitterfeld	15
1.2.2 Larned Research Site	17
1.3 Outline	18
2 Evaluation of methods for determining hydraulic conductivity from grain size distribution.....	20
2.1 Introduction.....	20
2.2 Field work.....	21
2.2.1 Sampling	22
2.2.2 Grain size analysis	23
2.2.2.1 Empirical formulas to calculate K from grain size distribution.....	25
2.2.2.2 Semi empirical formulas to calculate K from grain size distribution	25
2.2.3 Limitations and application range of the applied formulas	26
2.2.4 Effects of porosity on calculated K	28
2.3 Results of the grain size analyses	29
2.4 Comparison of calculated K from grain size analyses with Direct Push slug test results	32
2.5 Factors influencing K_{DPST} and $K_{Grains\ size}$ correlation.....	35
2.6 Effects of measuring inaccuracy on calculated K	36
2.7 Conclusion	39

3	Comparison of in situ water-content profiles obtained using frequency-domain and neutron-probe technology	40
3.1	Introduction.....	40
3.2	Applied methods	42
3.2.1	CPT deployed Water Content Profiler (WCP)	42
3.2.2	Neutron probe	44
3.3	Application of methods at the Larned Research Test Site (LRS).....	45
3.3.1	Larned test site field work	45
3.3.2	Results at Larned test site	46
3.4	Application of methods at the Bitterfeld test site	50
3.4.1	Bitterfeld test site field work	50
3.4.2	Results at Bitterfeld test site	51
3.5	Conclusion	53
4	Evaluation of approaches to estimate porosity of clastic sediments.....	55
4.1	Introduction.....	55
4.2	Classification of porosity	56
4.3	Approaches to estimate porosity.....	58
4.3.1	Theoretical models predicting total porosity in sedimentary mixtures.....	58
4.3.2	Empirical approaches to estimate porosity of sediments.....	59
4.3.3	Evaluation of porosity estimates with DPST data	61
4.4	Conclusion	64
5	The use of CPT and other Direct Push methods for (hydro-)stratigraphic aquifer characterization.....	66
5.1	Introduction.....	66
5.2	Direct Push technology	67
5.2.1	Direct Push Slug Test (DPST)	69
5.2.2	Sonic sampling and grains size analysis	70
5.2.3	Cone penetration testing with pore pressure and electrical conductivity measurement (CPTU-EC)	71
5.2.4	Direct Push Injection Logger (DPIL)	73
5.2.5	Hydraulic Profiling Tool (HPT)	75
5.2.6	Electrical conductivity logging.....	76

5.3	Results.....	78
5.3.1	Field data.....	78
5.3.2	Quantitative data evaluation	83
5.3.3	Data evaluation with DPST results	85
5.4	Conclusion	87
6	Summary and conclusion.....	89
	References.....	93
	Acknowledgment.....	102
	Appendix.....	103
	Appendix A.....	103
	Appendix B.....	107
	Appendix C.....	108
	Curriculum vitae	109

List of figures

Figure 1-1: Synthetic data set showing decreasing parameter scattering with increasing intrinsic volume, modified after Bear (1972).....	14
Figure 1-2: Location of the Bitterfeld test site with position of the sampling clusters and position of the DP profiles at each sampling cluster including neutron probe profiles. Repeat measurements are marked with an *	17
Figure 1-3: Location of the Larned Research Site and position and measuring date of neutron probe (NP) and Water Content Profiler (WCP) logs.	18
Figure 2-1: Selected grain size diameters and slug test intervals at sampling cluster 1 (SC1), sampling cluster 2 (SC2), and sampling cluster 4 (SC4); grain size diameters are given in mm.	22
Figure 2-2: Resulting deviation on calculated K after Kozeny-Köhler (1965) and Terzaghi (1925a, b) caused by uncertainties of porosity estimates. The Graph shows the magnitude of difference between calculated K with fixed porosity value (K_{ref}) of 0.55 in Fig. 2-2 a and 0.30 Fig. 2-2 b and calculated K for porosity values ranging between 0.25 and 0.65 (K_{dev}).....	29
Figure 2-3: Matrix plot of natural logarithm of K ($\ln(K)$) calculated from grain size analyses using different formulas. Histogram: x-axis: classes, y-Axis: frequency; scatter plots: x- and y-axis: $\ln(K)$	30
Figure 2-4: Correlation of measured K_{DPST} and calculated $K_{Grain\ size}$ of untreated data. Histogram plot: x-axis: classes, y-axis: frequency; scatter plots: x- and y-axis: $\ln(K)$	33
Figure 2-5: Matrix plots of K_{DPST} and calculated $K_{Grain\ size}$ of treated data. Histogram plot: x-axis: classes, y-axis: frequency; scatter plots: x- and y-axis: $\ln(K)$	34
Figure 2-6: Box plot of $\ln(K)$ values calculated with different formulas for the slug test intervals.....	36
Figure 2-7: Box plot showing the differences of determined d_{10} values within each ring analysis.....	38
Figure 3-1: Schematic view of the neutron probe field setup.	45
Figure 3-2: Overview of profiling results at the Larned test site. R_f is the friction ratio determined by the use of the cone penetrometer and θ_v is the volumetric water content in percent.....	47
Figure 3-3: Overview of profiling results at the Larned test site with normalized WCP results. R_f is the friction ratio determined by the use of the cone penetrometer.....	49
Figure 3-4: Comparison of NP and averaged WCP readings using Eq. 3-5 after Cameron (1970) of the 2009 campaign from LRS in a common scatter plot.....	50
Figure 3-5: Overview of profiling results at the Larned test site. R_f is the friction ratio determined by the use of the cone penetrometer and ϕ_v is the volumetric water content in percent.....	52

Figure 3-6: Comparison of NP and averaged WCP readings using Eq. 3-5 after Cameron (1970) at the Bitterfeld test site in a common scatter plot.	53
Figure 4-1: Total porosity, effective porosity, and volume of retained water in dependence of sediment type, modified after Davis & de Wiest (1966).	57
Figure 4-2: Intrinsic permeability (k) versus total porosity (ϕ) for different rocks and sediment types after Chouker (1970).	60
Figure 4-3: Matrix plot of calculated $K_{Terzaghi}$ (a) and $K_{Kozeny-Köhler}$ (b) based on porosity estimates after Szymczak et al. (2009) (Scz), Vukovic & Soro (1992) (V&S), Langguth (1980) (Langg), Chouker (1970) (Chou), Hölting & Coldewey (2005) (Hö), and a fixed porosity values of 0.4 with DPST data. Histogram y-axis labeling is frequency, scatter plot x- and y-axis labeling is $\ln(K)$	63
Figure 5-1: Schematic view of DP slug test field setup and components (Butler et al. 2000).	70
Figure 5-2: Schematic view of CPTU-EC probe and components.	72
Figure 5-3: DPIL probe design with different water injection elements (a) and field setup (b).	75
Figure 5-4: Schematic view of the HPT field setup (a) and probe design (b).	76
Figure 5-5: Schematic view of EC probe.	77
Figure 5-6: Repeat DP measurements. Repetitive measurements were taken at nearby locations at cluster 1 (CPTU, CPTU-EC, and HPT) and cluster 2 (DPIL). DPIL data: grey line indicates test intervals of 10 cm spacing, the black line test intervals of 30 cm spacing.	78
Figure: 5-7 (A-D): Results from DP (hydro-)stratigraphic profiling in comparison with results from DPST and grain size analyses at the Bitterfeld test site.	82
Figure 5-8: Scatter plot of DP profiling results at the Bitterfeld test site; histogram y-axis labeling is frequency. Units: d_e in mm, K_{Hazen} in m/s, R_f in %, EC in mS/cm, I_C (-), K_{HPT} (ml/min/kPa), K_{DPIL} (l/h/bar). All K values given as $\ln(K)$	84
Figure 5-9: Scatter plot of repeat CPT R_f (a) and CPTU-EC EC (b) measurements from two logs at sampling cluster 1 with approximately 1.5 m spacing.	84
Figure 5-10: Matrix plot of Bitterfeld DP and DPST data. Solid line is the line of simple regression, dashed line is 95% confidence interval; x-axis labeling of the scatter plot is $\ln(K_{DPST})$, y-axis are DP data. Units: K_{DPST} in m/s, K_{Hazen} in m/s, R_f in %, CPTU-EC EC in mS/cm, I_C (-), K_{HPT} (ml/min/kPa), K_{DPIL} (l/h/bar). All K values given as $\ln(K)$	86
Figure 6-1: Dependency of vertical profiling results in a heterogeneous aquifer on intrinsic volume of influence and spacing between point measurements. Illustration of the braided river deposit has been taken from Tronicke et al. (2002) and modified.	92

List of tables

Table 1-1: Quaternary stratigraphic sequence at the Bitterfeld test site, modified after Weiß et al. (2001).....	16
Table 2-1: Selected literature references for the evaluation of K determined from grain size distribution.	21
Table 2-2: Summary of the applied formulas to calculate K from grain size distribution; key parameters, and citations.	24
Table 2-3: Correlation matrix for calculated $\ln(K)$ values using different formulas. Triplets are listed top down in form of r , y , and b , where r is the correlation coefficient; $y*x$ is the slope and b is the intercept of the linear regression	31
Table 2-4: Overview of basic statistics for calculated K values derived from different formulas.	32
Table 2-5: Basic statistics for calculated $K_{Grain\ size}$ and measured K_{DPST} based on different formulas; $y*x$ is the slope and b is the intercept of the linear regression.	35
Table 2-6: Mean, upper tolerance limit, and lower tolerance limit for the fraction of each ring analysis.	37
Table 2-7: Maximum values, minimum values, and resulting deviation for determined d_{10} values and calculated K_{Hazen} values within each ring analysis.	38
Table 3-1: Major advantages and limitations of gravimetric, NP, and WCP measurements for determining volumetric water content.	41
Table 4-1: List of sediment types with respective grain size diameter after DIN EN ISO 14688-1 and corresponding empirical porosity values after Szymczak et al. (2009), Chouker (1970), and Hölting & Coldewey (2005).	61
Table 4-2: Basic statistics of $K_{Terzaghi}$ and $K_{Kozeny-Köhler}$ based on porosity estimates after Szymczak et al. (2009) (Scz), Vukovic & Soro (1992) (V&S), Langguth (1980) (Langg), Chouker (1970) (Chou), Hölting & Coldewey (2005) (Hö), and a fixed porosity values of 0.4 with DPST data. Linear regression is given as slope ($y*x$) in the upper value and intercept as lower value. Correlation coefficients are determined based on $\ln(K)$ values.	64
Table 5-1: Overview of DP (hydro-)stratigraphic profiling tools. Duration for continuous probing is given for a 10 m log, not including probe preparation (e.g. piezocone saturation). Durations for discontinuous and depth oriented tests are given for single tests at one depth interval, not including probe preparation or advancement of the probe to the individual depth. Further references are given in the text. State: ++ is fully developed, + is functioning and o is experimental.	68
Table 5-2: Basic statistics and correlation of DP profiling data and DPST results at the Bitterfeld test site; where $y*x$ is the slope and “b” is the intercept of the simple regression line. Units: K_{DPST} in m/s, K_{Hazen} in m/s, R_f in %, CPTU-EC EC in mS/cm, I_C (-), K_{HPT} (ml/min/kPa), K_{DPIL} (l/h/bar). Correlation coefficients were determined using $\ln(K)$ values.	87

Appendix A: Grain size diameter determined based from grain size analyses of soil samples. Depth is given in m below ground surface, all grain size diameters are given in mm. For chapter 2, grain size distribution from cores S1, S2, and S4 were used in data analyses; for chapter 5 grain size distributions from all samples were included 103

Appendix B: Grain size diameter for the slug test interval with d in mm. Grain size distribution of samples within individual slug test intervals were averaged according to their abundance and grain size diameters were derived. SC is Sampling Cluster, and CL is core loss observed on samples within the slug test interval. Where no grain size diameter is given, no material was retained. 107

Appendix C: Neutron probe soil water content measurements in dependency of the applied soil type based calibration at sampling cluster 1 and sampling cluster 2 in Bitterfeld. 108

List of symbols

Symbol	Denotation
b	intercept of linear regression
a	area ratio of the cone
C	capacitance
$C_B = f(U) = \log \frac{500}{U}$	coefficient after Beyer
C_H	coefficient after Hazen
C_i	dimensionless factor
cl	clay content
C_T	coefficient after Terzaghi
d	effective diameter of the grains
$\frac{1}{d_i} = \frac{1}{2} \times \left(\frac{1}{d_u} + \frac{1}{d_l} \right)$	harmonic mean of the i th fraction
d_i	diameter of grains in the i th percentile
d_u	upper grain size limit of a grain size fraction
d_l	lower grain size limit of a grain size fraction
d_m	largest diameter of the last, finest fraction of the material ($d < 0.002$ mm)
d_{50}	median grain size diameter
$de = \frac{0.1}{\frac{3}{2} \frac{\Delta g_m}{d_m} + \sum_{i=2}^{i=n} \frac{\Delta g_i}{d_i}}$	effective grain size diameter
$d_w = \frac{6}{S}$	effective grain size after Beyer (1964)
$f_l(s)$	shape factor
$f_2(\phi)$	porosity factor
f_s	unit sleeve friction resistance
$f(U)$	porosity function after Beyer (1964)
$F_r = f_s / (q_t - \sigma_{vo})$	normalized friction ratio
g	gravitational constant
I_c	soil behavior type index
j	standard imaginary unit
K	hydraulic conductivity

List of symbols

Symbol	Denotation
k	intrinsic permeability
K_i	hydraulic conductivity determined with method i
K_{ref}	reference K value calculated for a porosity of 0.55 and 0.3 respectively as shown in Figure 2-2; further information is given in the text
K_{dev}	K values calculated for porosities deviating from 0.55 an 0.3 respectively as shown in Figure 2-2; further information is given in the text
L	length
m	hydraulic radius
n	population size
P	percentage of fine grained material <0.06mm
p_{HPT}	corrected HPT injection pressure
p_{inj}	injection pressure
p_{trans}	pressure measured at pressure transducer
Q	flow rate
q_c	measured cone resistance
$q_t = q_c + (1 - a)u_2$	corrected cone resistance
$Q_{t1} = (q_t - \sigma_{vo}) / \sigma'_{vo}$	normalized cone resistance
R	coefficient of roughness
r	correlation coefficient
R_{total}	total flow resistance
R_{tube}	tube resistance
r_{tube}	tube radius
$R_f = \frac{f_s}{q_t} \times 100$	friction ratio
S	specific surface
T	temperature
$U = \frac{d_{60}}{d_{10}}$	coefficient of uniformity
u_0	in situ pore pressure
u_2	pore pressure measured behind the cone
V	bulk volume

List of symbols

Symbol	Denotation
V_p	volume of pore spaces
\bar{x}	arithmetic mean
y^*x	slope of a linear regression
yQ	slope of the DPIL regression analysis

List of Greek symbols

Symbol	Denotation
Δg_i	weight of a fraction in parts of total weight
Δg_m	weight of the last, finest fraction of material in parts of total weight
$\varepsilon = \varepsilon' - j\varepsilon''$	complex relative permittivity
ε_0	permittivity of free space
ε'	real part of the complex relative permittivity (dielectric constant in a static electrical field)
ε''	imaginary part of the complex relative permittivity
η	dynamic viscosity
η_T	dynamic viscosity at ground water temperature
η_{10}	dynamic viscosity at 10° Celsius
$\Theta = \frac{\phi}{1-\phi}$	void ratio
θ_v	volumetric water content
κ	geometry factor
ν	kinematic viscosity
σ^2	variance
σ_{vo}	total overburden stress
σ'_{vo}	effective vertical stress
$\tau = \frac{\nu_{10}}{\nu_T}$	ratio of kinematic viscosity at 10° Celsius and ground water temperature
ϕ	total porosity

List of abbreviations

Symbol	Denotation
BTF	Bitterfeld
CPT	Cone Penetration Testing
CPTU	Cone Penetration Testing with Pore Pressure Measurement
CPTU-EC	Cone Penetration Testing with Pore Pressure and Electrical Conductivity Measurement
DP	Direct Push
DPIL	Direct Push Injection Logger
DPST	Direct Push Slug Test
FD	Frequency Domain
EC	Electrical Conductivity
HPT	Hydraulic Profiling Tool
ln	natural logarithm
LRS	Larned Research Site
MADE	Macro Dispersion Experimental
Max	Maximum Value
Min	Minimum Value
NP	Neutron Probe
REV	Representative Elementary Volume
TDR	Time Domain Reflectometry
USBR	United States Bureau of Reclamation
UFZ	Helmholtz Centre for Environmental Research - UFZ
WCP	Water Content Profiler

1 Introduction

1.1 Motivation and objective

Environmental site investigations require high resolution information about lithology and hydraulic properties of the subsurface for understanding and modeling of flow and fluid transport processes. This is especially true for complex structured sedimentary deposits where spatial variability of hydrogeological parameters governs flow processes in saturated systems (Sudicky 1986, Gomezhernandez & Gorelick 1989, Eggleston & Rojstaczer 1998, Sudicky & Huyakorn 1991, Zheng & Gorelick 2003).

Many tools for the laboratory and field investigation of K exist. Butler (2005) gives a comprehensive overview of approaches including pumping tests, slug tests, laboratory analysis of core samples, geophysical logging, borehole flowmeter tests, direct push methods, and hydraulic tomography. These approaches vary significantly in the intrinsic area of influence. This is the volume over which a method measures and integrates the integral parameter value which is attributed to one measurement point, ranging from aquifer to particles size scale.

The minimum volume of a soil sample required from which a given soil parameter measurement becomes independent of the size of the sample is called representative elementary volume, REV (VandenBygaart & Protz 1998). Bear (1972) explains the REV in detail and provides a graphical explanation. Following this graphical explanation, Figure 1-1 shows a synthetic data set at which parameter scattering but also spatial resolution decreases with increasing intrinsic volume. Grain size analysis, Direct Push methods, slug test, and pumping test are plotted regarding their intrinsic volume; this illustrates the complex problem of comparing K values derived from methods using different intrinsic volumes in inhomogeneous media. Pumping tests e.g. yield an integral K value over a certain part of the aquifer while grain size analysis yield K values representative only of the sample or its closest vicinity.

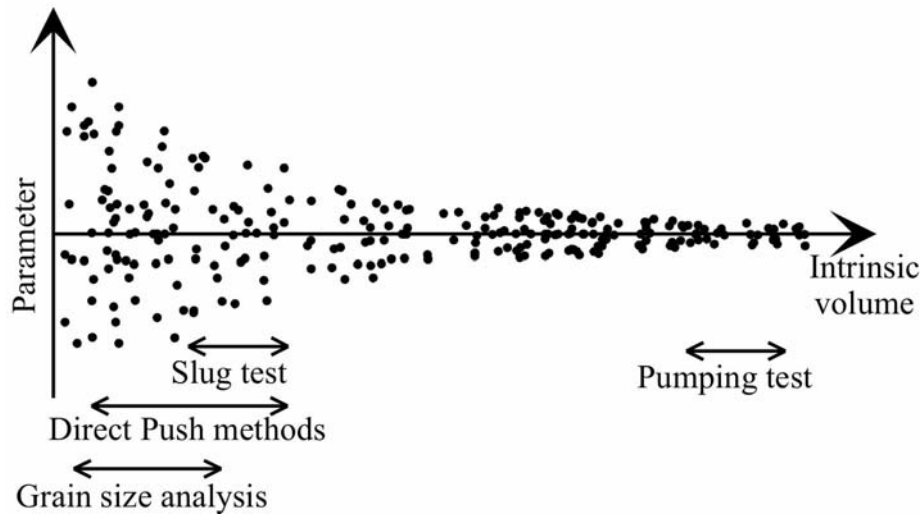


Figure 1-1: Synthetic data set showing decreasing parameter scattering with increasing intrinsic volume, modified after Bear (1972).

Often, traditional site investigation techniques (see EPA 1997a, Sevee 2005) such as pumping tests, slug tests or sampling and laboratory tests of hydraulic parameters cannot cope with the task of reliable high resolution aquifer characterization. A critical evaluation of the limitation or representativeness of the data within the geological framework or aim of investigation is necessary as the limiting momentum in flow and transport predictions is oftentimes the quality and quantity of underlying field data (Anderson 1997, Woodbury et al. 1995, Dekker & Abriola 2000). Ongoing research in the field of stochastic and deterministic modeling has lead to the development of increasingly complex flow and transport models for the saturated and unsaturated zone. However, adequate field methods have to be developed and reliably applied to describe soil variability in a way to keep pace with modeling (van Genuchten 1991).

The objective of this thesis is to provide a critical evaluation of methods for high resolution vertical K characterization in unconsolidated sedimentary aquifers regarding their ability to reflect the structure of a complex sedimentary aquifer and their ability to predict K . Therefore, extensive field testing was conducted at different test site. Novelties included in this study are the use of in situ measured high resolution K values for evaluation of the applied formulas to calculate K based on grain size analyses and the combined application of the variety of tools at one field site that is characterized by heterogeneous sedimentary deposits.

The main field work was performed at the Bitterfeld test site, Saxony-Anhalt, Germany. Additional field work presented in this thesis was performed at Larned Research Site, central Kansas, USA. Further field activities included work at Horstwalde, Brandenburg, Germany and at the macrodispersion experiment site (MADE), Mississippi, USA. The extensive data collected at Bitterfeld and Larned are presented within this thesis, an overview of the two test sites is given in the following section.

This introduction is to present the motivation and overall objective of this thesis. For each chapter, a detailed introduction is provided.

1.2 Field sites

1.2.1 Bitterfeld

The field work was conducted at the Helmholtz Centre for Environmental Research – UFZ test site in Bitterfeld, Germany. This site was chosen because of its strong heterogeneity and broad sedimentological spectrum of glacial and glazifluviatile deposits. A description of the quaternary stratigraphic sequence at the Bitterfeld test site after Weiß et al. (2001) is given in Table 1-1. The stratigraphic sequence presented by Weiß et al. (2001) is in good agreement with the results of soil sampling that was conducted at the test site in the course of this thesis.

The upper part of the quaternary unconsolidated sedimentary aquifer that was tested consists of a number of lithological horizons. The terrace gravel layers are composed of vast number of individual layers and lenses with limited vertical and lateral extent and high variability in thickness and composition (see Table 1-1). The test site is covered with backfill material of varying thickness. Changes in soil specific properties were therefore expected to range over several orders of magnitudes and to change over short horizontal and vertical distances. During the field work, ground water table fluctuated between 2.68 and 3.27 m below ground surface. Only profiling results below the backfill material at depths greater than 3 m below ground surface were used in the data analyses.

Table 1-1: Quaternary stratigraphic sequence at the Bitterfeld test site, modified after Weiß et al. (2001).

Stratigraphic unit	thickness	composition	characteristics	hydraulic behavior
oberer Terrassenschotter (upper terrace gravel)	3-4 m	diagonal- and cross-bedded gravelly fine sands and medium sands	partially replaced by backfill material of varying thickness	unsaturated zone
oberer Schluffhorizont (upper silt horizon)	0.5-0.7 m	grey-green to ocher sandy (fine to medium sand) silt	irregular fine sand lenses and layers	aquitard
mittlerer Terrassenschotter (middle terrace gravel)	2-3 m	diagonal- and cross-bedded partially gravelly grey fine sands and middle sands	small scale interbedding with variable gravel content	aquifer
unterer Schluffhorizont (lower silt horizon)	0.2-2 m	green-grey to dark green clayey-sandy silt	fine sand at top, with increasing clay content to the basis	aquitard
unterer Terrassenschotter (lower terrace gravel)	12-14 m	cyclic interbedding of gravelly sand and sandy gravel on decimeter to meter scale	Upper part: irregularly embedded layers of medium to coarse gravel	aquifer

For further information on the test site see Weiß et al. 2001, further information on the local geology of the Bitterfeld area is given by Eissmann (1994) and Knoth (1995).

DP profiling was conducted at four clusters along a 58 m long profile (Fig. 1-1) in the upper 12 m of the aquifer and included cone penetration testing with pore pressure and electrical conductivity measurements (CPTU-EC) and measurements of the dielectric constant, Neutron probe profiles, DP Injection Logger (DPIL) profiles, Hydraulic Profiling Tool (HPT) profiles as well as Direct Push slug testing (DPST) and soil sampling with extensive grain size analyses. Location of the sampling clusters and positions of the profiles at each cluster is shown in Figure 1-2.

analyses. Location of the sampling clusters and positions of the profiles at each cluster is shown in Figure 1-2.

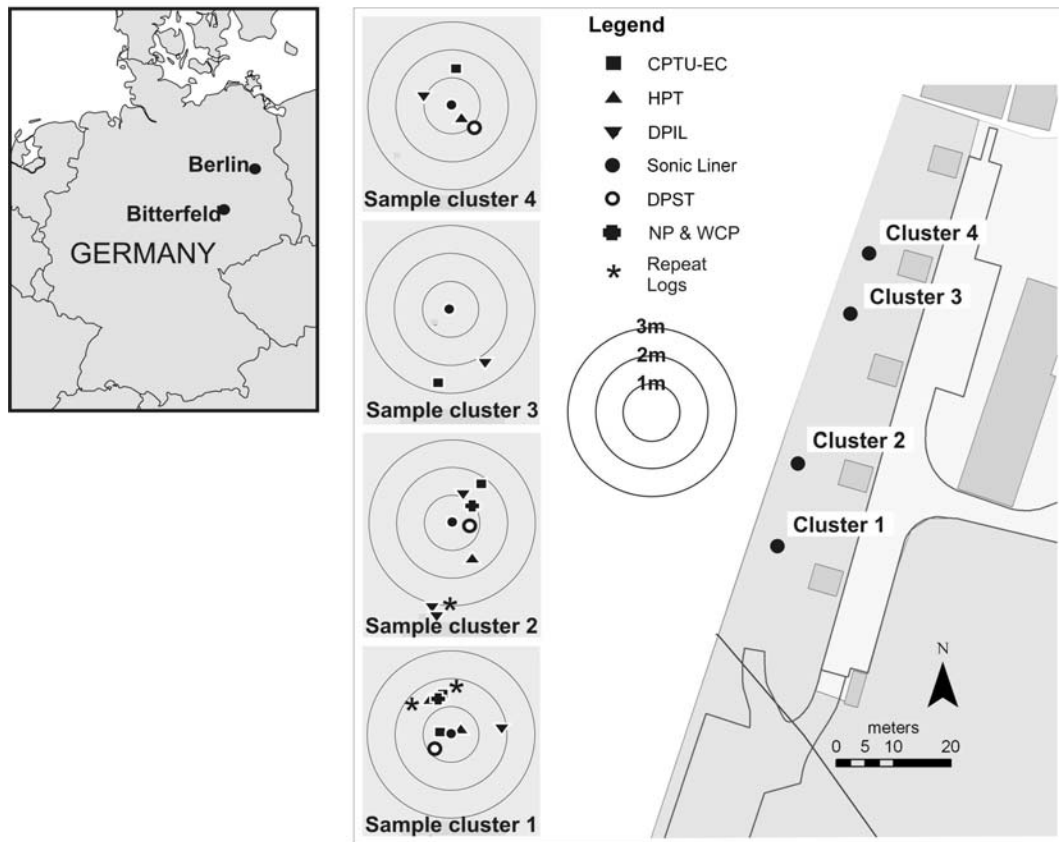


Figure 1-2: Location of the Bitterfeld test site with position of the sampling clusters and position of the DP profiles at each sampling cluster including neutron probe profiles. Repeat measurements are marked with an *.

1.2.2 Larned Research Site

The test site of the Kansas Geological Survey is located on the banks of the Arkansas river near the city of Larned, central Kansas, USA. It overlies an unconfined, coarse-sand and gravel aquifer that is in direct hydraulic connection with the intermittently flowing Arkansas river (see Butler et al. 2004 and Butler et al. 2007b). The field work was conducted during two campaigns in October/November 2008 and October 2009 and comprised volumetric water content measurements using neutron probe and frequency domain technology. The frequency domain probe was deployed in combination with a standard 15 cm² cone penetrometer. For further information on the test site see Butler et al. (2004) and Butler et al. (2007). Location of the test site as well as profiling location is

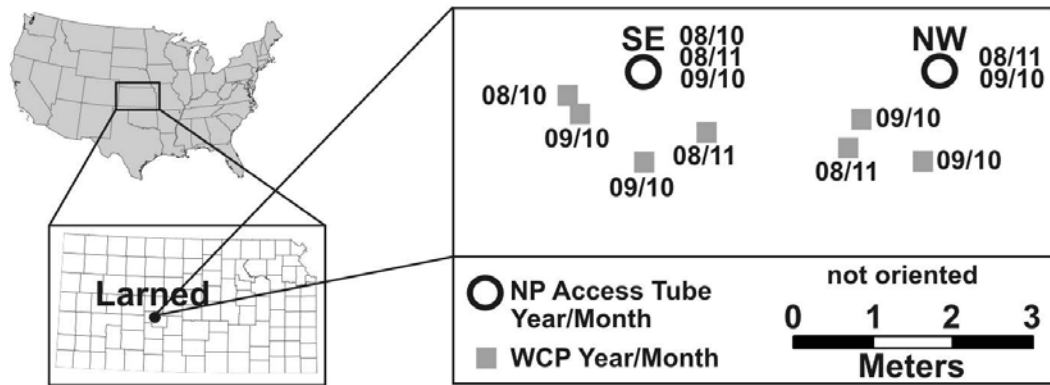


Figure 1-3: Location of the Larned Research Site and position and measuring date of neutron probe (NP) and Water Content Profiler (WCP) logs.

1.3 Outline

Chapter 2 is focused on grain size analysis as one of the most commonly employed method for high resolution vertical profiling in the hydrogeological practice. Results of different formulas to calculate K based on grain size distribution of 108 samples are compared. Precision of the individual formulas are evaluated with results of in situ measured K values using the Direct Push slug test data. In addition, effects of measuring inaccuracy of grain size analyses from repeat measurements on calculated K are investigated and effects of other factors influencing K , especially porosity, are shown.

The relevance of reliable porosity measurements for calculation of K from grain size distribution was shown in the previous chapter. However, sample disturbance and removal of the sample from its natural stress field among other factors often inhibit reliable porosity measurements ex situ. Therefore two methods, neutron probe and frequency domain technology, for volumetric soil water content determination are compared in chapter 3. The volumetric water content in the saturated zone equals the total porosity.

Two of the described formulas in chapter 2 to calculate K based on grain size distribution data require input of total porosity. Due to the complexity of frequency domain technology and resolution limits of the neutron probe technology, porosity values are in chapter 4 determined based on the geology and

grain size data using different empirical approaches. The empirical nature of the formula implies that different porosity values might be determined for the same sample. Therefore approaches are evaluated regarding their effects on calculated K .

Calculated K values based on grain size analyses can be used to reliably describe K distribution even in complex geological media. However, two of the main disadvantages of this method are that minimally disturbed samples are required and the high labor costs for laboratory work. Therefore, minimum invasive Direct Push deployed sensor probes and DP tools for the (hydro-)stratigraphic aquifer characterization as alternative to conventional site investigation techniques are evaluated in chapter 5. Analogue to chapter 2 and 3, methods are tested with the focus on vertical resolution and ability to reflect the hydraulic structure of the aquifer and to predict K . Results of the DP logging are compared to results of the grain size analyses and Direct Push slug testing from chapter 2.

A summary and final conclusion will be presented in chapter 6.

2 Evaluation of methods for determining hydraulic conductivity from grain size distribution

2.1 Introduction

Its high resolution and semi automated sample handling procedures make the grain size analysis a standard tool for site investigations. Since the work of Seelheim (1880) and especially Hazen (1893) who established a relationship between K and a certain grain size diameter, new formulas have been developed and existing refined. This led to a broad spectrum of formulas of which some are clearly defined while others are cited in a wide range of variations. Mostly site specific adaptations of the formulas were necessary as large uncertainties are associated with the (semi-) empirical nature of most of the frequently used formulas.

Relevant soil matrix properties, and therefore governing factors of K are grain- and pore size distribution, shape of grains and pores, tortuosity, specific surface, and porosity (see Bear 1972). Neither porosity nor tortuosity can be reliably determined from grain size analysis, as disturbance of the natural soil structure during commonly used sampling procedures is inevitable. Nevertheless, most of the semi empirical formulas rely on porosity measurements. Empirical relationships between K and the grain size distribution were often derived based on laboratory measurements. The calculation of K from grain size distribution is a standard method in practical hydrogeology (Langguth 1980, Holting & Coldewey 2005, Vukovic & Soro 1992). So derived K values are then often used to assess variability of hydraulic conductivity. However, uncertainties associated with this method have been addressed by Mishra et al. (1989), Alyamani & Sen (1993), and Sperry & Peirce (1995).

Therefore a clear need exists to test how prevalent grain size interpretation formulas compare when applied to the broad sedimentological spectrum of heterogeneous aquifers and how well these methods predict K . Many authors contributed to evaluate methods of the determination of hydraulic conductivity

from grain size analyses (see Table 2-1 for a number of selected references). However, often evaluation methods were chosen that differ significantly in intrinsic volumes from grain size analyses. Furthermore, methods suffer from soil disturbance during sampling. Developments in the soil sampling and high resolution in situ K determination techniques enable the revision of this comparison on a high resolution scale.

Table 2-1: Selected literature references for the evaluation of K determined from grain size distribution.

Reference	Methods compared to grain size analysis
Vukovic and Soro (1992)	pumping test
Chapius et al. (2005)	slug test, pumping test, numerical modeling
Cheong et al. (2008)	pumping test, slug test, numerical modeling
Song et al. (2009)	permeameter
De Ridder (1965)	pumping test, permeameter
Indelman et al. (1999)	tracer test
Schafmeister (2006)	permeameter, infiltration tests, borehole dilution test
Uma et al. (1989)	pumping test

Novelties employed include the retrieval of minimally disturbed cores with a minimum of core loss and high resolution in situ measurements of K using a semi automated Direct Push (DP) slug test kit.

In the following sections, the concepts of the applied formulas used to calculate K from grain size distributions, will be explained. Effects of porosities on calculated K will be shown and results of calculated K for 108 samples using seven different formulas will be compared. At last, calculated K values will be evaluated using slug test data.

2.2 Field work

The field work was conducted at the UFZ test site in Bitterfeld, Germany. For detailed information on the test site and sampling location see section 1.2.1. This site was chosen for the strong heterogeneity and broad sedimentological spectrum of the deposits. Soil samples were taken at three locations along a 58 m long profile (Figure 1-2) in the upper 12 m of a quaternary unconsolidated sedimentary

aquifer that consists of glacial and glaciofluvial deposits. Changes in soil specific properties are therefore within a range of several orders of magnitudes and occur within short horizontal and vertical distances. Figure 2-1 shows the variability of the d_{10} , d_{60} and d_e for the individual cores.

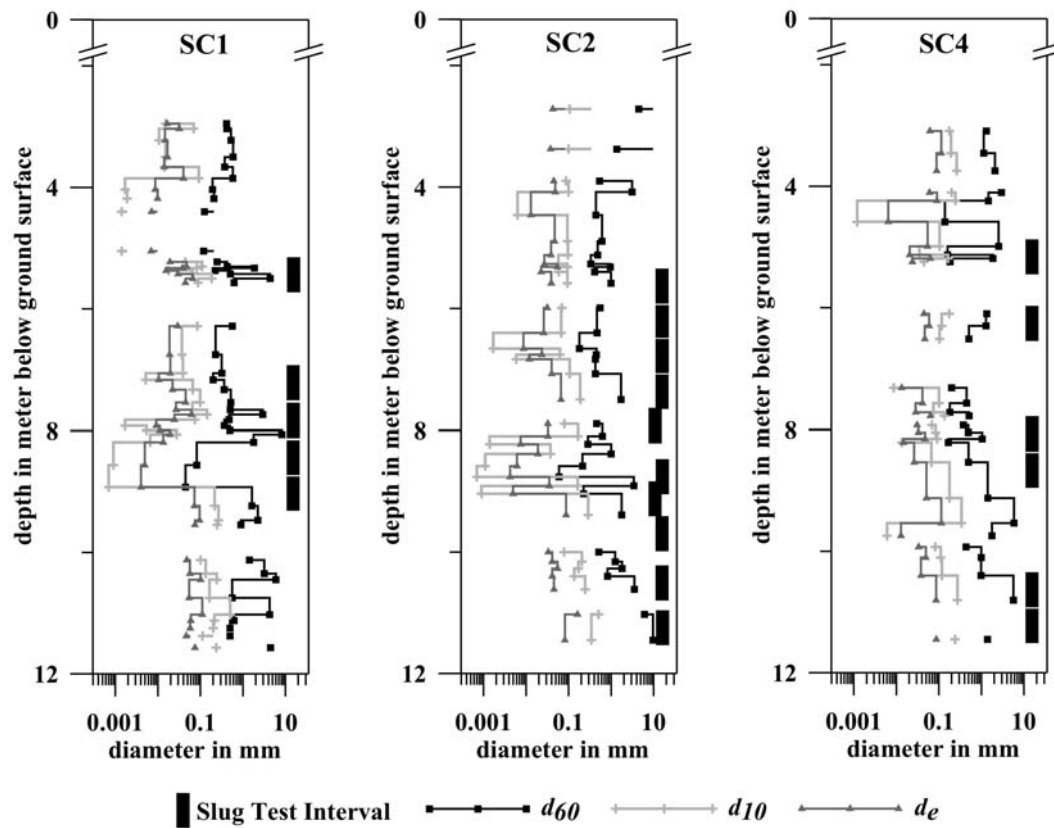


Figure 2-1: Selected grain size diameters and slug test intervals at sampling cluster 1 (SC1), sampling cluster 2 (SC2), and sampling cluster 4 (SC4); grain size diameters are given in mm.

2.2.1 Sampling

To collect the soil samples for grain size analyses, sonic sampling was employed (Barrow 1994). Thereby the rods are set into high frequency vibration causing the soil that is in direct contact with the rods to “liquefy”. This technique allows the retrieval of continuous and minimally disturbed soil cores. The cores were visually classified after lithological criteria and samples were taken at every observable change in lithology, color, and/or texture. Grain size analyses including the coarse and fine grained fraction were performed on the resulting 108 core samples at sampling cluster 1, 2, and 4. The rock, gravel and sand fractions

were sieved; the silt and clay fraction were automatically processed and manually weighed. Results of the grain size analyses are presented in Appendix A.

2.2.2 Grain size analysis

Relevant soil matrix properties, and governing factors of K , are grain- and pore size distribution, shape of grains and pores, tortuosity, specific surface, and porosity (see Bear 1972). A general form for the relationship between grain size diameter and the intrinsic permeability (k) is given by Bear (1972):

$$k = f_1(s) \times f_2(\phi) \times d^2 \quad (\text{Eq. 2-1})$$

where $f_1(s)$ is the shape factor; $f_2(\phi)$ is the porosity factor; and d is the effective diameter of the grains.

In most cases, $f_1(s)$ and $f_2(\phi)$ are combined in a dimensionless factor C_i (Bear 1972). K and k are related by the following equation after Bear (1972):

$$K = k \times \frac{g}{\nu} \quad (\text{Eq. 2-2})$$

where g is the gravitational constant; and ν is the kinematic viscosity. When combining eq. 1 and 2, a unit consistent form can be derived (Bear 1972)

$$K = \frac{g}{\nu} \times f_1(s) \times f_2(\phi) \times d^2 \quad (\text{Eq. 2-3})$$

Table 2-2: Summary of the applied formulas to calculate K from grain size distribution; key parameters, and citations.

Name	Type	Formula	K in	Relevant Parameter	Application Range	Tested on	References
Hazen	empirical	$K = C_H \times d_{10}^2 \times (0.7 + 0.03T)$ T= temperature $C_H = 1000$ (Coefficient)	m/d	d_{10} in mm	U < 5 0.1 < d_{10} < 3mm	Laboratory experiments on sand samples	Hazen (1893) Chapius (2004)
Beyer	empirical	$K = C_B \times d_{10}^2$ $d_e =$ effective grain size diameter	m/s	d_{10} in mm $\frac{d_w}{d_{10}} = f(U)$ $C = f(U) = \log \frac{500}{U}$	U < 20 0.06 < d_{10} < 0.6mm	Correlation of grain size analysis and pumping tests	Beyer (1964) Vukovic and Soro (1992)
Kozeny-Köhler	semi-empirical	$K = \frac{\tau}{R} \times 405 \times \frac{\Theta^3}{1 + \Theta} \times d_e^2$ $\Theta = \frac{\phi}{1 - \phi}$ $\tau = \frac{V_{Water} 10^\circ \text{ Celsius}}{V_{GW} \text{ Temperature}}$ R= 3.5 after Köhler (1965) as cited in Hütte (1956)	cm/s	$d_e = \frac{0.1}{\frac{3}{2} \frac{\Delta g_m}{d_m} + \sum_{i=2}^{i=n} \frac{\Delta g_i}{d_i}}$ (in cm) $\Delta g_m =$ weight of the last, finest fraction in parts of total weight $\Delta g_i =$ weight of the ith fraction $d_m =$ diameter of last fraction $\frac{1}{d_i} = \frac{1}{2} \times (\frac{1}{d_u} + \frac{1}{d_l})$ $d_l =$ lower class limit, $d_u =$ upper classer limit		Theoretical derivation, supported by sand and glass bead laboratory experiments	Kozeny (1953) Carman (1937) Hütte (1956) Köhler (1965) Bear (1972) Vukovic & Soro (1992)
USBR	empirical	$K = 0.0036 \times d_{20}^{2.3}$	m/s	d_{20} in mm	U < 5	-	Vukovic and Soro (1992)
Seelheim	empirical	$K = 0.00357 \times d_{50}^2$	m/s	d_{50} in mm		Laboratory measurements on sand, clay, and elutriated chalk	Seelheim (1880)
Kaubisch	empirical	$K = 10^{0.0005P^2 - 0.12P - 3.59}$	m/s	P < 0.06mm in %	60% > P > 10%	Permeameter tests	Kaubisch and Fischer (1985) Kaubisch (1986)
Terzaghi	semi-empirical	$K = C_T \times \frac{\eta_{10}}{\eta_i} \times (\frac{\phi - 0.13}{\sqrt[3]{1 - \phi}})^2 \times d_{10}^2$	cm/s	d_{10} in cm $C_T \sim 460 - 800$	0.26 < ϕ < 0.476	Theoretical derivation laboratory tests	Terzaghi (1925a,b) Vukovic and Soro (1992); Kasenow (2002)

Seven different formulas for the calculation of K from sieve data were compared (see Table 2-2). Formulas were chosen that cover a wide range of different approaches to represent the grain size diameter, shape and porosity functions.

2.2.2.1 Empirical formulas to calculate K from grain size distribution

As empirical solutions, the formulas after Hazen (1893), Beyer (1964), USBR (United States Bureau of Reclamation), Seelheim (1880), and Kaubisch (1986) were used. These formulas, except for Kaubisch (1986), use a power relationship between K and a certain grain size diameter that is derived from the cumulative grain size curve. Kaubisch (1986) based his formula upon a power relationship between K and the percental abundance of grain sizes <0.06 mm in the sample. No references could be found for the USBR formula, which is identical to the formula cited after Bialas and Kleczkowski (1970). Some authors cite USBR after Mallet and Pacquant (1954). A table of d_{20} and K values after USBR can be found in the work of Mallet and Pacquant (1954), the therein published K values however do not quite match the USBR formula. The semi empirical formulas include in contrast to the empirical solutions the grain size factor and porosity factor.

2.2.2.2 Semi empirical formulas to calculate K from grain size distribution

Two of the most frequently used semi empirical formulas are the Kozeny-Carman equation (see Carman 1937, Kozeny 1953, Bear 1972, Köhler 1965) and the formula after Terzaghi (1925a, b). The Kozeny-Carman equation includes two significant characteristics, the porosity function in the form of

$$\frac{\phi^3}{(1-\phi)^2} \quad (\text{Eq. 2-4})$$

and the introduction of the mean hydraulic radius (Carman 1937). The mean hydraulic radius (m) is linked to the porosity (ϕ) and the specific surface (S) by (Carman 1937):

$$m = \frac{\phi}{S} \quad (\text{Eq. 2-5})$$

Although various methods exist to measure the specific surface (see Bear 1972 for details) it is yet not a standard parameter to be measured during grain size analysis. As it is intended to use formulas that are close to the hydrogeological practice, the derivation of the Kozeny-Carman equation as cited in Köhler (1965) after Hütte (1956) was followed; from here referred as Kozeny-Köhler (1965). As one of many derivations, the Kozeny-Köhler (1965) approach uses the effective grain size diameter (d_e) which is calculated based on the harmonic mean of the grain size fractions. Vukovic & Soro (1992) cite a special derivation of d_e (see Table 2-2) without giving detailed references in their work that especially considers the clay fraction ($d < 0.002$ mm).

Also, various derivations of the formula after Terzaghi (1925a, b) exist. In this thesis the derivation cited by Vukovic & Soro (1992) referring to the d_{10} diameter was used. The formula after (Terzaghi 1925a, b) is characterized by the porosity function in form of

$$\frac{\phi - 0.13}{\sqrt[3]{1 - \phi}} \quad (\text{Eq. 2-6}).$$

From testing on sand, Terzaghi (1925a, b) developed an empirical factor (C_T) for his formula, ranging from 460 to 800. Other authors proposed different values. In this thesis a value of 800 was in good accordance to results of the Direct Push slug testing. When searching for references, it is important to note that Terzaghi used several forms of his name in his publications; two of these forms are Karl von Terzaghi and Charles Terzaghi (De Boer 2005).

Table 2-2 lists the applied formulas, relevant parameters, application range and main citations. The formulas were tested on all samples, even though sedimentary characteristics did not meet the dedicated application ranges.

2.2.3 Limitations and application range of the applied formulas

Most of the frequently used formulas are not unit consistent. Unit consistency is beneficial when temperature effects on the fluid viscosity must be considered. Most equations are based on an average ground water temperature of 10° Celsius. For Bitterfeld, where during testing an average groundwater temperature of 12° Celsius was measured, the temperature difference results in a 5.8% deviation in the kinematic viscosity (ν). A table of the water viscosity as a function of

temperature can be found in Kasenow (2002). However, temperature effects on K can easily be compensated using a simple correction factor like τ as applied in the Kozeny-Köhler formula (see Table 2-2).

Furthermore, a variety of application limits exist. As some formulas were originally developed against the background of other applications, i.e. as a proxy to predict water fluxes through sand filters (Hazen 1893); $f_1(s)$, $f_2(\phi)$, and C_i were derived from laboratory measurements that are not representative of natural geological conditions. Also, formulas based on actual field data were often correlated with either integral K values from pumping tests or permeameter tests. Often $f_1(s)$ and $f_2(\phi)$ were combined in C_i because effects of $f_1(s)$ and $f_2(\phi)$ on K are not distinguishable. Conventional sampling methods do not allow reliable ex-situ measurements of ϕ . The limited accessibility of extensive data sets for cross validation is a common problem (see Shepherd 1989).

Ideally, equations should be applicable over the complete sedimentary spectrum and usable for homogenous and highly heterogeneous sediment samples. However, as already discussed, certain limitations confine the application range; among those are the grain size ranges for applicability and the level of uniformity. The application is limited for small grains sizes mainly by the abundance of clay particles. A common model of flow through a porous medium is to visualize the void spaces of a porous medium as composed of a spatial network of interconnected tubes (Bear 1972). Hence, the laminated habitus of clay minerals in contrast to the rounded shape of sand grains causes an important difference in the mechanics of the percolation processes when the model of connected tubes is applied (see Terzaghi 1925a).

The heterogeneity of a sample is defined by the coefficient of uniformity expressed by Hazen 1893:

$$U = \frac{d_{60}}{d_{10}} \quad (\text{Eq. 2-7}).$$

An overview of application ranges for each formula is given in Table 2-2.

2.2.4 Effects of porosity on calculated K

The porosity function is an important part of the formulas after Kozeny-Köhler (1965), and Terzaghi (1925a, b). However, reliable ex-situ porosity measurements on soil samples can often not be performed as currently used soil sampling methods alter the soil structure, packing, and compaction of the sediment sample. Typically, empirical data or equations are used to estimate the total porosity of a sample. Two approaches will be briefly discussed here. The first approach is presented by Vukovic & Soro (1992) who approximated the change of ϕ as a function of U , based on literature data as

$$\phi = 0.255(1 + 0.83^U) \quad (\text{Eq. 2-8}).$$

Vukovic & Soro (1992) state that for the given formula, significant deviations are observed for materials comprising clay. In the proposed relationship no distinction is made between total and effective porosity. Especially when working with samples that contain clayey materials, the effective porosity must be considered. The second approach is based on ϕ values related to d_e as cited by Szymczak et al. (2009). Porosity values after Szymczak et al. (2009) and others are combined in Table 4-1.

When both approaches were applied significant differences for ϕ could be observed, ranging from 0.55 after Szymczak et al. (2009) to 0.255 for the calculated porosity after Vukovic and Soro (1992). This difference could be found in seven of the 108 samples. Effects of deviation of ϕ on the calculation of K are demonstrated in Figure 2-2. The plot shows the ratio of a reference K value (K_{ref}) calculated for a porosity of 0.55 (Figure 2-2a) and 0.30 (Figure 2-2b) versus K values (K_{dev}) calculated for porosity ranging from 0.25 to 0.65. When K_{ref} equals K_{dev} the ratio is 1. K_{ref} is calculated after Terzaghi (1925a,b) and Kozeny-Köhler (1965). In this plot, the observed porosity differences lead to significant differences for calculated $K_{Terzaghi}$ and $K_{Kozeny-Köhler}$. To follow the hydrogeological practice and in consideration of the clay content standard ϕ values cited by Szymczak et al. (2009) were used. Median values for the classes were chosen as previous studies at the Bitterfeld field site have indicated an increased compaction of the sediments due to increased overburden stress during glaciation periods.

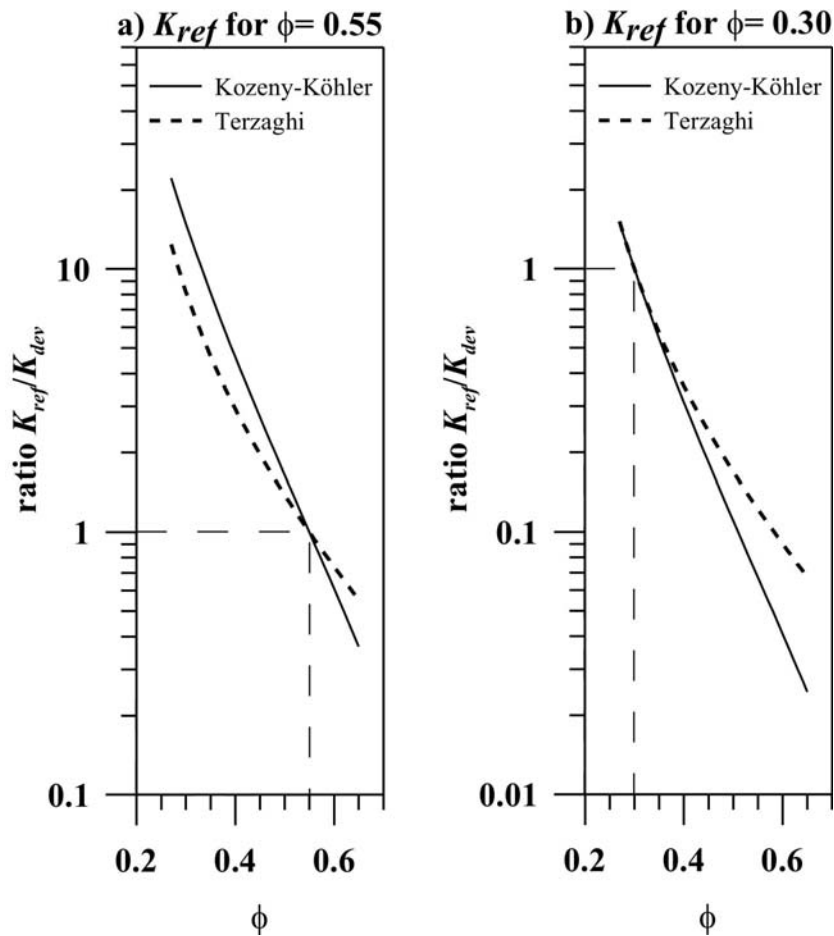


Figure 2-2: Resulting deviation on calculated K after Kozeny-Köhler (1965) and Terzaghi (1925a, b) caused by uncertainties of porosity estimates. The Graph shows the magnitude of difference between calculated K with fixed porosity value (K_{ref}) of 0.55 in Fig. 2-2 a and 0.30 Fig. 2-2 b and calculated K for porosity values ranging between 0.25 and 0.65 (K_{dev}).

2.3 Results of the grain size analyses

Calculated $\ln(K)$ values based on the results of the grain size analyses (Appendix A) are presented in the following section. Therefore, $\ln(K)$ values derived from different formulas are plotted against each other in scatter plots that are arranged in form of a matrix plot. This allows the fast visual recognition of linear correlation between the applied methods. In addition to the data points, a simple regression line and the line of equality ($x=y$) are plotted. Histogram plots (Figure 2-3) show the relative distribution of $\ln(K)$ for each of the applied formulas. While the histogram plots for Hazen (1893), Beyer (1964), Terzaghi (1925a,b), and USBR yield similar $\ln(K)$ distributions, differences for the remaining formulas can be observed. Results after Kaubisch (1986) show a trend towards higher $\ln(K)$

values. This formula is not coupled to the cumulative grain size curve, but to the percentage of fine grain material and yields relatively high K values for samples with low fine grain content. The $\ln(K)$ values after Seelheim (1880) concentrate in the mid range while results after $\ln(K_{\text{Kozeny-Köhler}})$ show, when compared to the other histogram plots, a relatively even distribution. The matrix plot of the results of the 108 analyzed soil samples reveals a qualitatively high level of correlation between the different applied formulas over the entire sedimentological spectrum (Figure 2-3); correlation coefficients are listed in Table 2-3. The correlation coefficient is a measure of the strength of the linear correlation between variables (Brown 1998). However, a high coefficient of correlation does not imply a 1 to 1 relationship between two variables. To identify differences in the results between applied methods the line of equality is plotted in addition to the simple regression line. Strong differences in the slope of the line of equality and simple regression line are especially prominent for results after Seelheim (1880) and Kozeny-Köhler (1965) although a high linear correlation exists between the results of these two formulas and all other tested methods. These differences clearly state the need for directly measured K values for evaluation purposes.

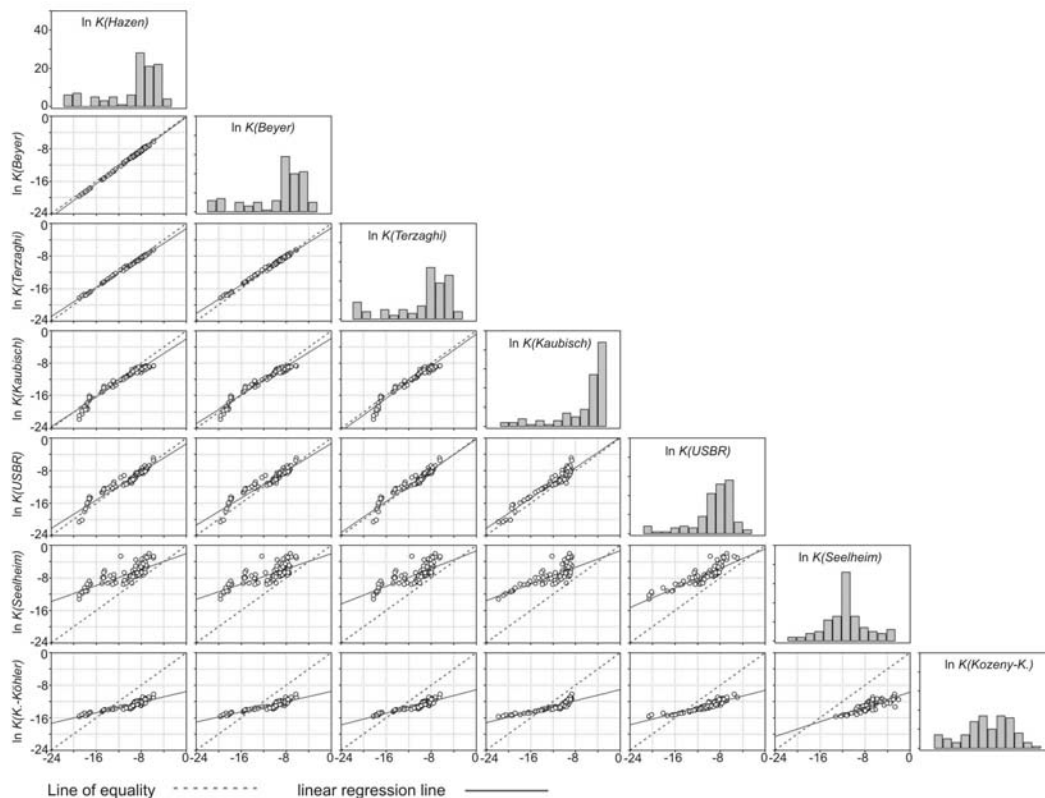


Figure 2-3: Matrix plot of natural logarithm of K ($\ln(K)$) calculated from grain size analyses using different formulas. Histogram: x-axis: classes, y-Axis: frequency; scatter plots: x- and y-axis: $\ln(K)$.

Table 2-3: Correlation matrix for calculated $\ln(K)$ values using different formulas. Triplets are listed top down in form of r , y , and b , where r is the correlation coefficient; $y*x$ is the slope and b is the intercept of the linear regression

$K_A \backslash K_B$	$\ln K_{Hazen}$	$\ln K_{Beyer}$	$\ln K_{Terzaghi}$	$\ln K_{Kaubisch}$	$\ln K_{USBR}$	$\ln K_{Seelheim}$
$\ln K_{Beyer}$	0.999 1.0262*x -0.1935	1.000				
$\ln K_{Terzaghi}$	0.999 0.9014*x -1.2426	0.998 0.8771*x -1.0863	1.000			
$\ln K_{Kaubisch}$	0.972 0.8996*x -1.9986	0.972 0.8764*x -1.8316	0.971 0.9963*x -0.7773	1.000		
$\ln K_{USBR}$	0.958 0.8664*x -1.4161	0.952 0.8389*x -1.3125	0.957 0.959*x -0.2452	0.959 0.9373*x 0.2138	1.000	
$\ln K_{Seelheim}$	0.777 0.4925*x -2.0077	0.758 0.4679*x -2.0469	0.776 0.5447*x -1.3471	0.749 0.5128*x -1.3098	0.860 0.6024*x -0.8474	1.000
$\ln K_{Kozeny-Köhler}$	0.933 0.3258*x -9.5476	0.927 0.3152*x -9.5105	0.931 0.3602*x -9.1108	0.899 0.3391*x -9.086	0.916 0.3538*x -9.2478	0.826 0.4553*x -9.6952

To quantify results, Table 2-4 shows the relevant statistic for the calculated $K_{Grain\ size}$ values. Results of the calculated K values reflect the broad sedimentological spectrum of the deposits; differences of 6 orders of magnitudes can be observed between Min and Max values after Hazen (1893), Beyer (1964), Kaubisch (1986) and USBR. Results after Kozeny-Köhler (1965) prevail with small Max and large Min values and thereof a narrow range of results. Seelheim (1880) provides highest K values.

Table 2-4: Overview of basic statistics for calculated K values derived from different formulas.

	K_{Hazen}	K_{Beyer}	$K_{Terzaghi}$	$K_{Kaubisch}$	K_{USBR}	$K_{Seelheim}$	$K_{Kozeny-Köhler}$
n	108	108	108	108	108	108	108
\bar{x}	2.57E-04	1.68E-04	1.51E-04	5.22E-05	2.49E-04	6.94E-03	4.30E-06
Min	5.67E-09	2.94E-09	1.18E-08	3.48E-10	1.15E-09	1.86E-06	1.54E-07
Max	3.05E-03	2.02E-03	1.58E-03	1.70E-04	7.34E-03	1.32E-01	3.68E-05
σ^2	2.25E-07	9.29E-08	6.12E-08	2.28E-09	6.81E-07	3.66E-04	2.56E-11

2.4 Comparison of calculated K from grain size analyses with Direct Push slug test results

Results of the previous section demonstrate that directly measured K values are needed to evaluate the different formulas used to calculate K . As shown at the beginning of this thesis, these reference K values should be measured in situ and must be determined by a method that works with an intrinsic volume similar to that of grain size analysis. This is especially important when the heterogeneity of the sedimentary deposits is considered. A technology that is especially suitable for the high resolution in situ K characterization is called Direct Push. Detailed information and references on DP and DP slug tests (DPST) is given in section 5.2 and 5.2.1. DP slug test was chosen as an established method to obtain absolute K values on a decimeter scale. Therefore DP multi level slug tests were performed in temporary DP monitoring wells with a screened interval of 57 cm length at the end of the rod string in close vicinity of the sample locations. Well installation procedures and details on the DP slug test and data analysis are given in section 5.2.1.

A number of 22 slug tests (see Figure 1-2 for test positions) were used to compare measured in situ $K_{\text{Slug test}}$ values and calculated $K_{\text{Grain size}}$ values. To derive relevant parameters for the calculation of $K_{\text{Grain size}}$ values, cumulative grain size curves of the individual slug test intervals were generated. Therefore, the grain size distributions of the individual layers were averaged according to their thickness within each slug test interval (Appendix B). $K_{\text{Grain size}}$ values were calculated and temperature corrected.

For 9 of 22 slug tests intervals generally minor core losses were observed (Appendix B). Similar to the comparison of the different formulas, calculated and measured K values are plotted in scatter plots arranged in a matrix. Again, not only the degree of linear correlation but also the difference in slopes between the simple regression line and line of equality are considered.

An example of the scatter plot for the slug test data and grain size data after three formulas (Figure 2-4) reveals that the correlation is strongly affected by several values. Three values of high $K_{Slug\ test}$ and very low $K_{Grain\ size}$ could be identified as K values derived from test intervals containing high contents of clay and gravel, resulting in high U values of 198.64, 328.47, and 399.69 respectively (Appendix B).

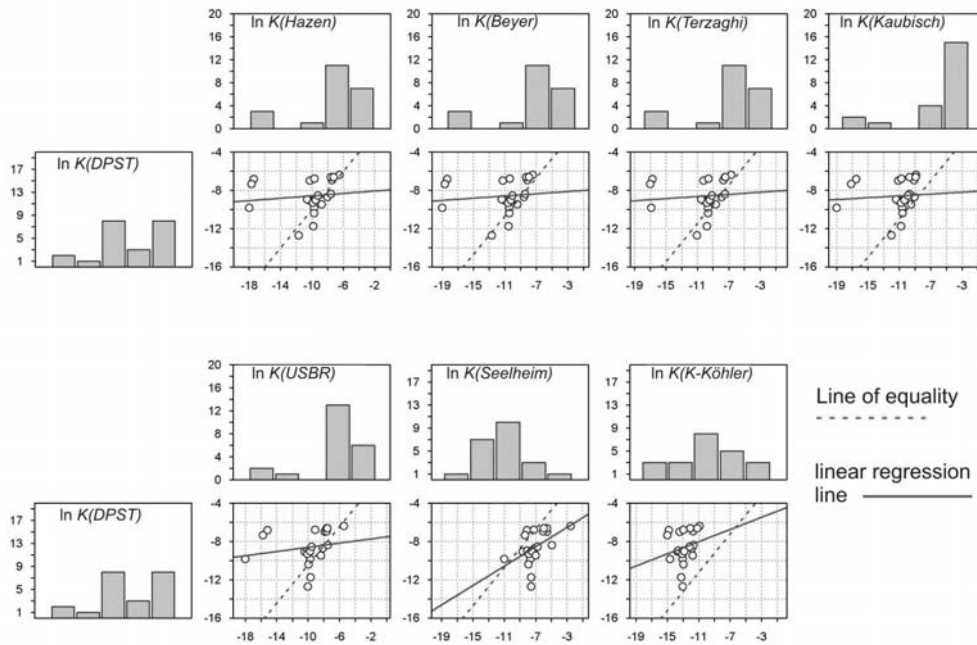


Figure 2-4: Correlation of measured K_{DPST} and calculated $K_{Grain\ size}$ of untreated data. Histogram plot: x-axis: classes, y-axis: frequency; scatter plots: x- and y-axis: $\ln(K)$.

These three values were removed and analysis continued with 19 slug test intervals. In addition, two K_{DPST} values were identified, that also strongly decreased the correlation coefficients. These K_{DPST} values were derived from slug tests intervals where grain size analysis revealed the presence of a thin (8-10cm) low K layer in between high K sediments. The presence on the low K layers had only minor effects on the measured K_{DPST} values but did significantly lower calculated K values. To account for this effect, $K_{Grain\ size}$ for the individual layers of these to slug test intervals were calculated and averaged according to their

thickness within the respective interval. By using the arithmetic mean, effects of small K values on the mean are reduced. The matrix plot of $\ln(K_{Slug\ test})$ and corrected $\ln(K_{Grain\ size})$ values are shown in Figure 2-5, correlation coefficients are presented in Table 2-5. The box plots (Figure 2-6) of the $\ln(K)$ data for the slug test intervals also demonstrate the wide range of results for measured and calculated K values.

The highest correlation coefficient of 0.82 was observed for $\ln(K_{Beyer})$ with good accordance between the simple regression line and line of equality. In good agreement with the results from Table 2-4, correlation coefficients for $\ln(K_{Hazen})$ and $\ln(K_{Terzaghi})$ are with 0.81 and 0.79 within the same range; the correlation coefficient for $\ln(K_{USBR})$ is 0.72; the regression lines corresponding to the equality lines. The correlation coefficient for $K_{Kaubisch}$ is high (0.77) and differences between the line of equality and linear regression can be observed. Lowest values of $r < 0.7$ can be seen for $\ln(K_{Kozeny-Köhler})$, and $\ln(K_{Seelheim})$. For results after $\ln(K_{Kozeny-Köhler})$ a strong difference between the regression line and equality line can be observed. The results of the simple linear regression for $\ln(K_{Grain\ size})$ versus $\ln(K_{Slug\ test})$ are shown in Table 2-5.

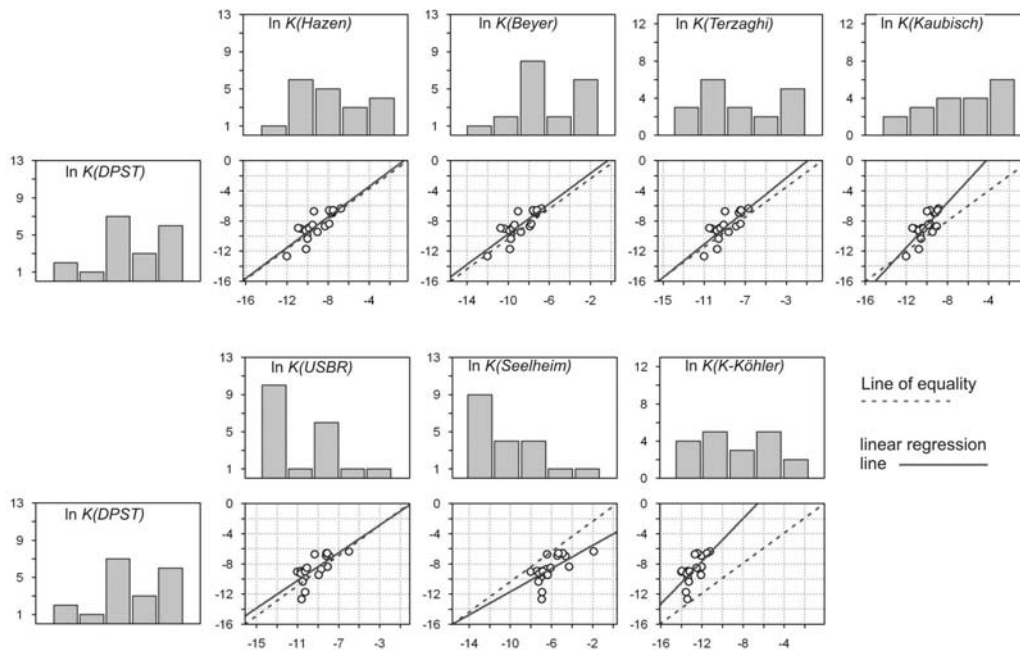


Figure 2-5: Matrix plots of K_{DPST} and calculated $K_{Grain\ size}$ of treated data. Histogram plot: x-axis: classes, y-axis: frequency; scatter plots: x- and y-axis: $\ln(K)$.

Table 2-5: Basic statistics for calculated $K_{Grain\ size}$ and measured K_{DPST} based on different formulas; $y*x$ is the slope and b is the intercept of the linear regression.

	K_{Hazen}	K_{Beyer}	$K_{Terzaghi}$	$K_{Kaubisch}$	K_{USBR}	$K_{Seelheim}$	$K_{K-Köhler}$	K_{DPST}
n	19	19	19	19	19	19	19	19
\bar{x}	2.98E-04	1.91E-04	1.76E-04	5.76E-05	2.78E-04	7.63E-03	4.49E-06	4.61E-04
Min	8.10E-06	4.19E-06	1.02E-05	6.15E-06	1.86E-05	2.32E-04	9.31E-07	3.07E-06
Max	1.54E-03	7.96E-04	7.94E-04	1.45E-04	2.80E-03	1.06E-01	1.49E-05	1.67E-03
$r(\ln K)$	0.81	0.82	0.79	0.77	0.72	0.63	0.67	
lin. Regr.								
y	$1.02*x$	$1.01*x$	$1.10*x$	$1.48*x$	$0.92*x$	$0.77*x$	$1.42*x$	
b	0.38	0.73	1.56	6.26	-0.19	-3.75	9.22	
σ^2	1.42E-07	4.73E-08	3.95E-08	1.85E-09	3.72E-07	5.47E-04	1.34E-11	3.00E-07

2.5 Factors influencing K_{DPST} and $K_{Grains\ size}$ correlation

Two effects decrease the correlation of $K_{Kozeny-Köhler}$ and K_{DPST} in this heterogeneous aquifer: the high effect of ϕ and calculation of d_e as harmonic mean. One systematic difference between slug tests and the grain size analysis should be further mentioned: When laboratory data and field data are compared differences in K estimates are often found, especially in low permeable media (Campbell et al. 1990). This is caused, as the natural soil structure is altered or destroyed by the sample recovery and handling. In this thesis, 3 samples of high clay and gravel content, and corresponding high U values, had impacted correlation, yielding small $K_{Grain\ size}$ and relatively high $K_{Slug\ test}$ values. The fine grain content is the governing parameter in the determination of K .

Here, the major difference between calculated and measured K becomes obvious. Calculated K values are either based on the harmonic mean of the grain size distribution (Kozeny-Köhler 1965) or rely on a certain grain size diameter determined from the grain size distribution curve of a sample (e.g. Hazen 1893). For the calculation of K from grain size distribution it is insignificant whether the fine grain content is homogeneously dispersed over the entire sample or accumulated within a small layer within this sample. In contrast, K values

measured with slug tests represent an arithmetic K value of the test interval. This means that results of measured K from slug tests will essentially be affected by the fact whether the fine grain material is homogeneously dispersed or accumulated in a small layer within the test interval. This could be clearly shown with the additional two samples where K values had to be corrected. If grain size analyses are performed on heterogeneous samples, the presence of small fine grained layers in a generally high permeable medium leads to a strong underestimation of calculated K .

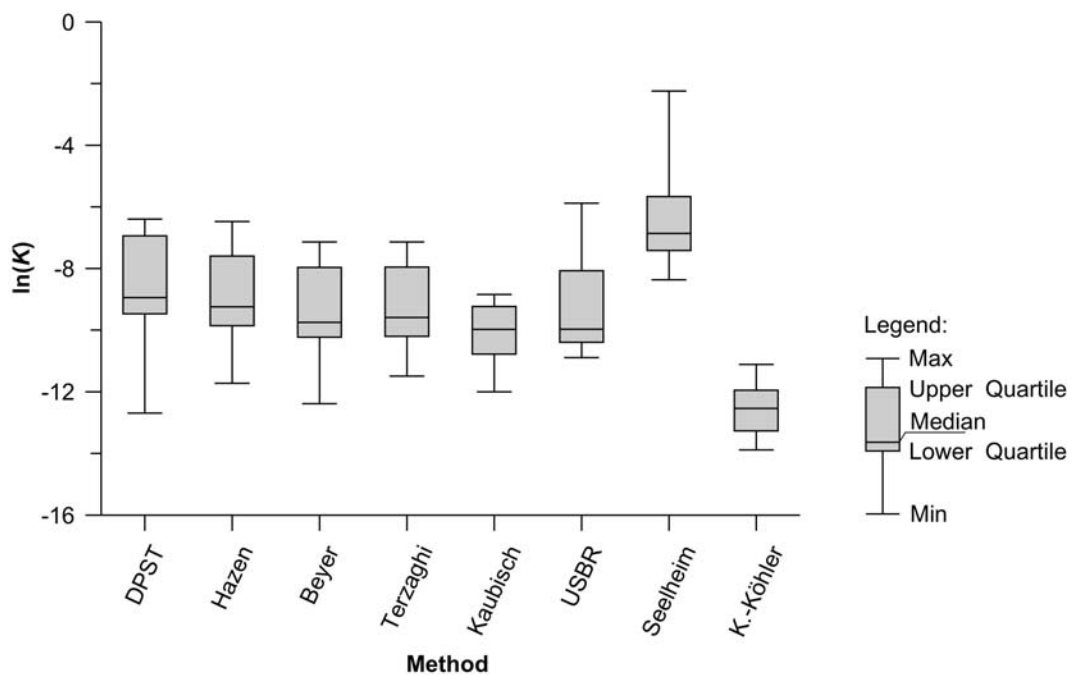


Figure 2-6: Box plot of $\ln(K)$ values calculated with different formulas for the slug test intervals

2.6 Effects of measuring inaccuracy on calculated K

To compare the effects of measuring inaccuracy of grain size analyses, results from ring analyses for grain size analysis were exploited that were initiated by the Verband Deutscher Landwirtschaftlicher Forschungs- und Untersuchungsanstalten (VDLUFA) between 2006 and 2010. The ring analysis is an interlaboratory test in the course of which specimen of the same samples are sent to different laboratories to evaluate the laboratory performance. Strong differences in the composition of the soil are seen between the individual ring analyses. Thus, results in the analyses of different soil types can be compared,

ranging from clay dominated to sand dominated soils. In this evaluation only those laboratory results were considered for which the total sum of all particle fractions of the grain size analyses ranged between 95 to 105 % and for which all of individual fractions were within the tolerance limits set by the VDLUFA. Execution of ring analyses and determination of tolerance limits were done in accordance with DIN 38402-41.

In the compared ring analyses no subdivision of the sand fraction is made. Hence, sand values were assigned to the medium sand fraction to determine the corresponding d_{10} values. Table 2-6 lists the mean values the fraction for each ring analyses as well as respective upper and lower tolerance limits.

Table 2-6: Mean, upper tolerance limit, and lower tolerance limit for the fraction of each ring analysis.

Name	Parameter	medium		medium		
		sand	coarse silt	silt	fine silt	clay
89_1	\bar{x}	13.02	12.77	18.58	13.39	42.51
	Lower limit	9.93	6.37	14.56	6.83	37.28
	Upper limit	16.22	20.83	23.39	20.81	47.95
89_2	\bar{x}	5.33	23.14	20.34	8.90	41.75
	Lower limit	1.65	15.33	16.24	3.85	31.48
	Upper limit	10.08	32.61	25.21	18.78	51.24
88_1	\bar{x}	81.75	6.61	4.48	2.47	4.81
	Lower limit	78.42	3.81	2.42	1.09	2.90
	Upper limit	85.36	9.39	6.69	4.45	7.35
88_2	\bar{x}	14.52	30.33	18.38	6.77	29.16
	Lower limit	12.27	23.64	14.65	3.53	24.85
	Upper limit	16.59	36.82	22.31	10.51	33.91
87_1	\bar{x}	5.64	12.91	21.41	19.83	40.45
	Lower limit	2.86	5.13	17.00	14.05	31.65
	Upper limit	8.20	20.12	25.99	26.82	47.88
87_2	\bar{x}	59.74	20.39	8.94	4.08	6.81
	Lower limit	55.83	15.32	5.89	1.26	4.72
	Upper limit	63.27	25.00	11.74	7.01	9.19
86_1	\bar{x}	73.3	12.5	6.3	2.9	4.9
	Lower limit	70.40	7.60	5.14	1.23	2.90
	Upper limit	76.66	16.28	7.66	4.41	7.19

Effects of the variability of measurements on the determination of d_{10} values for each ring size analyses are shown in Fig. 2-7. Significant differences can be found for those ring analyses performed on sand dominated soils. Here differences between determined d_{10} values as high as 212% are seen for ring analysis 86_1, leading to differences in calculated K_{Hazen} of 448%. Minimum and maximum values of determined d_{10} values and calculated K_{Hazen} is given in Table 2-7.

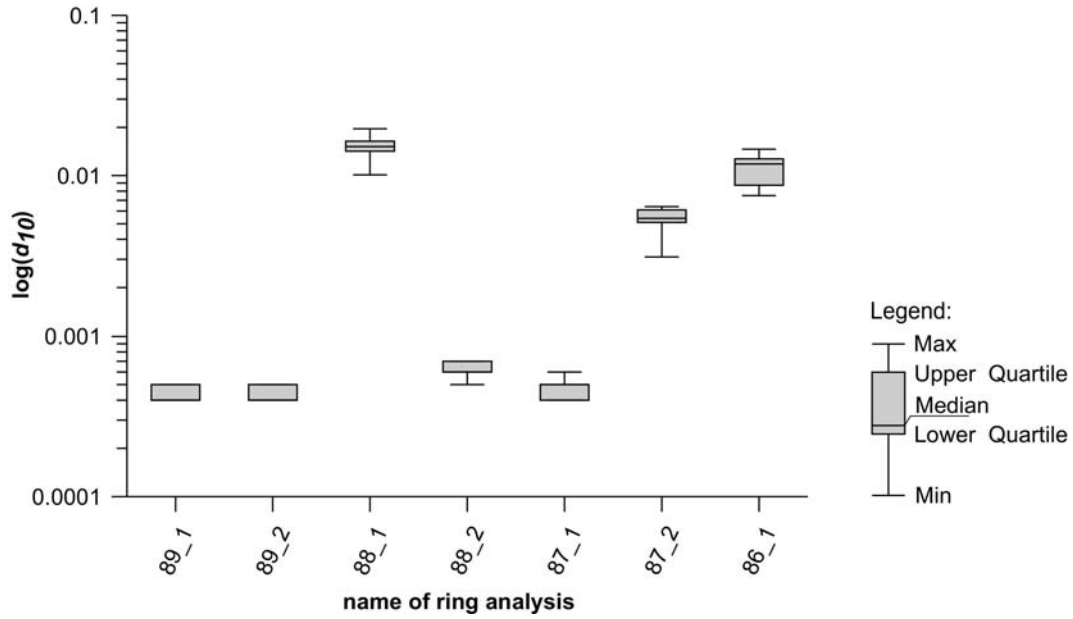


Figure 2-7: Box plot showing the differences of determined d_{10} values within each ring analysis.

Table 2-7: Maximum values, minimum values, and resulting deviation for determined d_{10} values and calculated K_{Hazen} values within each ring analysis.

	89_1	89_2	88_1	88_2	87_1	87_2	86_1
Max d_{10}	0.0005	0.0005	0.0196	0.0007	0.0006	0.0064	0.0146
Min d_{10}	0.0004	0.0004	0.0101	0.0005	0.0004	0.0031	0.0075
Deviation in %	125	125	194	140	150	206	195
Max K_{Hazen}	2.89E-09	2.89E-09	4.45E-06	5.67E-09	4.17E-09	4.74E-07	2.47E-06
Min K_{Hazen}	1.85E-09	1.85E-09	1.18E-06	2.89E-09	1.85E-09	1.11E-07	6.51E-07
Deviation in %	156	156	377	196	225	426	379

2.7 Conclusion

Comparison of results of 108 grain size analyses revealed a high correlation between the different applied formulas to calculate K based on grain size distribution. Despite the high correlation, differences in the results of the applied formulas became obvious when the simple regression line and line of equality were compared in the scatter plots. This indicated the need to evaluate the applied formulas with directly measured K values using the DP slug testing. A high correlation between $K_{Grain\ size}$ and 19 K_{DPST} values and low deviation between the simple regression line and line of equality could be shown with correlation coefficients of 0.82 for $\ln(K_{Beyer})$, 0.81 for $\ln(K_{Hazen})$, and 0.79 for $\ln(K_{Terzaghi})$. Strongly heterogeneous sample influenced $\ln(K_{DPST})$ and $\ln(K_{grain\ size})$ correlation. This clearly revealed the difference between calculated and measured K . Calculated K values are based either on the harmonic mean of the grain size distribution or rely on a certain grain size diameter determined from the grain size distribution curve while K_{DPST} values represent the arithmetic mean of the K distribution within the test interval. Porosity was identified as an important factor for calculating K after Terzaghi (1925 a,b) and Kozeny-Köhler (1965). In addition, strong effects on determined d_{10} values and respective K_{Hazen} were seen in repeat measurements of sand dominated soil in the comparison of ring analyses that caused differences in calculated K_{Hazen} as high as factor 4.26 for the same sample.

The calculation of K from grain size distribution is a suitable method to predict K even in heterogeneous deposits. However as shown in this chapter, uncertainties are associated with these methods, that must be especially considered if $K_{Grain\ size}$ data is used for calculations of flow velocities.

"NOTICE: this is the author's version of a work that was accepted for publication in Journal of Hydrology. Changes resulting from the publishing process, such as peer review, editing, corrections, structural formatting, and other quality control mechanisms may not be reflected in this document. Changes may have been made to this work since it was submitted for publication. A definitive version was subsequently published in Journal of Hydrology, published online February 23rd, 2011, doi:10.1016/j.jhydrol.2011.01.022."

3 Comparison of in situ water-content profiles obtained using frequency-domain and neutron-probe technology

3.1 Introduction

The importance of determining volumetric water content has been long recognized for agricultural water management. Water content information is also important in subsurface hydrology for assessments of conditions in the vadose zone and estimation of total porosity in the saturated zone. Total porosity is a fundamental parameter for flow and fluid transport modeling and is required for certain formulas to calculate hydraulic conductivity (K) from grain size distribution data (see Terzaghi 1925, Carman 1937, Kozeny 1953, Vukovic & Soro 1992) as shown in section 2.2.2.

Commonly, volumetric water content is determined by gravimetric analyses in the laboratory on field samples. Disturbance during sampling, removal of the sample from its natural stress field, transport to the laboratory, and labor costs are all disadvantages of this method. In situ measurements are therefore preferable, and can be obtained using an active source neutron probe in a cased borehole or access tube to determine a vertical profile of water content with depth. However, the handling, transport, and storage of the radioactive source require special training and are subjected to regulatory approval in most countries.

Both of the above methods are limited in terms of their vertical resolution. Higher resolution measurements are possible with minimally invasive direct-push (DP) probes that have been developed to measure in situ water content profiles based on the dielectric properties of the subsurface material (see Robertson et al. 1996, Lunne et al. 1997, Shinn et al. 1998, McCall et al. 2005, and Brouwer 2007). These sensor probes can be operated independently or in combination with other DP probes, such as cone penetrometers (CPT). Different names can be found in the literature for probes to measure volumetric water content based dielectric measurements, including capacitance probe (Atkins et al. 1998, Starr &

Paltineanu 2002, Vera et al. 2009) and soil moisture probe (Shinn et al. 1998, Brouwer 2007). As these names can be misleading and do not represent the full application range for the probe, i.e. use of the probe in the unsaturated and saturated zone, the name Water Content Profiler (WCP) is proposed for such DP deployed sensor probes to measure volumetric water content in this thesis at the centimeter scale. Table 3-1 lists the major advantages and disadvantages of gravimetric, neutron probe, and WCP measurements for determining volumetric water content.

Different studies of the design, development and application of sensors and sensor probes for the dielectric measurement and its relation to volumetric water content exist (Evet & Steiner 1995, Hilhorst 1998, Shinn et al. 1998, Robinson et al. 2003, Kim et al. 2007, Evett et al. 2009, Vera et al. 2009). However, little information on the performance of commercially distributed CPT deployed sensor probes for continuous water content measurements, especially in comparison to other in situ techniques, has been published to date. The performance of a CPT deployed WCP to estimate volumetric water content was assessed through a comparison with neutron probe profiles at a test site overlying a coarse sand and gravel aquifer.

Table 3-1: Major advantages and limitations of gravimetric, NP, and WCP measurements for determining volumetric water content.

	Gravimetric method	Neutron Probe	Water Content Profiler
Type	laboratory	in situ	in situ
Vertical spacing of point measurements	depth oriented	discontinuous	continuous
Effort	high	medium (low for repetitive measurements)	medium
Spatial Resolution	sample size dependent	decimeter scale	centimeter scale
Causes for possible measurement bias	sample disturbance removal from natural stress field	high clay content hydrocarbons water within access tube	loss of electrode contact hydrocarbons

3 Comparison of in situ water-content profiles obtained using frequency-domain and neutron-probe technology

	Gravimetric method	Neutron Probe	Water Content Profiler
Restrictions	intact samples required	subjected to regulatory requirements	complex underlying dielectric theory deployment only with DP equipment
Application	Soil investigation, if additional information such as grain size distribution is needed	Soil moisture monitoring	Soil moisture mapping

3.2 Applied methods

3.2.1 CPT deployed Water Content Profiler (WCP)

Using dielectric properties of soil to determine soil water content is based on the findings of Topp et al. (1980) who introduced an empirical relationship between the dielectric constant (ϵ') and soil water content. Since then, major advancements have been made in sensor developments including the first sensors which implemented the Time Domain Reflectometry (TDR) principle. TDR investigations determine the propagation velocity of an electromagnetic wave in a transmission line of a known length (Topp et al. 1980). However, TDR can only be used for short cable distances, and high conductivity soils can attenuate the TDR signal (Shinn et al. 1998).

These limitations were overcome with the development of Frequency Domain (FD) sensors. Hilhorst (1998) describes that the FD technology is characterized by the application of a single sine wave where capacitance and conductance can be calculated from the impedance measured between the electrodes. Capacitance (C) and complex relative permittivity (ϵ) are coupled by

$$C = \epsilon \epsilon_0 \kappa \quad (\text{Eq. 3-1})$$

where ϵ_0 is the permittivity of free space and κ is a geometry factor which is determined by the distances of the electrodes and their surface areas (Hilhorst 1998).

Furthermore, ε can be split by

$$\varepsilon = \varepsilon' - j\varepsilon'' \quad (\text{Eq. 3-2})$$

into a real part ε' (also referred as dielectric constant in a static electrical field) which is a measure of the total polarisability of a material and an imaginary part ε'' which represents the total energy absorption or energy loss (Hilhorst 1998); and j is the standard imaginary unit with

$$j^2 = -1 \quad (\text{Eq. 3-3})$$

Due to the dipole structure of the water molecule, water has a high dielectric constant of approximately 80 (Briscoe 1935, Langmuir 1997, Millero 2001) whereas the dielectric constant of dry soil ranges between 3-6 (Shinn et al. 1998). Only limited information is available on the intrinsic area of influence (section 1.1) for FD dielectric constant measurements. Starr & Paltineanu (2002) give area of influence for axial and radial components for capacitance probes on a centimeter to decimeter scale respectively, depending on the sensor geometry.

Topp et al. (1998) formulated the relationship between dielectric constant and volumetric water content (θ_v) in the following empirical formula:

$$\theta_v = -5.3 \times 10^{-2} + 2.92 \times 10^{-2} \varepsilon' - 5.5 \times 10^{-4} \varepsilon'^2 + 4.3 \times 10^{-6} \varepsilon'^3 \quad (\text{Eq. 3-4}).$$

However, as the soil represents a multiphase system of soil gas, pore fluid and soil matrix, the measured dielectric properties are influenced by a number of factors. Hilhorst (1998) introduces a new dielectric mixture equation to account for these influences and couple dielectric properties as measured on macroscopic scale and the impact of microstructural and compositional soil properties. The employed probe is based on a newly described FD sensor technology after Hilhorst (1998), however, the technical details of the probe design and working principles are proprietary details of the manufacturer and are not available.

This further stresses the need for independent evaluation by comparison to other in situ methods.

The WCP that measures electrical conductivity and relative permittivity can be deployed alone or in combination with a standard 15 cm² cone penetrometer. In the latter setup, the cone penetrometer is pushed into the ground at a constant rate of 2 cm/s while the standard CPT- based parameters are measured: the cone

resistance (q_c), the sleeve friction (f_s), and the dynamic pore water pressure (u_2). Detailed information on CPT parameters is given in section (5.2.3).

A primary indicator of sediment type is the friction ratio (R_f) as defined in Eq. 5-1. The probe used in this research, Fig 1a, records WCP and CPT parameters every centimeter during a profile. The WCP is mounted above the CPT probe where the dielectric constant and electrical conductivity are measured using four equally spaced ring shaped electrodes. The WCP includes the advantages of Direct push (DP) profiling, e.g. cost and time efficiency (EPA 1997b). However, limitations of the WCP include the complex underlying dielectric theory and the multiple factors influencing ϵ as well as practical problems that can arise through insufficient coupling of the probe to the soil.

3.2.2 Neutron probe

Neutron probe measurements are a standard technique for the determination of soil water content (Lal & Shukla 2004, Topp & Ferré 2002, Benson 2005). Hignett and Evett (2002) give a comprehensive overview of the neutron probe (NP) principles, equipment and measurement procedures. The working principle of NP measurements is based on a radioactive source that emits fast neutrons and a detector that records slow (thermalized) neutrons. When emitted in the subsurface, fast neutrons are slowed to thermal energy levels by collisions with hydrogen nuclei. Changes in hydrogen content are assumed to be primarily driven by changes in volumetric water content. Therefore, the concentration of thermal neutrons can be related to the volumetric water content (see Hignett & Evett 2002).

However, soil density and chemical composition of the subsurface (e.g. presence of hydrocarbons) can affect the neutron measurements. In heterogeneous media with changing sediment textures, the probe may require a separate calibration for each sediment type. Using a common regression line between volumetric water content and neutron count ratio can introduce considerable error to the data interpretation under these conditions, especially in the presence of clay (see Hignett & Evett 2002). Thus, at sites that have a broad range of sediments, previous knowledge of the sediment distribution is essential for data interpretation. Vertical profiling with the neutron probe uses previously installed

access tubes that must be completely dry. Fig. 3-1 gives a schematic view of the neutron probe design and measurements setup. The intrinsic volume of influence, i.e. the volume over which the probe measures an average of the volumetric water content, can be estimated from Cameron (1970) as a sphere with the radius of:

$$R_v = 15(\theta_v)^{-1/3} \quad (3-5)$$

where R is the radius of the intrinsic volume of influence in cm and θ_v is the volumetric water content in $\text{m}^3 \text{m}^{-3}$.

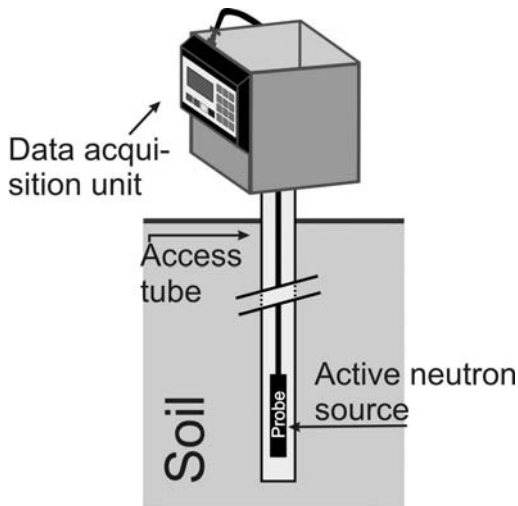


Figure 3-1: Schematic view of the neutron probe field setup.

3.3 Application of methods at the Larned Research Test Site (LRS)

3.3.1 Larned test site field work

The field work was conducted during two campaigns in October/November 2008 and October 2009 at the Kansas Geological Survey Larned Research Site (LRS) in west-central Kansas, USA (Figure 1-3). Information on the test site and a figure showing the location of the test site as well as logging positions is given in section 1.2.2. During these campaigns, 3 WCP and 3 NP logs were taken in October/November 2008 and 4 WCP and 2 NP logs were taken in October 2009. WCP profiles were recorded in close vicinity to neutron probe measurements that were performed in two permanently installed access tubes (see Figure 1-3 for position of access tubes and WCP logs). These access tubes (maximum depth of 5.9 m below land surface) are constructed of standard 1.5 inch pipe with 40 mm

inner diameter that was emplaced in a manner to maximize formation contact. A Campbell Pacific Nuclear Model 503 DR Hydroprobe Moisture Depth Gauge was used to take neutron-probe readings to a depth of 5.5 m in 0.152 m (0.5 ft.) intervals.

The volumetric water content (m^3m^{-3}) for the neutron probe profiles is calculated with an equation based on laboratory calibrations by the manufacturer and an adjustment for the PVC pipe (Butler et al. 2005). Although the equation is not based on calibrations using LRS sediments, it should provide reasonable estimates in sands and gravels. WCP values were recorded in 1 cm intervals to a depth of at least 6m. Tests were performed in the vadose and phreatic zone.

3.3.2 Results at Larned test site

Figure 3-2 presents an overview of the CPT friction ratio and calculated water contents for the WCP and NP. The friction ratio (R_f) can be used as a simple parameter to infer sediment lithology. Generally low R_f values indicate sand and gravel dominated deposits at the LRS. The CPT profiles show comparable results for the upper 6 m with only minor variations in the first meter and between 5-6 m depth with a high degree of lateral homogeneity between the profile locations. The increases in EC and R_f values at 0-1m and 5-6m indicate an increasing fine grain content at these depths. Also, an isolated EC and R_f peak, most likely indicating an isolated clay lens, can be seen in one of the 2009 profiles at the NW access tube location at about 2.35 m depth. This isolated peak is also observed in the corresponding WCP results.

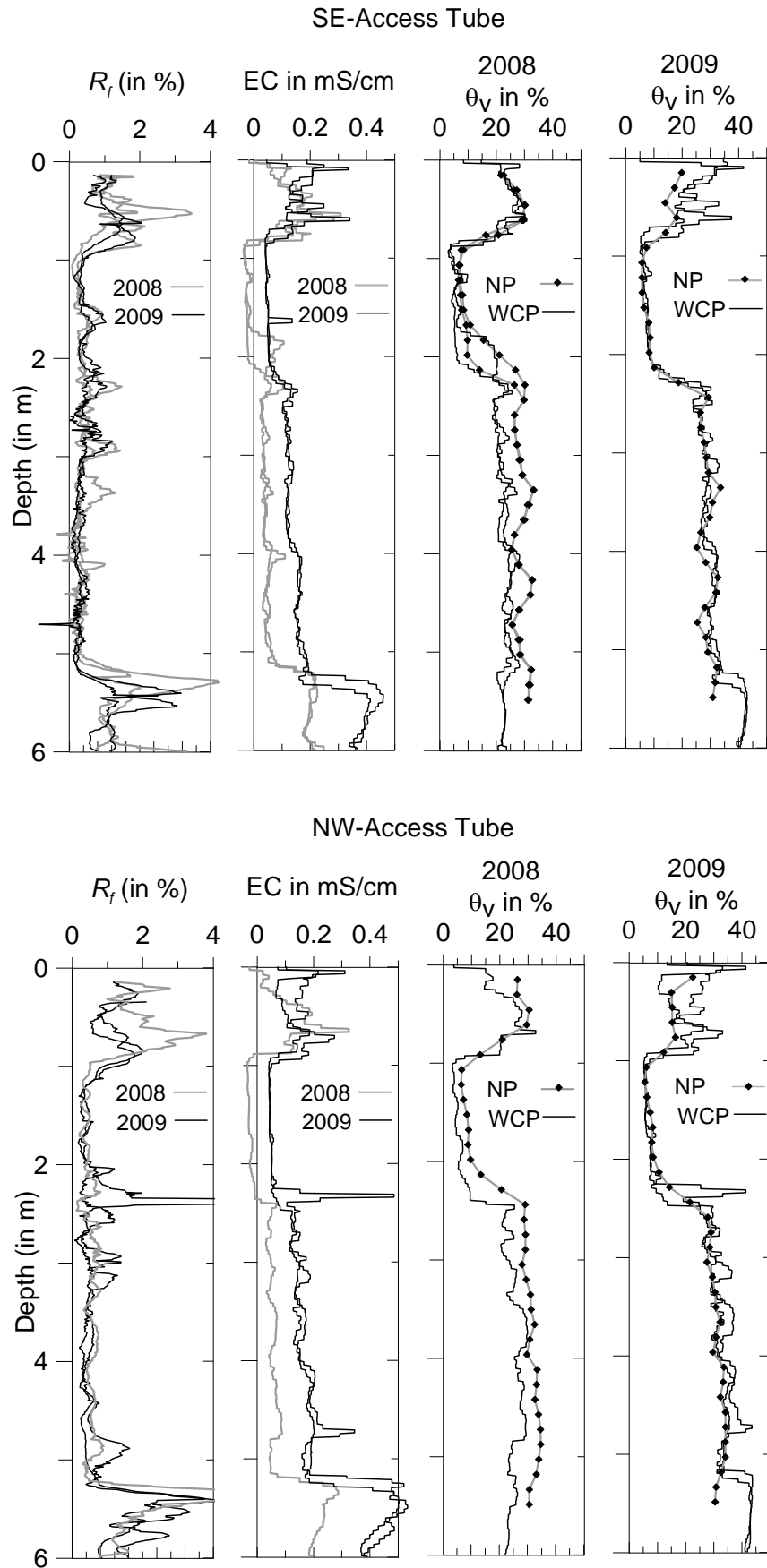


Figure 3-2: Overview of profiling results at the Larned test site. R_f is the friction ratio determined by the use of the cone penetrometer and θ_v is the volumetric water content in percent.

The WCP volumetric water content estimates were compared to the neutron probe measurements from the nearby access tubes. There was an offset between the WCP and neutron profiles in 2008, but the profiles from the two approaches were in good agreement in 2009 (Figure 3-2). The offset in the 2008 profiles that is also clearly visible in the EC data, was found to be a result of an incorrect calibration relationship for the WCP. The probe was recalibrated by the manufacturer prior to the 2009 profiles; the differences in WCP performance, relative to the neutron probe profiles, between the two years demonstrate the importance of probe calibration.

Due to this offset, the 2008 WCP measurements were only used for a qualitative comparison. For this comparison, the 2008 WCP data were normalized using the arithmetic mean of the 2008 WCP data of the unsaturated zone between 1.2 to 2 m depth for the November 2008 measurements and 1.2 - 1.7 m depth for the October 2008 measurement as the minimum value and the arithmetic mean of the saturated zone between 3.0 to 5.0 m depth as the maximum value (1.0). This way, a qualitative comparison between the individual 2008 WCP measurements and the neutron probe results is possible.

The qualitative comparison between neutron probe and WCP data for 2008 shows good agreement for most depths (Figure 3-3). Also, normalized WCP results indicate a change in groundwater level of about 0.35 m at the SE access tube between the October 2008 and November 2008 measurement that was also observed in the groundwater monitoring well in close vicinity of the access tube. The October 2008 data that were collected only at the SE access tube were taken a few days after a strong precipitation event.

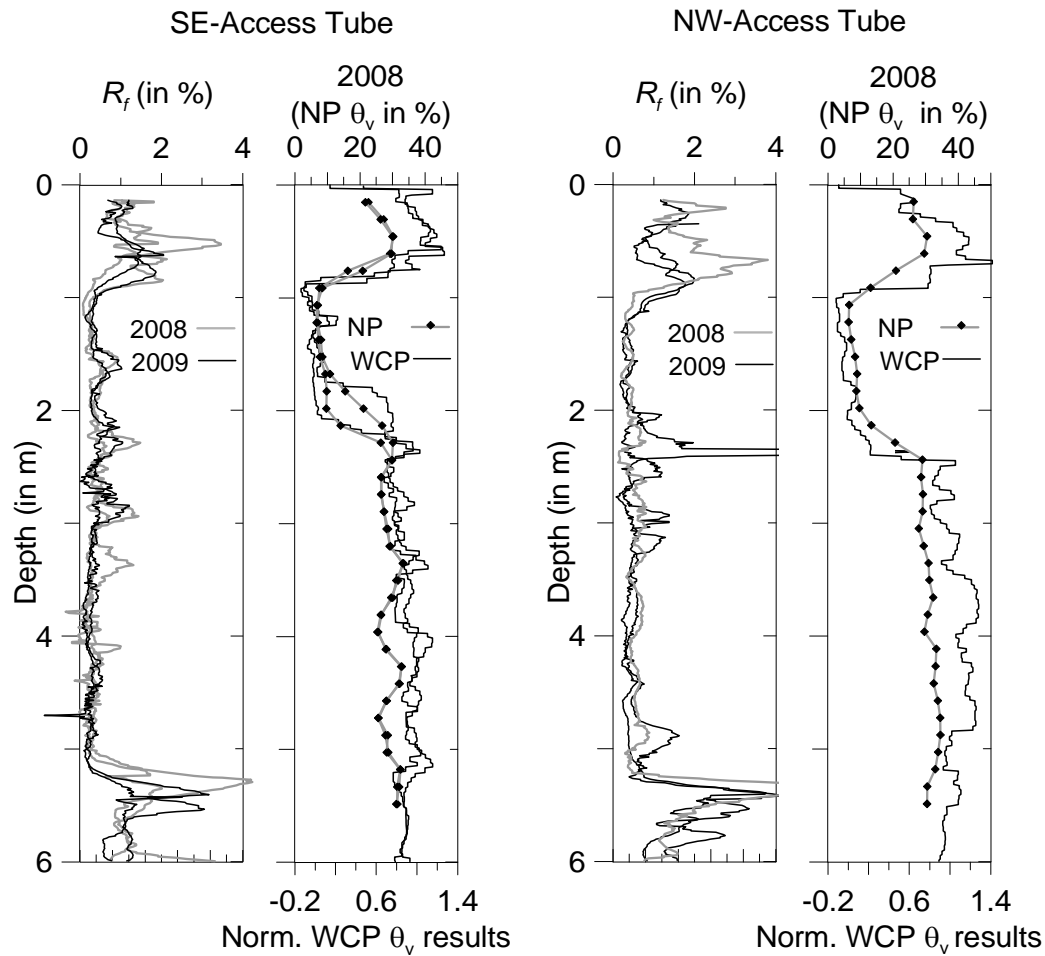


Figure 3-3: Overview of profiling results at the Larned test site with normalized WCP results. R_f is the friction ratio determined by the use of the cone penetrometer.

Good agreement between the actual WCP measurements and the neutron probe measurements was found in 2009 for most depths. Natural soil moisture variation is reflected by differences in the WCP measured water content of the uppermost part of the vadose zone for the 2009 measurements. Figure 3-4 shows a comparison of NP and averaged WCP readings of the 2009 campaign from LRS in a common scatter plot. The area of influence for neutron probe measurements was calculated using Eq. 3-5 after Cameron (1970) and WCP values were averaged over the corresponding intervals using the geometric mean. The available data covers a wide range of water content and the scatter plot confirms the results of the qualitative comparison (Figure 3-3).

LRS water content data exhibit a high consistency between neutron probe and WCP results with the majority of data pairs showing less than 5 percent difference between applied methods. The correlation of neutron probe and WCP data is

characterized by a correlation coefficient of 0.94. However, those values that are outside the 5 percent deviations show almost all higher ϕ_v values measured with the WCP than with the NP. This effect might be related to differences in the intrinsic area of influence that enables the WCP to resolve layers of limited thickness that might be present within the upper (0-1m depth) and lower (5-6m depth) of the profiles better than the NP.

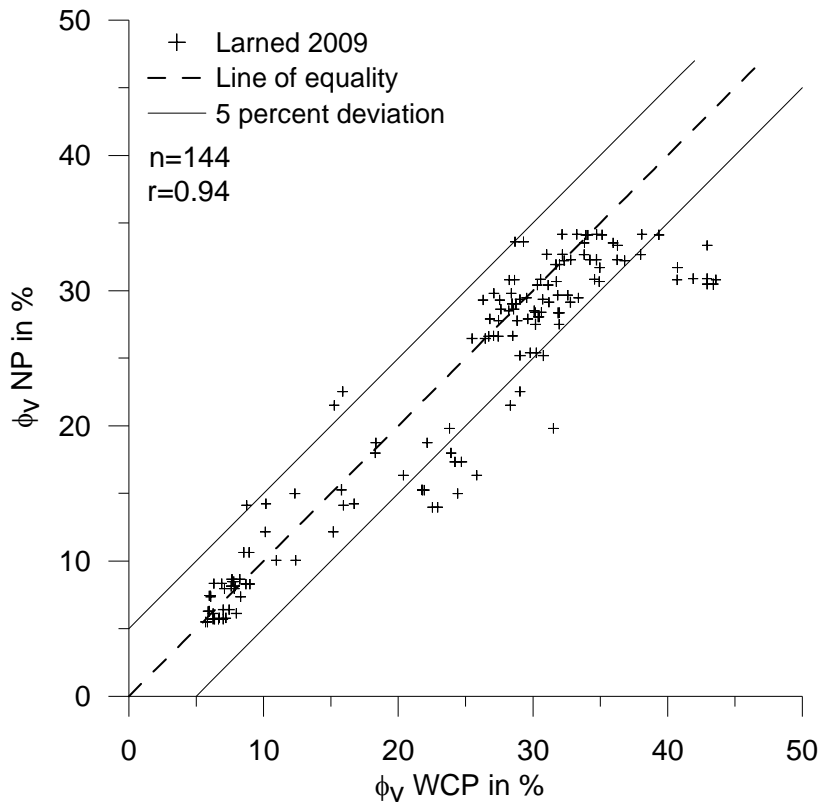


Figure 3-4: Comparison of NP and averaged WCP readings using Eq. 3-5 after Cameron (1970) of the 2009 campaign from LRS in a common scatter plot.

3.4 Application of methods at the Bitterfeld test site

3.4.1 Bitterfeld test site field work

Additional field work that comprised two NP and two WCP profiles was conducted at the UFZ test site in Bitterfeld, Germany in 2009. Tests were performed below the backfill material (depth > 3m) only in the saturated part of the aquifer. At the Bitterfeld test site, 28 mm outer diameter steel access tubes were installed to a depth of 12 m shortly before the NP measurements. Discontinuous measurements were performed in 0.2 m intervals. After the NP

measurements had been finished the access tubes were removed and WCP profiling was subsequently done at the same positions. Due to the larger diameter of the WCP probe in respect to the NP access tubes the exact same location for the WCP profiling could be chosen. See Fig. 1-2 for location of the test site as well as position and measurement dates of the individual profiles.

3.4.2 Results at Bitterfeld test site

WCP measurements were performed at the same position of NP logs after the access tubes had been removed. Influences of soil disturbance on the CPT-data were presumed and therefore R_f data from nearby locations were chosen for Fig. 3-5 which gives an overview of the CPT R_f and measured ϕ_v using the WCP and NP. R_f and EC data indicate two fine grained dominated layers between 4-5m and 8-8.5m depth, respectively. The overall qualitative correlation between water content after WCP and NP data is less consistent. Results of calculated water content appear contrarily in the fine grain dominated layers. The WCP data reveals a high degree of variability in the water content up to a depth of approximately 8.5 m. Only below this depth, a better consistency between WCP and NP data is reached. This depth interval of better consistency between WCP and NP data also corresponds to an interval of low EC values of approximately 0.2 mS/cm.

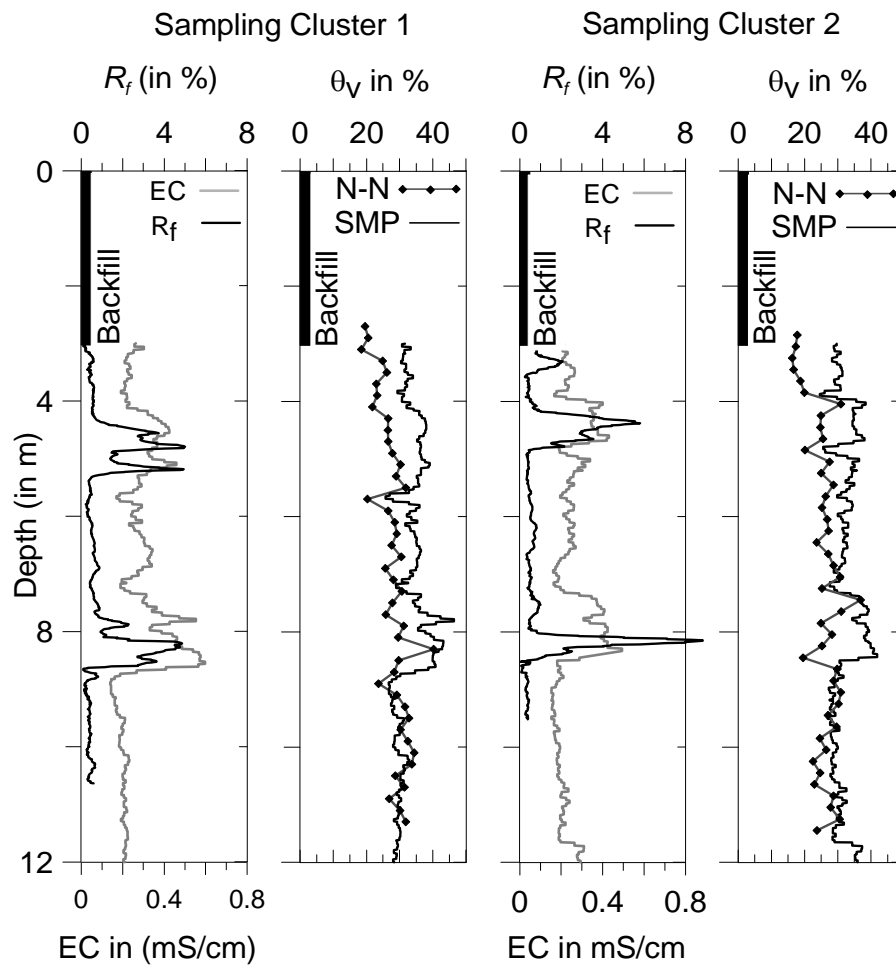


Figure 3-5: Overview of profiling results at the Larned test site. R_f is the friction ratio determined by the use of the cone penetrometer and ϕ_v is the volumetric water content in percent.

The Bitterfeld test site offers geological conditions (see Table 1-1), that appear to be beyond resolution and application ranges of NP measurements. Especially the abrupt and small scale changes in lithology, and increased amounts of clay affect NP measurements. Different NP calibrations had to be used for data interpretation, especially for areas of high clay content. These areas were identified with CPT data as areas of higher R_f . Without this additional information about sediment distribution at the test site, NP results would have been misinterpreted. Differences in determined water content of NP measurements in dependency of the applied calibration are shown in Appendix C. However, it cannot be precluded that also WCP results, especially in the upper part of the profile to a depth of 8.5m depth, are biased. Here, influences of increased electrical conductivity of the soil on the measured data must be considered. Results of WCP and NP measurements from the Bitterfeld test site are shown in

Fig. 3-6 in a common scatter plot. A low correlation with a correlation coefficient of 0.25 between WCP and NP results is observed. In most of the cases, larger θ_v are measured with the WCP than with the NP. As stated before, this effect might relate to resolution differences. The correlation between the applied methods is with a correlation coefficient of 0.25 low.

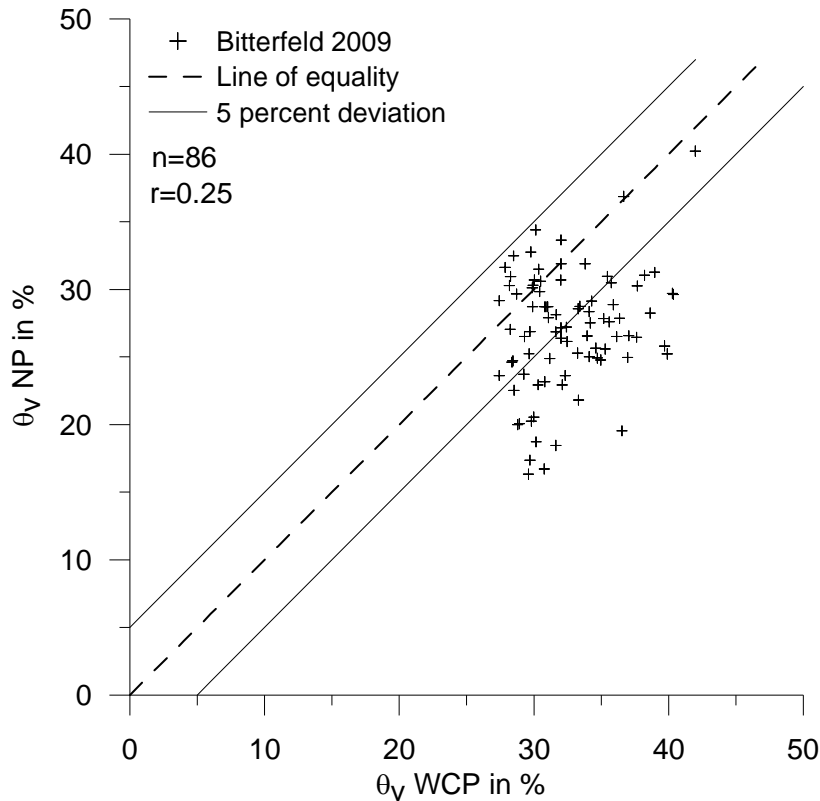


Figure 3-6: Comparison of NP and averaged WCP readings using Eq. 3-5 after Cameron (1970) at the Bitterfeld test site in a common scatter plot.

3.5 Conclusion

Good agreement between the actual WCP measurements and the neutron-probe measurements was found at Larned for the 2009 field data for most depths with a resulting correlation coefficient of 0.94 between methods. Nevertheless an apparent offset in the 2008 WCP profiles that is also clearly visible in the EC data, was found to be a result of an incorrect calibration relationship for the WCP. This indicates the importance of correct calibrations to obtain reliable FD measurements. At the Bitterfeld site that is characterized by heterogeneous fluvial mixed deposits only a limited correlation between the two methods was

observed with a respective correlation coefficient of 0.25 between the tested methods.

Abrupt and small scale changes in lithology and increased amounts of clay affected NP measurements. Different NP calibrations had to be used for data interpretation for areas of high clay content that identified with CPT data. The use of a one common calibration for NP data would have lead to a misinterpretation of results. Strongest differences between WCP and NP measurements were observed at the Bitterfeld test site in areas of increased electrical conductivity. Due to these differences the accuracy of measured water content of the WCP in a complex geological deposit as encountered at the Bitterfeld test site could not be proven.

For sand dominated fairly homogeneous deposits the tested DP deployed WCP at its current state is a reliable alternative to conventional neutron probe water content measurements if vertical profiles of soil water content at multiple locations are needed, e.g. for soil moisture mapping in coarse grained sediments. The WCP reaches higher resolution, while transport, handling, and deployment of the probe equipment do not require special regulatory approval as opposed to NP measurement equipment. For repeat measurements at the same location in the framework of soil moisture monitoring, the NP technology remains the better alternative if access tubes remain in place as deployment of the WCP probe requires use of pushing equipment. Limits of both, the NP and WCP technology were reached in this comparison, clearly stating the need for the conducted rigorous field testing in addition to commonly conducted laboratory tests.

4 Evaluation of approaches to estimate porosity of clastic sediments

4.1 Introduction

In chapter 2 the strong effects were demonstrated that arise from deviations in estimated porosity values on calculated K after Terzaghi (1925 a,b) and Kozeny-Köhler (1965). As stated in chapter 2, reliable ex situ measurements are often hindered by sample disturbance and removal of the sample from its natural stress field. However, in situ measurements of porosity are often not viable due to financial or technical restrictions. Results of chapter 3 have shown that neither neutron probe nor the WCP at its current state are suitable for the high resolution in situ measurements of porosity in heterogeneous sedimentary deposits as encountered at the Bitterfeld site.

Various empirical and theoretical based approaches exist to predict porosity for unconsolidated sedimentary deposits as alternative to porosity measurements (Chouker 1970, Vukovic & Soro 1992, Langguth 1980, Schön 1996, Hölting & Coldewey 2005, Todd & Mays 2005, Szymczak et al 2009, Ryjov & Sudoplatov 1990, Koltermann & Gorelick 1995). Especially a broad range of empirical porosity estimates exist. The empirical nature of the relations implies that different porosity estimates for one sample may be derived depending on the chosen approach.

In this chapter, different empirical approaches for estimating porosity will be evaluated concerning effects of deviating porosity estimates of calculated K after Terzaghi (1925a, b) and Kozeny-Köhler (1965). A brief overview of different types of porosity in unconsolidated sedimentary deposits is given, followed by a brief description of selected empirical approaches to estimate porosity of clastic sediments.

In a later step, porosity values based on different approaches were determined for the slug test intervals as described in chapter 2. Subsequently, $K_{Terzaghi}$ and $K_{Kozeny-}$

Köhler values were calculated based on the different porosity estimates and compared to measured K_{DPS} values. A comparison of results is then used to identify which of the applied porosity estimates is best to predict porosity against the background of calculated K based on grain size distribution.

4.2 Classification of porosity

For materials consisting of equally sized and perfectly formed spheres, porosity is independent of the radius of the spheres (Bear 1972). In a simple model of equally sized spheres, porosity is governed by particle packing; resulting porosities can be calculated ranging from 0.2596 for rhombohedral packing to 0.4764 for cubical packing (Dandekar 2006). In natural soils that consist of grain size mixtures with differently shaped grains, porosity is determined by various factors, such as the shape of the grains, grain size composition, mineralogical content, degree of compactness and cementation (Bear 1972, Vukovic & Soro 1992). Schön (1996) presents different classifications for porosity types based on the petrographic fabric of the rock, formation and alteration of the rock, and interconnection of pores. The latter porosity classification after Serra (1984) is best applicable to unconsolidated sedimentary deposits as presented in this work. After Serra (1984), four types of porosity exist:

A) Total porosity (ϕ) is defined as the volume of pore spaces (V_p) within a given bulk volume (V):

$$\phi = \frac{V_p}{V} \quad (4-1)$$

(see Bear 1972, Schön 1996, Todd & Mays 2005). Total porosity consists of primary and secondary porosity. The primary porosity is the native porosity of the material that is developed in the deposition of the material; the secondary porosity is developed post depositional by some geological process (Dandekar 2006), e.g. through leaching of minerals (Weight 2008).

B) Interconnected porosity describes porosity formed only by connected spaces. Pores are considered to be connected when electrical current and fluids can flow between (see Schön 1996).

C) The potential porosity is that part of the interconnected porosity in which the diameter of the connecting channels is large enough to permit fluid to flow (Schön 1996). The maximum thickness of a layer of electrostatic bound retained water is $4\ \mu\text{m}$ (Höltling & Coldewey 2005). Therefore, the minimum pore size that allows water movements must be at least twice the size of the thickness of the retained water layer.

D) Effective porosity is the porosity that is available for free fluids; it excludes all non-connected porosity including the space occupied by the clay-bound water (Schön 1996).

Calculated K after Terzaghi (1925 a, b) and Kozeny-Köhler (1965) require input of total porosity. In hydrogeological practice, total porosity is used, however, often without a critical evaluation of the suitability of this parameter. Only those pores that actually allow transport of water contribute to the hydraulic conductivity. Against this background, effective porosity is favorable to calculate hydraulic conductivity. Especially clay rich materials are associated with a high total porosity while the effective porosity is significantly smaller. The relation between total porosity and effective porosity is presented in Figure 4-1 modified after Davis & de Wiest (1966):

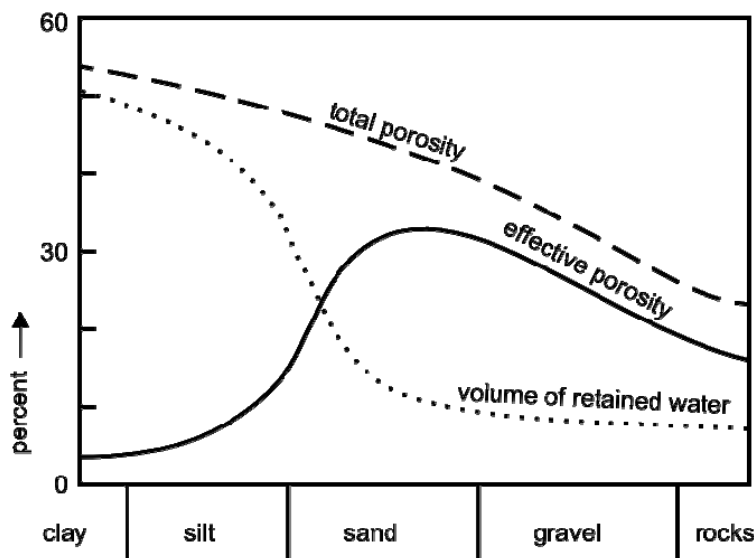


Figure 4-1: Total porosity, effective porosity, and volume of retained water in dependence of sediment type, modified after Davis & de Wiest (1966).

4.3 Approaches to estimate porosity

4.3.1 Theoretical models predicting total porosity in sedimentary mixtures

The following equation, after Ryjov & Sudoplatov (1990) as cited in Shevnin et al. (2006), is an example for theoretical derivation of porosity:

$$\phi = (\phi_s - cl) + \phi_c \times cl \quad (4-2)$$

where cl is the clay content, ϕ_c is the clay porosity, and ϕ_s is the sand porosity. Equation 4-2 is valid for $cl < \phi_s$; for $cl \geq \phi_s$ the following equation applies:

$$\phi = cl \times \phi_c \quad (4-3)$$

This theoretical model that has been refined by Koltermann & Gorelick (1995) and Kamann et al. (2007) considers particle packing and the role of interporous fines. This model is based upon the assumption that if the fine grain content of a sediment mixture is smaller than the porosity of the coarse grained fraction, the fine grained material will fill the pores between the coarse grained particles. With increasing fine grain content, the pores between the coarse grained components are subsequently filled. In this case, porosity is dominated by the coarse grained material. If the fine grain content exceeds the porosity of the coarse grained components, the coarse grained material is embedded in the fine grained material. In this case, porosity is dominated by the fine grained material. A minimum porosity values is reached, when the fine grain content equals the porosity of the coarse grained fractions and all interporous spaces of the coarse grained material are completely filled with fine grain material.

Discussions of this model by Koltermann & Gorelick (1995) have shown that in this case, not all pores are filled and the minimum porosity value is not as low as predicted by the original models. The disadvantage of these models is that they requires knowledge of the clay and sand porosity. This information is often not available and empirical porosity values have to be used, introducing an additional degree of uncertainty. Also, it is questionable how these models can represent the complex multicomponent sedimentary mixtures as found at the Bitterfeld test site that cover a large part of the grain size spectrum. Therefore, this theoretical approach was not further pursued in the evaluation.

4.3.2 Empirical approaches to estimate porosity of sediments

Empirical porosity estimates of sediments rely mainly upon correlations of soil specific properties (such as effective grain size or coefficient of uniformity) with porosity data or direct correlation of sediment types with porosity data. All empirical approaches bear certain disadvantages. Often, it is uncertain how reliable porosity measurements of the underlying empirical data are and how well the empirical literature data is generally applicable to represents soils of different composition, stress history or diagenetic alteration. Hence, a broad variety of approaches exists to estimate porosity of sedimentary deposits. Five different approaches will be evaluated in the following.

Literature porosity values based on sediment types are taken from Langguth (1980), Chouker (1970), and Hölting & Coldewey (2005). Langguth (1970) cites sieve data and specific hydraulic properties of fluvial basin sediments of the Friant-Kern Canal Service area in southern California after Johnson (1967). Estimates of total porosity in dependence of sediment classification rely on approximately 500 core samples of typical terrigen sediments that were deposited under semiarid to arid conditions (Langguth 1980). Sediment composition included a broad grain size spectrum ranging from clay to coarse sand. Langguth (1980) assigns a general validity to these values due to the clear lithological characterization of the sediments. Chouker (1970) presents a plot of intrinsic permeability versus total porosity for different rocks and sediment types in his work. Further information on the data is not given. Figure 4-2 was drawn after Chouker (1970) and used to determine total porosity values for sediments as listed in Table 4-1

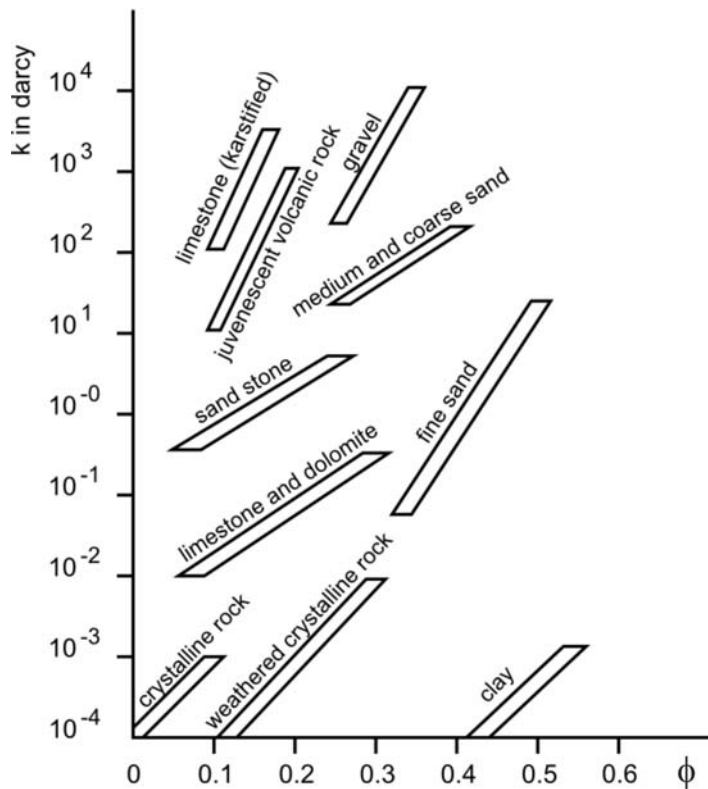


Figure 4-2: Intrinsic permeability (k) versus total porosity (ϕ) for different rocks and sediment types after Chouker (1970).

Hölting & Coldewey (2005) cite values for effective porosity. However, no further information on the underlying data is given. A practical problem that arises from assigning porosity values based on sediment classification is the limited reproducibility, especially when dealing with sedimentary mixtures.

Based upon the work of Istomina (1957), Vukovic & Soro (1992) present a scatter plot of porosity versus coefficient of uniformity (U). From this data set Vukovic & Soro (1992) derive the following relationship between porosity and U :

$$\phi = 0.255(1 + 0.83^U) \quad (4-4)$$

Although Vukovic & Soro (1992) point out that the application of this relation is confined to clay free deposits, the relationship was tested on the presented data. Details of the underlying data set are not available, as the original work of Istomina (1957) is published in Russian and Vukovic & Soro (1992) do not provide further information on the origin or composition of the data. Szymczak et al. (2009) relate porosity to the effective grain size diameter. Again, no further reference or information on the underlying data is given. Although the validity of the given empirical porosity after Szymczak et al. (2009) and Vukovic & Soro (1992) on the

presented data has yet to be tested, the correlation of porosity with a measurable soil specific property increases reproducibility of the approach in comparison to the approaches after Langguth (1980), Chouker (1970), and Hölting & Coldewey (2005). Table 4-1 gives an overview of porosity estimates in respect to various sediment types after Szymczak et al. (2009), Chouker (1970), and Hölting & Coldewey (2005).

Table 4-1: List of sediment types with respective grain size diameter after DIN EN ISO 14688-1 and corresponding empirical porosity values after Szymczak et al. (2009), Chouker (1970), and Hölting & Coldewey (2005).

sediment	d_e in mm after DIN EN ISO 14688-1	total porosity after (Szymczak et al. 2009)	total porosity after Chouker (1970)	effective porosity after Hölting & Coldewey (2005)
clay	<0.002		0.4-0.54	<0.05
Fine silt	0.002-0.0063	0.45-0.65		
silt	0.0063-0.02	0.40-0.55		
coarse silt	0.02-0.063	0.35-0.45		
fine sand	0.063-0.2	0.33-0.40	0.32-0.5	0.10-0.20
medium sand	0.2-0.63	0.30-0.38		0.12-0.25
coarse sand	0.63-2	0.28-0.35		0.15-0.30
medium to coarse sand	0.2-2		0.24-0.42	
gravelly sand	0.2-63			0.16-0.28
fine gravel	2-6.3	0.25-0.35	0.24-0.36	0.15-0.25
medium gravel	6.3-20	0.25-0.35	0.24-0.36	0.14-0.24

4.3.3 Evaluation of porosity estimates with DPST data

In the following the applicability of the different described empirical porosity estimates on the available slug test data is evaluated (see section 2.4 and 5.2.1 for further information on the slug test intervals and results). The described approaches were applied to determine porosity values for calculated grain size distribution data of the slug test intervals. Based on the respective porosity estimates, K after Terzaghi (1925 a, b) and Kozeny-Köhler (1965) was calculated and compared to results of the 19 slug tests. Calculation of K and treatment of outliers is done analog to the procedures described in section 2.4.

In addition, K after Terzaghi (1925 a, b) and Kozeny-Köhler (1965) was calculated for a fixed porosity value of 0.4 to determine the effect of the porosity term on K estimates and resulting correlation with DPST data. Results are shown in Fig. 4-3, basics statistics of the comparison are given in Table 4-2. Calculated $K_{Terzaghi}$ values show that correlation coefficients between $K_{Terzaghi}$ and K_{DPST} range between 0.78 for effective porosity values after Hölting & Coldewey (2005) and 0.83 for porosity estimates after Chouker (1970). However, the correlation coefficient for $K_{Terzaghi}$ based on the fixed porosity values is with 0.82 as high as K based on porosity values after Langguth (1980) and even higher than calculated K based on porosity estimates after Szymczak et al. (2009), Vukovic & Soro (1992), and Hölting & Coldewey (2005). However, $K_{Terzaghi}$ based on porosity values after Hölting & Coldewey (2005) show the best agreement between the simple line of regression and the line of equality.

When different porosity estimates are applied, strong differences in calculated K especially regarding the minimum values are observed for $K_{Terzaghi}$ (see Table 4-2). Correlation between $K_{Kozeny-Köhler}$ and K_{DPST} are strongly affected by the application of different porosity estimates with a correlation coefficient ranging from 0.67 for porosity values after Szymczak et al. (2009) to 0.78 for porosity estimates after Langguth (1980). Also, K estimates based on the fixed porosity values reach a correlation coefficient as high as 0.76. Despite a large offset between $K_{Kozeny-Köhler}$ based on porosity values after Hölting & Coldewey (2005) and K_{DPST} values, these values show best agreement between the line of equality and regression line of the tested porosity approaches in respect to $K_{Kozeny-Köhler}$ data.

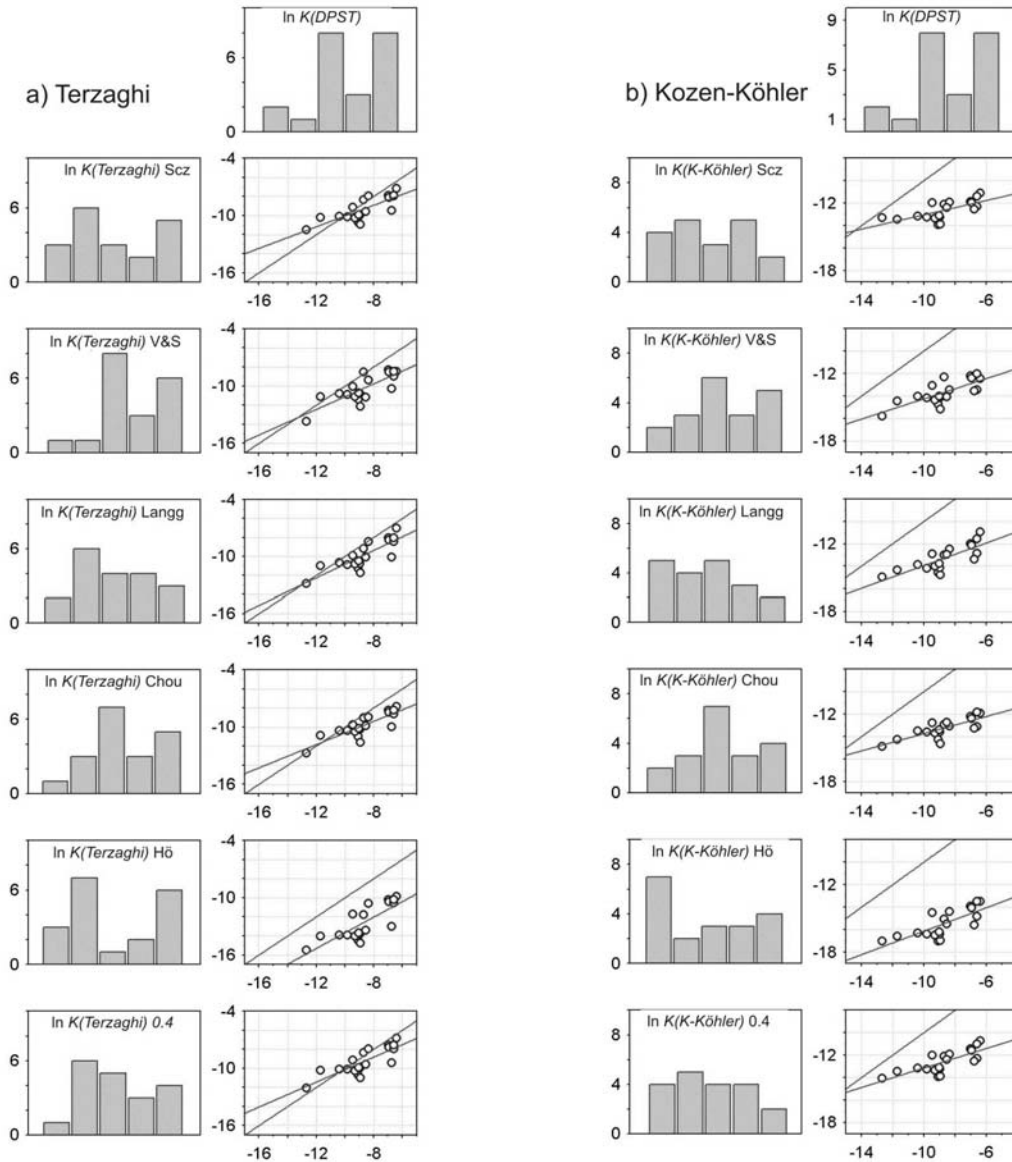


Figure 4-3: Matrix plot of calculated $K_{Terzaghi}$ (a) and $K_{Kozeny-Köhler}$ (b) based on porosity estimates after Szymczak et al. (2009) (Scz), Vukovic & Soro (1992) (V&S), Langguth (1980) (Langg), Chouker (1970) (Chou), Hölting & Coldewey (2005) (Hö), and a fixed porosity values of 0.4 with DPST data. Histogram y-axis labeling is frequency, scatter plot x- and y-axis labeling is $\ln(K)$.

Table 4-2: Basic statistics of $K_{Terzaghi}$ and $K_{Kozeny-Köhler}$ based on porosity estimates after Szymczak et al. (2009) (Scz), Vukovic & Soro (1992) (V&S), Langguth (1980) (Langg), Chouker (1970) (Chou), Hölting & Coldewey (2005) (Hö), and a fixed porosity values of 0.4 with DPST data. Linear regression is given as slope ($y*x$) in the upper value and intercept as lower value. Correlation coefficients are determined based on $\ln(K)$ values.

ϕ after	$K_{Terzaghi}$					
	(Scz)	(V&S)	(Langg)	(Chou)	(Hö)	($\phi=0.4$)
n	19	19	19	19	19	19
geometric mean	8.99E-05	3.59E-05	5.12E-05	5.35E-05	3.34E-06	9.35E-05
Min	1.02E-05	1.16E-06	2.61E-06	2.92E-06	1.94E-07	5.73E-06
Max	7.94E-04	2.54E-04	9.12E-04	3.89E-04	5.18E-05	1.09E-03
σ_2	3.95E-08	7.65E-09	4.51E-08	1.14E-08	2.62E-10	7.19E-08
$r \ln(K)$	0.79	0.79	0.82	0.83	0.78	0.82
linear regression	0,565*x -4,4006	0,6702*x -4,4026	0,7203*x -3,6108	0,6091*x -4,5355	0,8193*x -5,4798	0,6552*x -3,5766
	$K_{Kozeny-Köhler}$					
	(Scz)	(V&S)	(Langg)	(Chou)	(Hö)	($\phi=0.4$)
n	19	19	19	19	19	19
geometric mean	3.28E-06	1.16E-06	1.67E-06	1.77E-06	1.93E-07	3.42E-06
Min	9.31E-07	1.44E-07	3.16E-07	3.57E-07	4.12E-08	7.92E-07
Max	1.49E-05	6.10E-06	1.77E-05	7.47E-06	1.42E-06	2.20E-05
σ_2	1.34E-11	3.27E-12	1.72E-11	4.02E-12	1.88E-13	3.14E-11
$r \ln(K)$	0.67	0.74	0.78	0.77	0.74	0.76
linear regression	0,3186*x -9,8564	0,4494*x -9,7558	0,5061*x -8,8962	0,3821*x -9,9219	0,5215*x -10,9214	0,4337*x -8,8112

4.4 Conclusion

Different approaches to determine porosity of clastic sediments exist. Often, underlying data of the empirical relations between sediment type and porosity or soil specific properties and cited porosity values are not available. Due to the empirical nature of the relations, differences in estimated porosity between approaches for the same sample can arise. Especially against this background, five different approaches for estimating porosity were evaluated concerning the effects of deviating porosity estimates on calculated K after Terzaghi (1925 a,b) and Kozeny-Köhler (1965). For the presented data, the observed effects of differences

in porosity estimates on $K_{Terzaghi}$ were large concerning the absolute values with calculated Min and Max K values ranging between $1.02 \cdot 10^{-5}$ to $1.94 \cdot 10^{-7}$ and $1.09 \cdot 10^{-3}$ to $5.18 \cdot 10^{-5}$ respectively. Effects on the correlation with DPST data were small with correlation coefficients ranging between 0.78 and 0.83 for the different applied porosity estimates. In contrast, effects on absolute values for $K_{Kozeny-Köhler}$ were small. However, correlation between $K_{Kozeny-Köhler}$ and K_{DPST} was strongly influenced by the use of different porosity estimates with correlation coefficients ranging between 0.67 and 0.78.

The slope of the simple regression line between calculated and measured K indicates that the use of total porosity leads to an over prediction of calculated K in low K sediments. The best agreement between the linear regression line and line of equality between calculated and measured K was found for calculated K based on effective porosity values after Hölting & Coldewey (2005).

It could also be shown that if a fixed porosity value is applied to calculate K , correlation coefficients remain high while differences between the simple line of linear regression and line of equality are observed. However, for calculation of K after Kozeny-Köhler (1965) and Terzaghi (1925a, b) the appropriate method for estimating porosity must be identified as effects on calculated K from inappropriate porosity values are large. For the presented data highest correlation between calculated K after Kozeny-Köhler (1965) and Terzaghi (1925 a, b) and measured K_{DPST} values was found for porosity estimates after Chouker (1970) and Langguth (1980).

5 The use of CPT and other Direct Push methods for (hydro-)stratigraphic aquifer characterization

5.1 Introduction

In the previous section K_{DPST} were correlated with $K_{Grain\ size}$ data and it was shown that a reliable K characterization of sedimentary aquifers based on grain size analyses is possible. However, grain size analyses are time demanding and sample disturbance as well as removal of the sample from its natural stress field can bias results. In addition, as shown in chapter 2, the occurrence of fine grained layers of limited thickness within a sample of highly permeable media, can lead to a significant underestimation of calculated K . This clearly shows the need for high resolution, efficient in situ measurements of soil specific properties that may be used to measure K or derive K proxies.

Direct Push (DP) sensor probes and tools are promising methods for the in situ (hydro-) stratigraphic aquifer characterization and are therefore frequently applied to generate high resolution vertical profiles of various soil specific properties of un- or weakly consolidated sedimentary soils for a reliable description of subsurface structures. Various sensor probes and other DP tools for the in situ (hydro-)stratigraphic subsurface characterization have been engineered. Among these, CPT is the most commonly applied DP method. Despite the broad variety of DP tools that differ in working principle, application range, and resolution, no tool exists to measure continuous vertical K profiles.

Hydraulic characterization tools are constraint to generate vertical profiles of soil specific properties or to yield depth-oriented measurements of absolute K . Thus, (semi-)continuous K profiles rely on site specific correlations between absolute K values and K related parameters. This section aims to compare commonly applied DP tools for the (hydro-)stratigraphic subsurface characterization in a heterogeneous unconsolidated sedimentary aquifer. The objective is to show how well the applied DP methods can reflect soil variability and predict K . One aspect of the comparison is the consideration of the different operating modes and the

resulting difference in intrinsic area of influence (see section 1.1) For this thesis, DP profiling was carried out at the test site Bitterfeld (see section 1.2.1) and included cone penetration testing with pore pressure and electrical conductivity measurements (CPTU-EC), DP Injection Logger (DPIL), Hydraulic Profiling Tool (HPT) as well as Direct Push slug testing (DPST) and soil sampling with extensive grain size analyses. In the following the applied methods are briefly introduced with a focus on their capability to resolve vertical K distributions. Logging results were then evaluated for reproducibility and qualitatively compared and, in a later step, correlated with DP slug test data.

5.2 Direct Push technology

Direct Push (DP) technology refers to a growing family of tools used for performing subsurface investigations by driving, pushing and/or vibrating small-diameter hollow steel rods into the ground (EPA 1997a). Therefore, multiple tools can be attached at the end of the rod string. With the use of sampling devices, soil, soil gas, and ground water samples can be retrieved from the subsurface. If continuous or discontinuous information about the vertical distribution of soil specific properties are needed, sensor probes and tools can be deployed at the end of the rod string that measure in situ electrical, dielectrical, textural, and hydraulic soil properties, soil color or detect the presence of hydrocarbons. In addition a variety of other parameters can be derived based on these measurements.

DP can also be used to install temporary or permanent ground water or soil gas monitoring wells. Its minimum invasive nature, the broad variety of DP tools, probes, and sampling devices, the broad variety of equipment for advancing DP tools make it a promising technology for the high resolution vertical subsurface investigation. Thereby, DP includes many advantages over traditional site investigation technology, e.g. time and monetary efficiency, advanced data analysis that allows on-site decision making, and limited exposure to contaminated soil as no soil cuttings are produced by the rod advancement (EPA 1997b, McCall et al. 2005).

A general overview over DP technologies is given e.g. in Butler (2005), McCall et al. (2005), Dietrich & Leven (2006), Quinnan (2010). However, the application of DP technology is in most cases restricted to surface near weakly or unconsolidated sedimentary deposits. Table 5-1 lists major DP applications for the (hydro-)stratigraphic site characterization, operational specifications and selected references.

Table 5-1: Overview of DP (hydro-)stratigraphic profiling tools. Duration for continuous probing is given for a 10 m log, not including probe preparation (e.g. piezocone saturation). Durations for discontinuous and depth oriented tests are given for single tests at one depth interval, not including probe preparation or advancement of the probe to the individual depth. Further references are given in the text. State: ++ is fully developed, + is functioning and o is experimental.

Method	Derivation of K by means of:	Modus & Duration	Robustness	State	Reference
Electrical conductivity logging	Identification of lithological units. Site specific correlations with absolute K only possible in rare cases.	continuous/ < 1h	high	+	Christy et al. (1994) Schulmeister et al. (2003) Sellwood et al. (2005)
Cone Penetration Testing	Dissipation test, proxy for hydraulic conductivity	depth oriented/ seconds to days	medium	+	Meigh (1987) Lunne et al. (1997) Brouwer (2007)
Cone Penetration Testing	Identification of soil behavior type. Correlation of soil behavior with laboratory K data.	continuous/ < 1h	medium push only	++	Robertson et al. (1986) Robertson (1990) Lunne et al. (1997) Robertson (2009)
Direct Push Slug Test	Direct estimation of hydraulic conductivity at individual vertical test intervals	depth oriented/ 45 minutes	high	++	Butler (1997) Hinsby et al. (1992) Sellwood et al. (2005)

Method	Derivation of K by means of:	Modus & Duration	Robustness	State	Reference
Direct Push Injection Logger	Identification of hydrostratigraphic units. Proxy of hydraulic conductivity ($K_{relative}$)	semi continuous/ 3 minutes	high	+	Dietrich et al. (2008)
Hydraulic Profiling Tool	Identification of hydrostratigraphic units. Proxy of hydraulic conductivity ($K_{relative}$)	continuous/ < 1h	medium	+	McCall et al. (2009)
Direct Push Permeameter	K absolute	depth oriented/ 10-15 minutes	medium	o	Butler et al. (2007a)
High Resolution K Tool	K relative K absolute	continuous depth oriented	medium	o	Liu et al. (2009)
Waterloo Ground Water Profiler	Sampling and identification of hydrostratigraphic units.	continuous	high	++	Pitkin (1999) EPA (2004)

5.2.1 Direct Push Slug Test (DPST)

DP slug test is an established method for estimating horizontal hydraulic conductivity (Butler et al. 2002, Butler 2002, Hinsby et al. 1992). Butler (1997) describes the slug test as measuring the recovery of head in a well after a near-instantaneous change in head at the well. This instantaneous change of head can be realized by introducing or removing a known volume of water or by any other means (Papadopulos et al. 1973). In this thesis, a pneumatic slug test assembly was employed based on Hinsby et al. 1992; initiating a change in head by pressurized air. A schematic view of the DPST field setup and components is given in Fig 5-1. All slug tests were performed in temporary DP monitoring wells with a screened interval of 57 cm length at the end of the rod string. For well installation, the rods are driven into the soil while the screen is protected inside a sheath. Upon reaching the desired depth, an expandable tip at the end of the sheath is pushed out and the rod string is pulled back. While holding the screen in

place, it is exposed to the formation (see Sellwood et al. 2005 and McCall et al. 2005 for a description of installation procedures). At each sampling cluster multilevel slug testing was performed. Therefore, the temporary monitoring well was installed and the screen was subsequently pulled until reaching the desired depths. Slug tests were analyzed after Zlotnik & Mc Guire (1998) and Butler (1997).

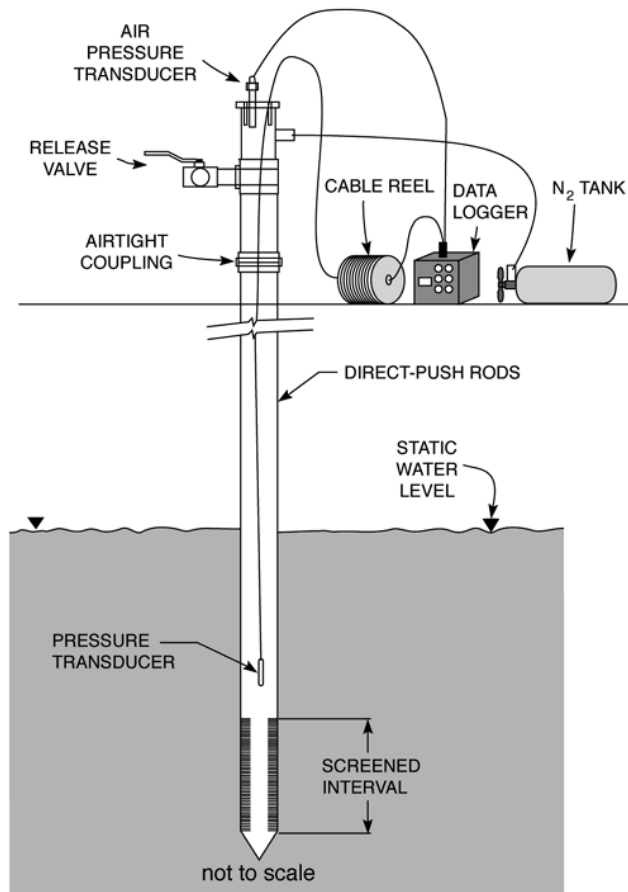


Figure 5-1: Schematic view of DP slug test field setup and components (Butler et al. 2000).

5.2.2 Sonic sampling and grains size analysis

108 grains size analyses were available (see section 2.2.1) that were supplemented with an additional number of 33 grain size analyses from sampling cluster 3 (see Figure 1-2). Results of all grain size analyses are listed in Appendix A. Based on the high correlation between K_{DPST} and K_{Hazen} (see section 2.4) and broad application range of the formula (see Table 2-2), calculation of K after Hazen (1893) was chosen. Despite the high correlation with DPST data, for layers of higher clay content extremely low K values as low as $6 \cdot 10^{-9}$ m/s were calculated,

indicating the application limit of this formula for fine grain dominated sediment mixtures.

5.2.3 Cone penetration testing with pore pressure and electrical conductivity measurement (CPTU-EC)

Among the Direct Push tools, cone penetration testing with pore pressure measurement (CPTU) is one of the most commonly used and versatile applications. Detailed information on cone penetration testing (CPT) is given by Meigh (1987), Lunne et al. (1997), and Brouwer (2007). While the cone penetrometer is statically pushed into the ground at a constant rate of 2 cm/s the probe measures the resistance (q_c) at the cone tip and friction (f_s) along the cone sleeve. Cone resistance (q_c) is defined as the total force acting on the cone divided by the projected area of the cone and sleeve friction (f_s) as total force acting on the sleeve divided by the total area of the sleeve (Lunne et al. 1997). A first indicator for soil behavior that can be linked to lithology is the friction ratio (R_f) which is defined as

$$R_f = \frac{f_s}{q_t} \times 100 \quad (\text{Eq. 5-1})$$

where q_t is the corrected cone resistance defined as

$$q_t = q_c + (1 - a)u_2 \quad (\text{Eq. 5-2})$$

where a is the area ratio of the cone (cone specific) and u_2 is the dynamic pore water pressure measured behind the tip.

In addition, the in situ pore pressure is measured. In this thesis a heavy duty subtraction-type piezocone with a projected tip area of 15 cm² and sleeve area of 225 cm² was used for the CPTU profiling. Pore pressure was measured at the u_2 position behind the tip. For this comparison, electrical conductivity was measured with a probe extension that in addition measures the relative permittivity of the soil. A schematic view of the CPTU-EC probe and components is given in Figure 5-2.

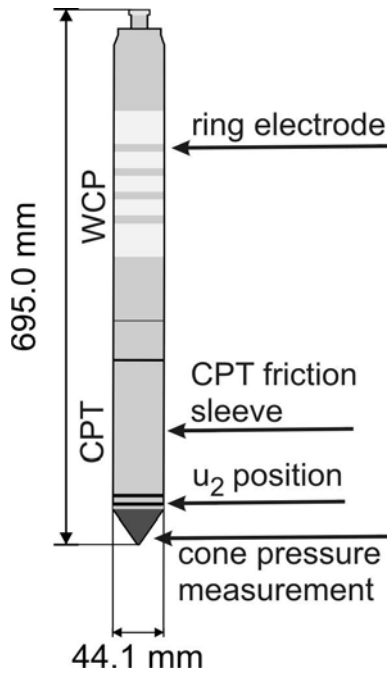


Figure 5-2: Schematic view of CPTU-EC probe and components.

Hydraulic conductivity values can be assessed from CPTU data in different ways. Two established methods are CPTU dissipation testing and identification of soil behavior type. To conduct dissipation tests during the probing the advancement of the CPTU cone is halted and the dissipation of the generated excess pore water pressure is logged. Lunne et al. (1997) describe methods to derive K from dissipation testing. Dissipation tests require fine grained soils with undrained or partially drained conditions in the soil, i.e. this test can not be performed in clean sands or gravels as the pore water pressure dissipates too rapidly to be measured with conventional CPTU cones. Also, pore pressure measurements are directly dependent on the quality of cone saturation.

The second approach is to characterize soil behavior type and is also applicable to coarse grained materials. Soil behavior type can either be estimated from soil behavior type diagrams or can be calculated. Various soil behavior type diagrams that are based on different parameters exist (Schmertmann 1978, Douglas & Olsen 1981; Robertson et al. 1986; Robertson 1990; Jefferies & Davis 1991). K values have been assigned to soil classes after Robertson et al. (1986) and Robertson (1990), see Lunne et al. (1997). Soil behavior can also be calculated using the formula after Jefferies & Davies (1991) that was modified by Robertson & Wride

(1998) to be applied to the chart after Robertson (1990) as cited in Robertson (2009):

$$I_C = ((3.47 - \log Q_{tl})^2 + (\log F_r + 1.22)^2)^{0.5} \quad (\text{Eq. 5-3})$$

where I_C is essentially the radius of concentric circles that can be plotted in the soil type behavior diagram after Robertson (1990) as shown in Robertson (2009). Soil behavior can be assigned based on where the circle segments fall within the diagrams; Q_{tl} is the normalized cone resistance:

$$Q_{tl} = (q_t - \sigma_{vo}) / \sigma'_{vo} \quad (\text{Eq. 5-4})$$

where σ_{vo} is the total overburden stress (Lunne et al. 1997) and σ'_{vo} is the effective vertical stress, that is derived from the difference between σ_{vo} and hydrostatic pressure; F_r is the normalized friction ratio:

$$F_r = f_s / (q_t - \sigma_{vo}) \quad (\text{Eq. 5-5})$$

It is important to note that this characterization is based on soil behavior and not soil types. Lunne et al. (1997) stress the uncertainty associated with the approach of assigning K values to soil behavior. In this thesis I_c will be directly correlate with soil type or soil properties (e.g. K).

5.2.4 Direct Push Injection Logger (DPIL)

The DPIL was introduced by Dietrich et al. (2003) and Butler & Dietrich (2004). Detailed information on the DPIL probe design and data analysis is given by Dietrich et al. (2008). This tool is used to derive discontinuous vertical profiles of the distribution of relative hydraulic conductivity within an aquifer (Table 5-1). At desired depth intervals (typically at vertical distances of less than 0.3 m), the advancement of the probe is stopped and the water pressure in the injection tubing is measured at different injection rates using a pressure transducer and flow meter at the surface. A schematic overview of the DPIL probe design with different injection elements and DPIL field setup is given in Figure 5-3.

A broad range of injection rates of more than 400 l/h can be used with the DPIL leading to intrinsic volume of influence of variable sizes. Especially, in heterogeneous media high injection rates can cause water flow along preferential flow paths instead of spherical water migration. Through its design, this tool is

very robust in the field and can measure relative hydraulic conductivity (K_{DPIL}) over a broad spectrum. K_{DPIL} is calculated as the reciprocal value of the difference of total flow resistance R_{total} and the resistance of the tube (R_{tube}) after:

$$K_{DPIL} = \frac{1}{R_{total} - R_{tube}} \quad (\text{Eq. 5-6})$$

R_{total} can be derived from the relation of the injection pressure (p_{inj}) and the flow rate (Q) that is measured with the flow meter:

$$R_{total} = p_{inj} / Q \quad (\text{Eq. 5-7})$$

The injection pressure is the sum of the pressure measured with the transducer (p_{trans}) at the surface and the pressure of the water column with a length that equals the distance from the pressure transducer above the surface to the depth of the water table.

With the given instrumentation, Q and p_{trans} are taken from analog instrumentation and can be processed in an excel sheet on a laptop computer on-site while logging.

For laminar flow, the tube resistance is mainly governed by the length of the tube and the tube diameter and can be calculated based on the Hagen-Poiseuille equation after:

$$R_{tube} = \frac{8L\eta}{\pi r_{tube}^4} \quad (\text{Eq. 5-8})$$

where L is the length of the tube between the pressure transducer and the screen; r_{tube} is the radius of the tube, and η is the dynamic viscosity of the injected fluid.

For turbulent flows, the tube resistance is a function of the flow rate. The tube resistance can be determined following:

$$R_{tube} = yQ + b \quad (\text{Eq. 5-9})$$

where y and b are parameters that are obtained from different flow and pressure measurements with the probe above the ground. Following equation 11, the tube resistance is calculated by the relation of injection pressure and flow rate and plotted versus the flow rate. Using the linear regression, the function of tube resistance in dependency of flow rate can be derived for various flow rates.

This pre-logging procedure is also used to identify the critical flow rate, i.e. the flow rate at which the system changes from laminar to turbulent flow. For further information on the DPIL and detailed instructions on calculation of K_{DPIL} see Dietrich et al. (2008).

To derive vertical K_{DPIL} distribution profiles, test intervals of 30 cm were chosen and, in a later step, reduced to 10 cm for increased resolution.

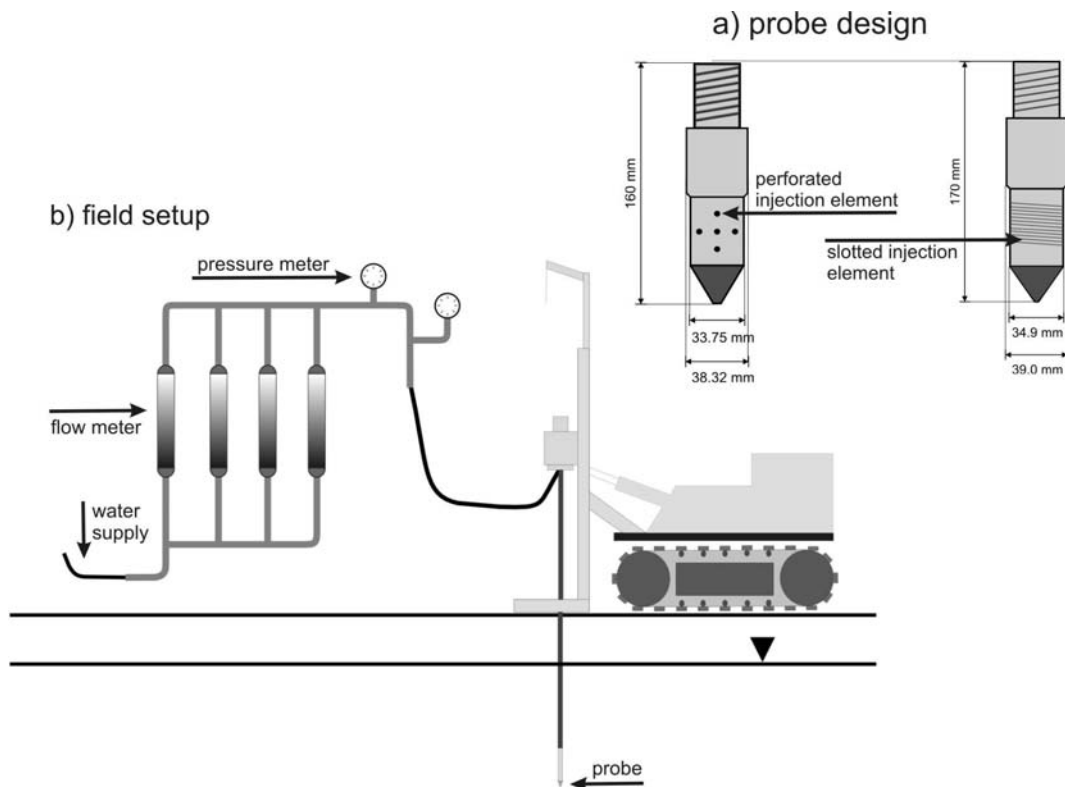


Figure 5-3: DPIL probe design with different water injection elements (a) and field setup (b).

5.2.5 Hydraulic Profiling Tool (HPT)

The HPT is used to evaluate the hydraulic properties of the subsurface (see McCall et al. 2009). It provides information that can be used to distinguish between units of varying hydraulic properties in the soil. The probe is advanced into the soil at a constant speed of 2 cm/s either by pushing and/or using a percussion hammer. While the probe is advanced, water is injected into the ground through a screen on the side of the probe. A build-in transducer measures the pressure response of the soil to the water injection. In addition, this tool is equipped with a 4 point electrode array to measure the electrical conductivity of the soil.

Flow rate, in situ/downhole back pressure, and electrical conductivity are logged in 1.5 cm vertical spacing. A schematic view of the HPT field setup and probe design is given in Figure 5-4. The injection rates of typically around 18 l/h lead to

a relatively small intrinsic area of influence for the water injection. High back pressure and low flow rates are normally corresponding to less permeable sediments, low backpressure and high flow rates indicate highly permeable sediments. An increase of the electrical conductivity can be an indicator for an increased abundance of fine material in the soil. In addition, Christy & McCall (2009) suggested using the HPT data to derive order-of-magnitude estimates of K based on the Q/p_{HPT} ratio:

$$K_{HPT} = Q / p_{HPT} \quad (\text{Eq. 5-10})$$

where Q is the flow rate; p_{HPT} is the pressure response data corrected for atmospheric and hydrostatic pressure. However, detailed studies of this approach are not available.

System dependent parameters, e.g. tube resistance, are not considered in Eq. 5-10 as p_{HPT} is measured downhole.

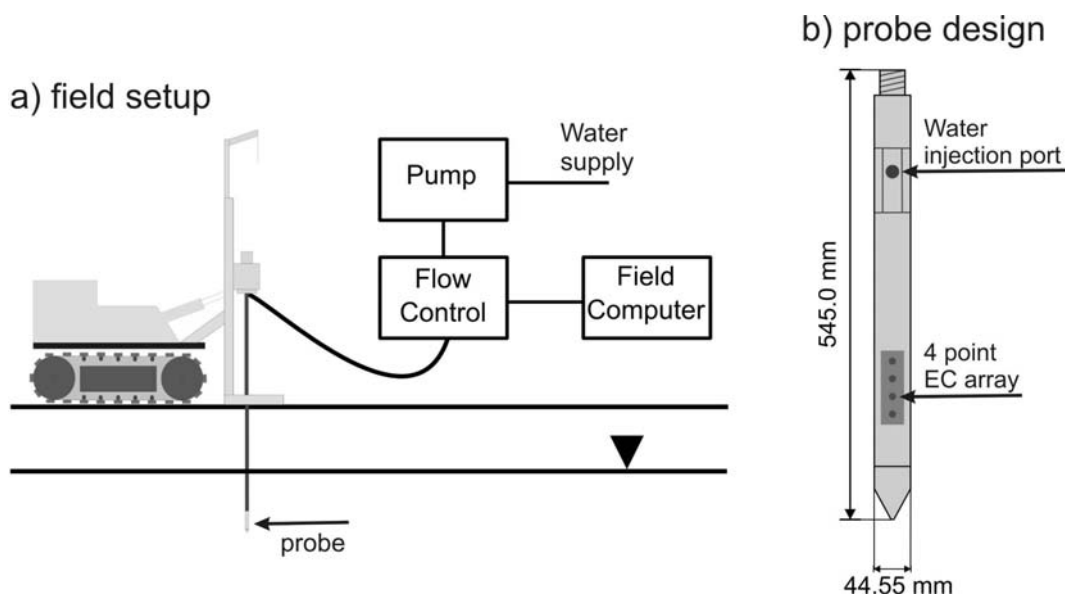


Figure 5-4: Schematic view of the HPT field setup (a) and probe design (b).

5.2.6 Electrical conductivity logging

The electrical conductivity logging is an efficient tool to gain high resolution vertical profiles of the distribution of electrical conductivity of the soil. Based on this information, soil stratification or layer boundaries within the subsurface can be inferred, as an increase of the electrical conductivity can indicate increased abundance of fine material in the soil. Therefore, often site specific correlations

between EC and K are established. Specific detail on electrical conductivity logging is given by Schulmeister et al. (2003), Sellwood et al. (2005).

While the probe is advanced, an electrical current is applied to the ground. The current and the resulting voltage are measured. The HPT and EC probe were operated in a Wenner configuration, i.e. with equally spaced electrode points (see Figure 5-5). The resistivity extension of the CPTU cone works with a Dipole array; here electrode rings instead of point electrodes are used. As the electrical conductivity is measured over the electrode array, the vertical extend of the intrinsic area of influence equals at least the total length of the electrode array. In our case, the total length of the electrode array at the HPT and EC probe is 6.5 cm, the length of one dipole electrode array of the CPTU-EC extension is 4.3 cm with 2.2 cm spacing between the 2 dipole sets. EC data of the CPTU-EC extension were used in the further analysis.

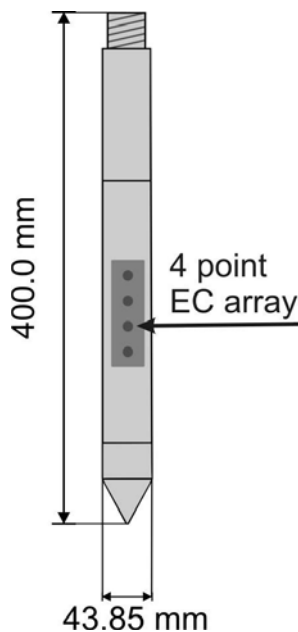


Figure 5-5: Schematic view of EC probe.

5.3 Results

5.3.1 Field data

The field work was conducted at the Bitterfeld test site. For information on the site and an overview of sampling points see section 1.21.

In the previous section the different applied DP methods were described. Differences in working principle and intrinsic area of influence were shown. For the evaluation of methods it is critical to first test reproducibility of the applied methods. Therefore, repetitive measurements at nearby locations were taken. Results (Fig. 5-6) indicate a high degree of reproducibility.

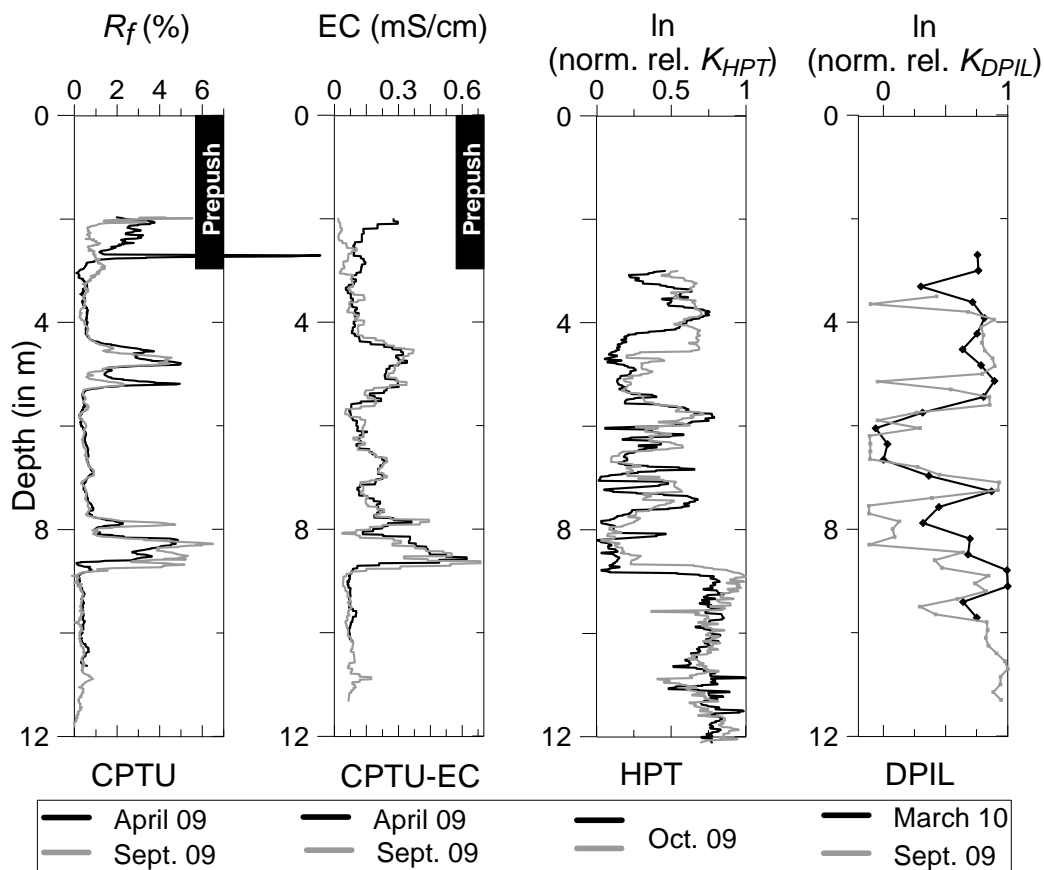


Figure 5-6: Repeat DP measurements. Repetitive measurements were taken at nearby locations at cluster 1 (CPTU, CPTU-EC, and HPT) and cluster 2 (DPIL). DPIL data: grey line indicates test intervals of 10 cm spacing, the black line test intervals of 30 cm spacing.

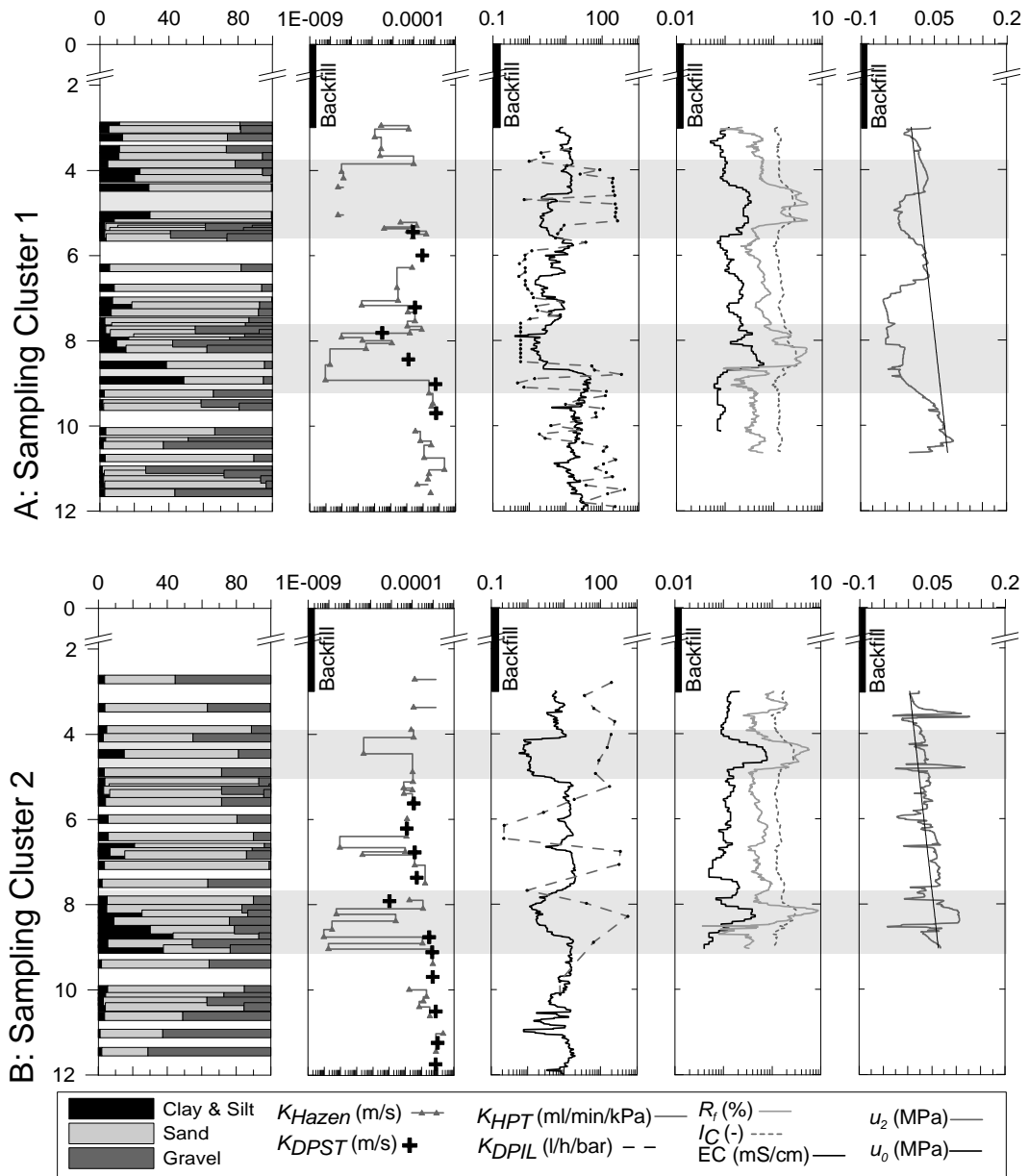
Also, possible effects of natural vertical soil variability on the comparison must be considered. Grain size data (Fig. 5-7) illustrate the high degree of soil variability on vertical and lateral scale. Natural soil variability is mainly caused by vertical and lateral facies variation - especially in fluvial sedimentation regimes, discontinuity of layers and lenses, and inclination or irregularity of stratum boundaries. Even though distances between logs are small (Fig. 1-2) effects of soil variability on the comparison and correlation of the methods must be considered. In addition, technical factors such as core disturbance or log inclination can affect comparison of DP results. In this thesis inclination effects are negligible due to the limited penetration depths of 12 m. However, CPTU-EC results were corrected for inclination, which was generally smaller than 5 degrees with a resulting difference of penetration length and penetration depth of less than 5 cm on 12 m penetration length.

An overview of all DP results including K distributions calculated from grain size data after Hazen (1893) (K_{Hazen}); CPT based R_f , EC and I_c ; relative K after HPT (K_{HPT}); and relative K after DPIL (K_{DPIL}) is given in Fig. 5-7. K_{Hazen} and slug test data show an overall high qualitative consistency. HPT and CPT profiling results can be used to characterize the major aquifer structure. Low K_{HPT} and high CPT R_f , I_c and EC data indicate two fine grain dominated layers of variable thickness at each of the sampling clusters (see grey shaded areas in Fig. 5.7). It is interesting to note that in 8 m depth of sampling cluster 3, sediment distribution does not indicate the presence of a fine grain layer as opposed to the DP data. Whether the fine grain horizon was not detected due to core loss or whether sedimentary effects such as compaction influenced CPT, HPT and DPIL results is unclear. HPT data offers a high resolution profile of hydraulic properties of the aquifer. However, data in Fig. 5-7 a, b, and d reveal an apparent upper resolution limit for high K soils in the lower section of the graph. Here, K_{HPT} reaches a system induced upper limit of about 10-30 ml/min/kPa. Higher K_{HPT} values cannot be resolved due to the limited injection rate.

In contrast, the DPIL oftentimes does not capture the fine grained layers at all or to their full extent which is most likely due to the lower vertical resolution. Also, hydraulic responses of the formation and the DPIL setup to high injection rates in

low permeable layers and effects of the filter design have yet to be further tested. Nevertheless, the DPIL does reflect the general K distribution over the aquifer and is especially suitable to reveal high K layers within the aquifer. The R_f also reflects the main structure of the aquifer, small structures on centimeter scale cannot be resolved due to the measurement principle. Distances over which the cone is influenced by a change in sediment behavior can be as large as 10-20 cone diameters in stiff materials (Lunne et al. 1997).

EC and I_c values show a qualitatively good correlation with the grain size and other DP data. Pore water pressure gives valuable information of the sediment behavior; however u_2 measurements in Bitterfeld must be evaluated carefully. The backfill material was prepunched to a depth of 3m with a solid dummy tip to avoid instrument loss. At the Bitterfeld test site mainly undrained soil behavior is found (see Fig. 5-7), i.e. fine grain dominated sediments and/or compaction normally lead to the generation of excess pore water pressure while probing. At the Bitterfeld site however, overconsolidated clays, i.e. clays that have been exposed to higher consolidation stresses in the past than at present, cause negative pore water pressure responses in the undrained sections of the aquifer that restrain dissipation testing. The piezocone was saturated with silicone oil. Damped pore water pressure responses (see Fig. 5-7 a,c,d) indicate a loss of saturation and negative pore water pressures impede recovery of cone saturation while probing.



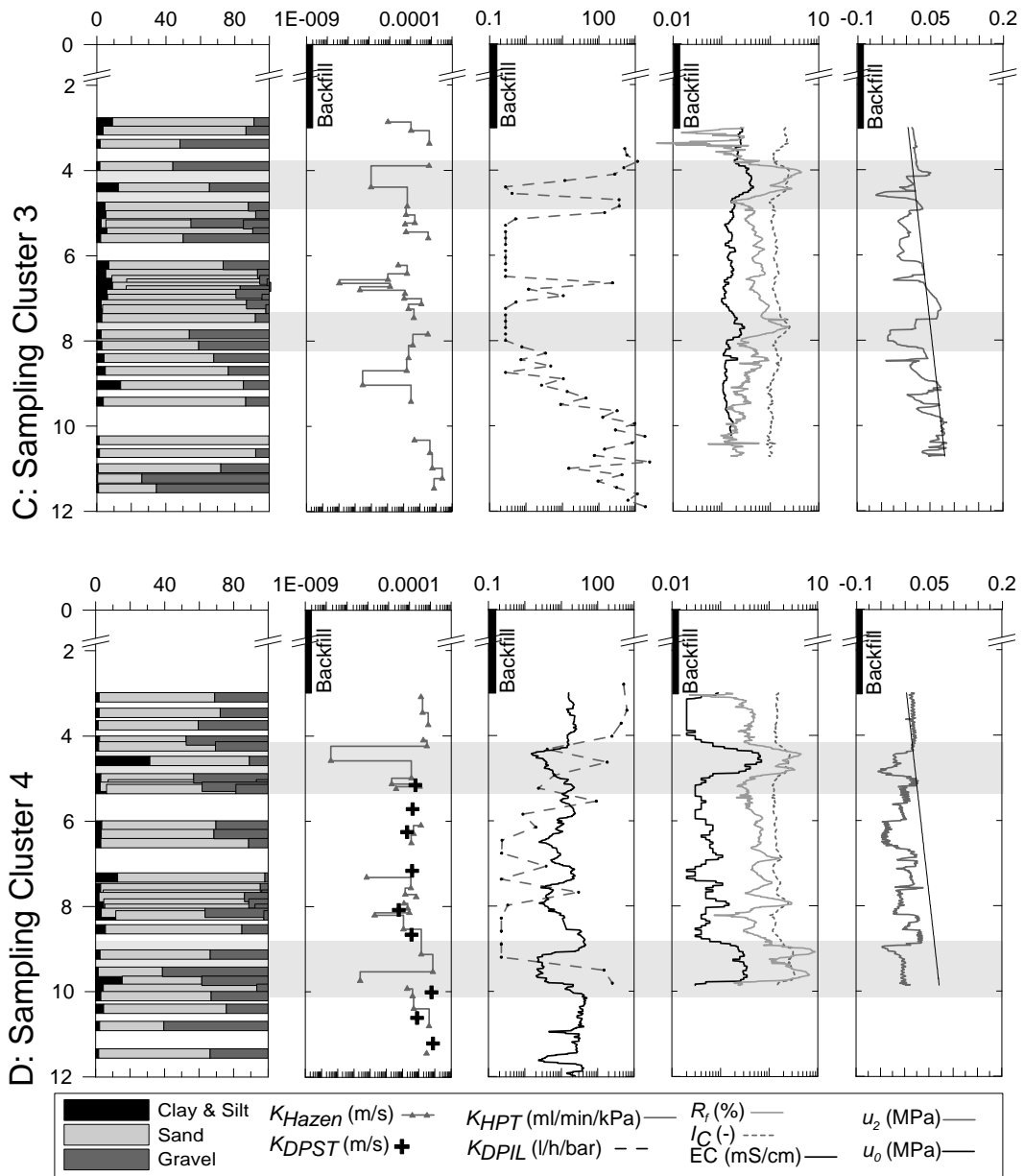


Figure: 5-7 (A-D): Results from DP (hydro-)stratigraphic profiling in comparison with results from DPST and grain size analyses at the Bitterfeld test site.

5.3.2 Quantitative data evaluation

After the qualitative comparison, the data is compared quantitatively. Therefore a dataset was generated that comprised grain size analyses, CPTU-EC, HPT and DPIL data from all sampling clusters at collocated depths in 10 cm vertical spacing. Values from above the ground water table or within the backfill material were discarded. Linear interpolation was used to determine missing data points from logging data that was generated with larger spacing than 10 cm between point measurements (DPIL) or at depths deviating from the collocated depth steps at which values are compared (DPIL, HPT). Effective grain size diameter, $\ln(K_{Hazen})$, EC from CPTU-EC measurements, EC from HPT measurements, R_f , I_C , $\ln(K_{HPT})$ and $\ln(K_{DPIL})$ are plotted in a common matrix plot (Fig. 5-8). Strong data scattering with low or no observable correlation especially for the comparison of DP in situ profiling data and results of the grain size analyses, effective grain size diameter (d_e) and $\ln(K_{Hazen})$, is dominating. Also no considerable correlation is observed between different DP profiling methods. Exemptions are thereby correlation of R_f and I_C , where calculation of I_C includes the normalized R_f values (F_r) and $\ln(K_{Hazen})$ and d_e .

Correlation between EC values derived from the CPTU-EC and HPT profiles show strong data scattering, even though the same parameter is measured. Although different probes with different electrodes arrays were employed, systematic differences should rather result in a difference of slope between the linear regression and the line of equality instead of data scattering. These results are caused by the high degree of vertical and lateral soil variability as described under section 1.2.1.

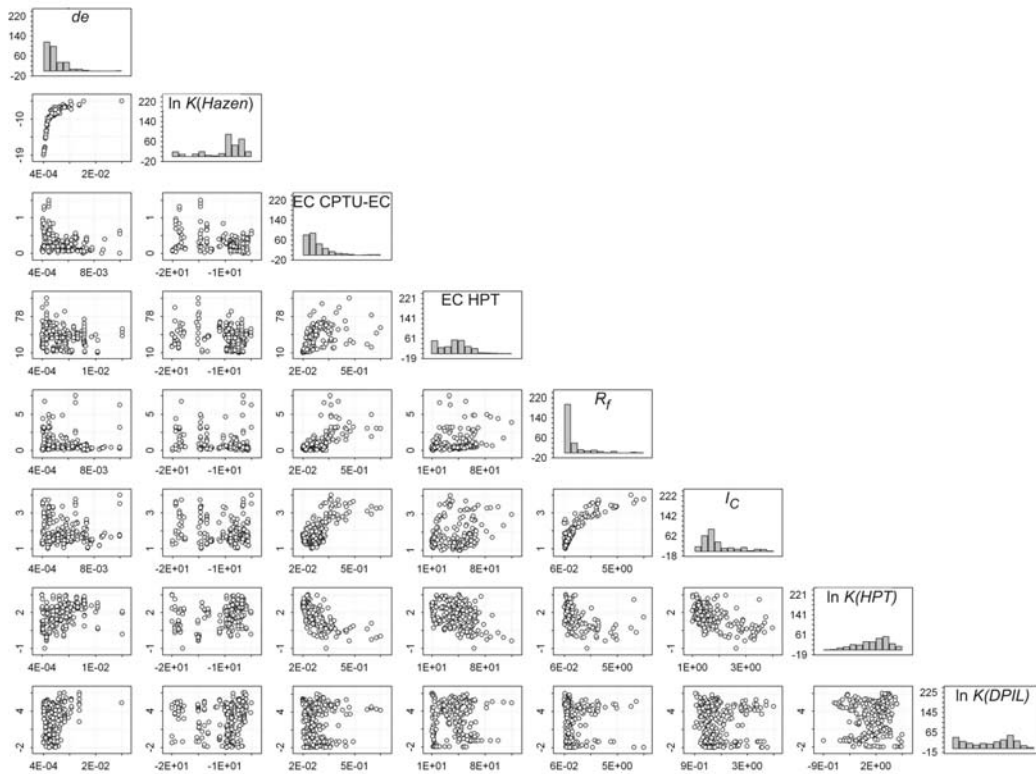


Figure 5-8: Scatter plot of DP profiling results at the Bitterfeld test site; histogram y-axis labeling is frequency. Units: d_e in mm, K_{Hazen} in m/s, R_f in %, EC in mS/cm, I_C (-), K_{HPT} (ml/min/kPa), K_{DPIL} (l/h/bar). All K values given as $\ln(K)$.

To further demonstrate the effect of soil variability on the correlation of logging results, R_f and CPTU-EC data are shown in scatter plots (Fig. 5-9). The underlying R_f and CPTU-EC data were measured with the same probe at two points that are 1.5 m apart (see Figure 1-2). Despite the high qualitative agreement between logs (Fig 5-6), data scattering indicates the effects of soil variability on the measurements.

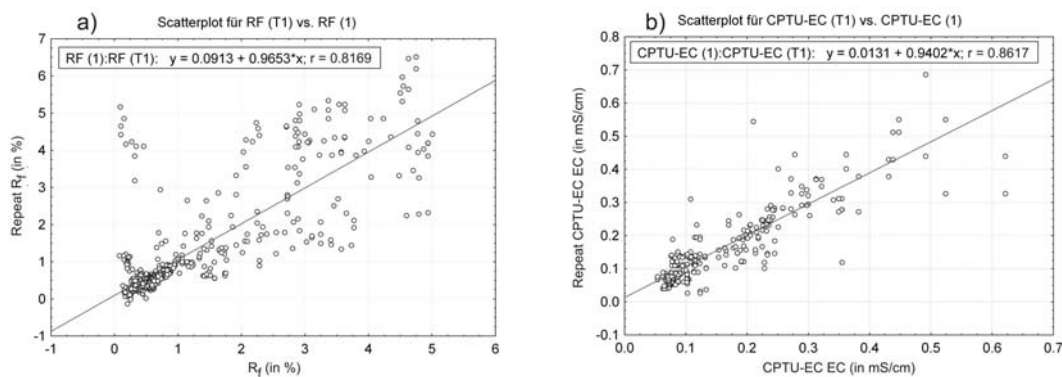


Figure 5-9: Scatter plot of repeat CPT R_f (a) and CPTU-EC EC (b) measurements from two logs at sampling cluster 1 with approximately 1.5 m spacing.

5.3.3 Data evaluation with DPST results

To test the ability to describe K , DP logging data were compared to multi level DP slug testing results from sampling cluster 1, 2, and 4. Outliers in the averaged DP profiling data, i.e. values deviating more than 2 standard deviations from the mean, were removed prior to the analyses. Three outliers were identified in the $\ln(K_{Hazen})$ data. These outliers represent extremely low K values calculated for strongly heterogeneous layers.

However, averaging the grain size data over the slug test intervals introduces an additional source of error (see section 2.5). R_f , I_c and EC data are influenced by one outlier. This outlier corresponds to a slug test interval over which the underlying R_f , I_c and EC considerably change. In addition, one $\ln(K_{DPIL})$ outlier was found and removed from the analyses. Outliers were not removed from slug tests data, as corrupt slug test data was already identified in the data analysis. Table 5-2 lists basic statistics and correlation coefficients between DPST results and the other DP methods, a matrix plot of the correlation is shown in Fig. 5-10.

A high degree of correlation can be observed between the DPST data and R_f , I_c data and calculated K_{Hazen} values. Correlation between DPST and EC , HPT , and $DPIL$ values are similar and range between 0.60 and 0.63. Values of the slopes of the regression lines (Table 5-2) reveal differences in the sensitivity of the parameters. The smaller the slope of the linear regression is, the less sensitive does the parameter on the y-axis respond to parameter changes on the x-axis. Slopes vary between -0.02 for EC values and 0.74 for $DPIL$ values. This shows that the $DPIL$ directly measures the hydraulic behavior as opposed to measuring sediment characteristics, e.g. fine grained content, and inferring K based on these parameters. Also, due to the variable injection rates, the $DPIL$ covers a broad K range.

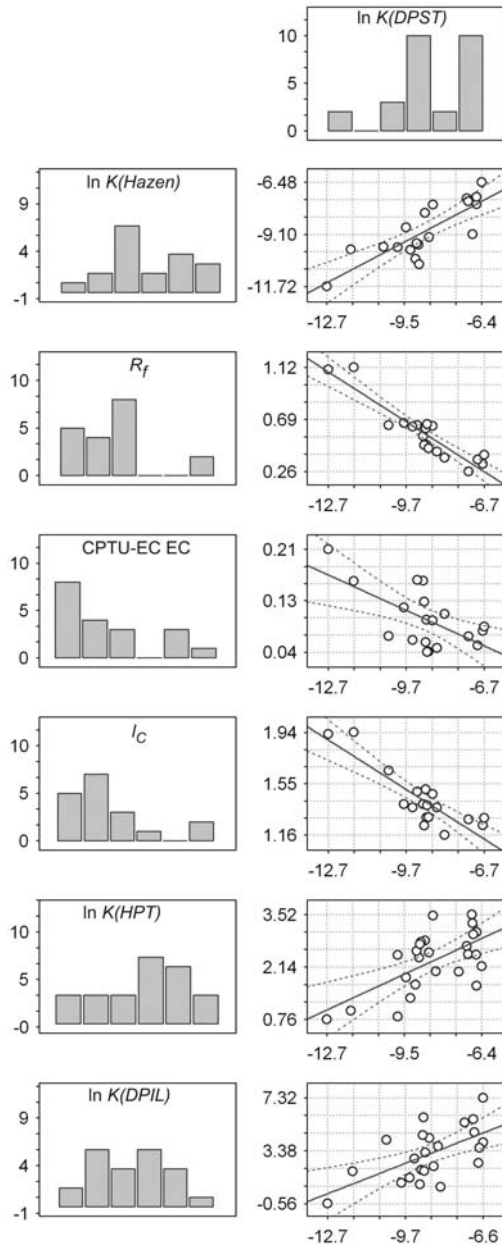


Figure 5-10: Matrix plot of Bitterfeld DP and DPST data. Solid line is the line of simple regression, dashed line is 95% confidence interval; x-axis labeling of the scatter plot is $\ln(K_{DPST})$, y-axis are DP data. Units: K_{DPST} in m/s, K_{Hazen} in m/s, R_f in %, CPTU-EC EC in mS/cm, I_C (-), K_{HPT} (ml/min/kPa), K_{DPIL} (l/h/bar). All K values given as $\ln(K)$.

Table 5-2: Basic statistics and correlation of DP profiling data and DPST results at the Bitterfeld test site; where $y*x$ is the slope and “b” is the intercept of the simple regression line. Units: K_{DPST} in m/s, K_{Hazen} in m/s, R_f in %, CPTU-EC EC in mS/cm, I_c (-), K_{HPT} (ml/min/kPa), K_{DPL} (l/h/bar). Correlation coefficients were determined using $\ln(K)$ values.

	K_{DPST}	K_{Hazen}	R_f	EC	I_c	K_{HPT}	K_{DPL}
n	27	19	20	20	19	25	24
geometric mean	2.10E-04	3.97E-05	0.57	8.82E-02	1.46	10.01	19.76
Min	3.07E-06	1.48E-08	0.26	3.62E-02	1.16	2.14	0.22
Max	1.67E-03	1.54E-03	2.28	3.82E-01	2.62	33.95	1504.27
σ^2	2.90E-07	1.33E-07	0.19	6.26E-03	0.11	74.39	9.18E+04
r		0.81 (LN)	-0.92	-0.62	-0.86	0.63 (LN)	0.60 (LN)
lin reg y		0.65*x	-0.14*x	-0.02*x	-0.13*x	0.30*x	0.74*x
b		-3.27	-0.68	-0.09	0.29	4.81	9.60

5.4 Conclusion

The objective in this chapter was to compare commonly applied Direct Push tools for the (hydro-)stratigraphic subsurface characterization in a heterogeneous unconsolidated sedimentary aquifer. Results of the applied DP methods are reproducible and all of the employed DP methods are suitable to reflect the general aquifer structure. Small scale heterogeneities cannot be resolved by all DP methods equally well as the volumetric intrinsic area of influence for these methods is a multiple of the probe diameter. In this context, the HPT is able to provide the highest vertical resolution with respect to hydraulic property distribution.

Small scale soil variability, especially the presence of isolated lenses that may not be penetrated by all DP logs at the same cluster, can introduce uncertainty in the comparison of DP performance. This was evident in the results of the quantitative data evaluation. The matrix plot of DP profiling data on 10 cm resolution revealed small to no correlation between results of the grain size analyses and DP in situ profiling data as well as little to no correlation between the results of the in situ profiling data. However, the DPST and DP data indicates high correlations between DPST and R_f ($r = -0.92$), I_c ($r = -0.86$), and K_{Hazen} ($r = 0.81$). In this thesis,

K was best described by methods that are primarily based on soil behavior or grain size distribution. The averaging process of the logging data over the 57 cm slug test interval in comparison to slug test results, that themselves represent averaged K values over the test interval, reduced the effects of soil variability on the comparison. Nevertheless, hydraulic conductivity is affected by other relevant soil matrix properties, such as grain- and pore size distribution, shape of grains and pores, tortuosity, specific surface, and porosity (see Bear 1972). Therefore, the established correlations between DPST and DP data are site specific and not generally applicable.

However, it is possible to describe the hydraulic structure of this complex aquifer on less than a meter scale by combining DPST data and continuous DP measurements. Even though the appropriate DP tools must be chosen in terms of spatial and parameter resolution and instrument robustness must match the site specific geological conditions, DP methods are reliable and efficient tools for characterization even strongly heterogeneous site with an intricate sedimentary architecture.

6 Summary and conclusion

High resolution data is needed to describe complex sedimentary flow systems. Different tools for the high resolution vertical (hydro-)stratigraphic profiling of sedimentary deposits exist, that differ in resolution and working principle. A critical evaluation of the limitation or representativeness of the data within the geological framework or aim of investigation is necessary as the limiting momentum in flow and transport predictions is oftentimes the quality and quantity of underlying field data. In this thesis methods for high resolution vertical aquifer characterization were evaluated regarding their ability to identify the complex structure of a sedimentary aquifer and their ability to predict K .

A commonly applied method for high resolution aquifer characterization is soil sampling with laboratory analyses of the soil samples. A broad spectrum of empirical and semi empirical formulas exist to calculate K from grain size distribution. Based on grain size analyses and results from Direct Push slug testing (DPST), seven commonly applied formulas were tested concerning their ability to predict K . Results of calculated K for 108 samples vary over several order of magnitudes for the calculated mean between the applied formulas, clearly indicating the need to evaluate calculated K with in situ measured K . Correlation between calculated K values and DPST data differed between applied formulas with respective correlation coefficients ranging from 0.63 to 0.82.

Uncertainty of K estimates is introduced through the empirical and semi-empirical nature of the applied formulas and the fact that during the grain size analyses the soil structure is eventually destroyed. In addition, other factors were identified in this thesis, that limit the reliability of calculated K ; among these are sample disturbance, heterogeneity of the analyzed samples, measuring inaccuracy, and uncertainty of porosity estimates. Results of ring analyses showed that measuring inaccuracy, which was well within acceptable tolerance limits, affected calculated K after Hazen (1893) by a factor of 4.26 for a sand dominated sample. Effects of deviating porosity estimates were shown to have an effect on calculated K after

Terzaghi (1925a, b) and Kozeny-Köhler (1925) of more than one order of magnitude.

To overcome the uncertainty associated with porosity estimates on calculated K values, in situ water content measurements were performed. Results from neutron probe and DP deployed WCP that works based on frequency domain technology were tested at two field sites under different geological settings. A high correlation with a respective correlation coefficient of 0.94 between results of both probes was seen at the Larned test site where fairly homogeneous sand and gravel dominated deposits are present. The NP could not resolve the strong heterogeneous deposits of the Bitterfeld test site due to small scale changes in lithology and a respective large intrinsic area of influence of the NP. Neither could the DP deployed WCP at its current state depict the soil moisture distribution reliably with a resulting correlation coefficient of 0.25 between the two methods.

As both of the in situ methods failed to determine soil water content, respectively total porosity in the saturated zone, empirical methods to determine porosity were subsequently compared. In the literature, porosity values based on sediment types and empirical relations between soil specific properties and porosity are found. Empirical literature data and proposed soil property-porosity correlations were used to calculate hydraulic conductivity for the slug test intervals. Results demonstrate strong effects on calculated K that are introduced through the use of empirical data. For $K_{Terzaghi}$ differences in calculated Min and Max K values ranging from $1.02 \cdot 10^{-5}$ to $1.94 \cdot 10^{-7}$ and $1.09 \cdot 10^{-3}$ to $5.18 \cdot 10^{-5}$ were observed between the different applied methods to estimate porosity. For $K_{Kozeny-Köhler}$ differences in correlation coefficients between calculated and measure K ranged between 0.67 and 0.78 in dependency of the applied method to estimate porosity.

In addition, the use of total porosity leads to an under prediction of calculated K for high permeable sediments and an over prediction of calculated K for low permeable sediments. This effect was reduced by the application of effective porosity. A strong offset between calculated and measured K values could in this case be observed that may be reduced by adaption of the empirical coefficients in

the formula. Large uncertainties are associated with the determination of K based on grain size distribution stressing the need for direct and in situ measurement of K or K related proxies.

DP technology has become a promising alternative for high resolution vertical (hydro-)stratigraphic profiling of sedimentary systems. In this work, DP profiling was carried out at the test site Bitterfeld and included cone penetration testing with pore pressure and electrical conductivity measurements (CPTU-EC), DP Injection Logger (DPIL), Hydraulic Profiling Tool (HPT) as well as Direct Push slug testing (DPST) and soil sampling with extensive grain size analyses. All of the applied DP methods for (hydro-)stratigraphic profiling were suitable to qualitatively reflect the general aquifer structure of the Bitterfeld test site.

Despite the broad variety of tools, no DP tool exists to measure a continuous vertical profile of the distribution of horizontal K . Such vertical profiles rely upon parameter relations. A high correlation between DPST and R_f ($r = -0.92$), I_c ($r = 0.86$), and K_{Hazen} ($r = 0.81$) is found. This work shows that it is possible to characterize even a strongly heterogeneous aquifer with a resolution scale of less than one meter by combining DPST and high resolution DP profiling data.

However, parameter relations could not be established on a centimeter scale although high resolution data were available. Differences of the intrinsic volume of influence and vertical spacing of point measurements had notable effects on the correlation of methods; especially in combination with the complex sedimentary architecture of the sedimentary deposits that was encountered at the Bitterfeld test. To reduce effects of soil variability, profiling was conducted at different sampling clusters where individual profiles were taken in close proximity to each other. Despite this approach, effects of soil variability could not be eliminated. Fig. 6-1 illustrates how soil variability affects the comparison of closely spaced DP profiles; therefore depth oriented measurements that average a soil specific property over vertical distances and continuous profiling with 30 cm, 15 cm and 1cm spacing between single measurements are plotted in a highly heterogeneous sedimentary deposit. Layers of limited thickness are not captured by measurements with low vertical resolution and irregular stratum boundaries,

lateral facies variation, and discontinuity of layers and lenses hinder a comparison of results on centimeter scale.

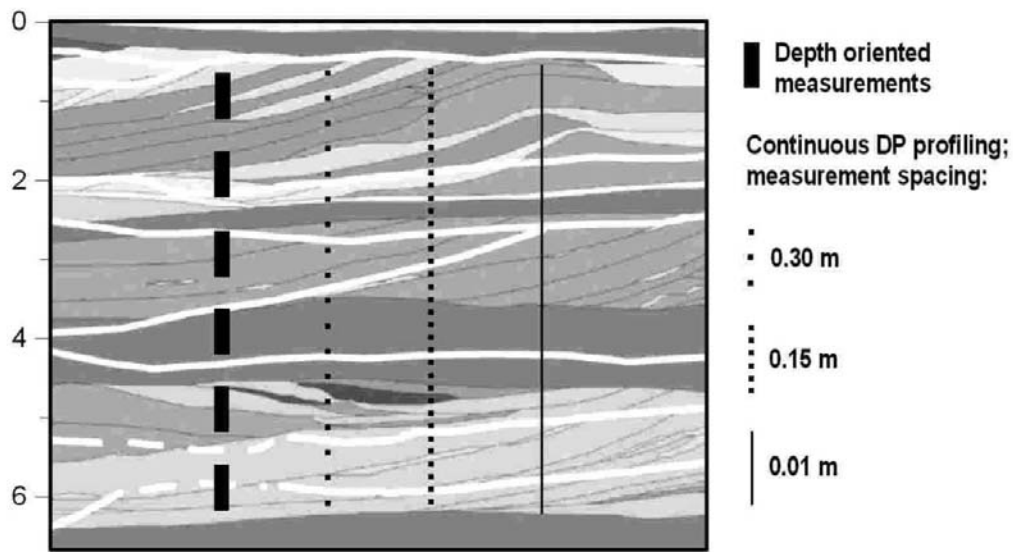


Figure 6-1: Dependency of vertical profiling results in a heterogeneous aquifer on intrinsic volume of influence and spacing between point measurements. Illustration of the braided river deposit has been taken from Tronicke et al. (2002) and modified.

In this thesis, large uncertainties were shown to affect the determination of K based on grain size distribution. DP tools proved to be a sound alternative to conventional site investigation methods for high resolution in situ aquifer characterization of sedimentary aquifers that can provide high resolution in situ data for flow and transport modeling. Established parameter relations between DPST and high resolution profiling data in this thesis are site specific.

Appropriate DP tools must be chosen to meet the demands of the investigation in consideration of the local geology. Obtained DP data needs to be carefully evaluated. Hence, further rigorous testing of DP methods in the laboratory and especially under field condition is needed. This work has set the foundation of a dataset that combines a large quantity of grain size and corresponding DP data. Expansion of this dataset will further contribute to ongoing research of whether generally valid parameter relations between DP data and K or grain size data can be established.

References

Alyamani, M.S. and Sen, Z., 1993. Determination of Hydraulic Conductivity From Complete Grain-Size Distribution Curves. *Ground Water*, 31(4): 551-555.

Anderson, M.P., 1997. Characterization of geological heterogeneity. In: G. Dagan and S.P. Neumann (Editors), *Subsurface Flow and Transport: A Stochastic Approach*. Cambridge University Press, Cambridge, pp. 23-43.

Atkins, R.T., Pangburn, T., Bates, R.E. and Brocket, B.E., 1998. *Soil Moisture Determinations Using Capacitance Probe Methodology*, US Army Corps of Engineers.

Barrow, J.C., 1994. The Resonant Sonic Drilling Method - an Innovative Technology for Environmental Restoration Programs. *Ground Water Monitoring and Remediation*, 14(2): 153-160.

Bear, J., 1972. *Dynamics of fluids in porous media*. American Elsevier, New York.

Benson, R.C., 2005. Remote Sensing and Geophysical Methods for Evaluation of Subsurface Conditions In: D.M. Nielsen (Editor), *Practical Handbook of Environmental Site Characterization and Ground-Water Monitoring*. CRC Press Taylor and Francis Group, Boca Raton, pp. 249-295.

Beyer, W., 1964. Zur Bestimmung der Wasserdurchlässigkeit von Kiesen und Sanden aus der Kornverteilungskurve. *WWT - Wasserwirtschaft Wassertechnik*(14): 165-168.

Bialas, Z. and Kleczkowski, A.S., 1970. O przydatności niektórych wzorów empirycznych dla określenia współczynnika filtracji k. *Archiwum Hydrotechniki (Archives of Hydrotechnics)*(17).

Briscoe, H.T., 1935. *The Structure and Properties of Matter*. McGraw-Hill Book Company Inc., New York, 420 pp.

Brown, C.E., 1998. *Applied Multivariate Statistics in Geohydrology and Related Sciences*. Springer, Berlin.

Brouwer, J.J.M., 2007. *In-situ soil testing*. Lankelma, East Sussex, 144 pp.

Butler, J.J., 1997. *The design, performance, and analysis of slug tests*. Lewis Publishers, Boca Raton.

Butler, J.J., 2002. A simple correction for slug tests in small-diameter wells. *Ground Water*, 40(3): 303-307.

Butler, J.J., 2005. Hydrogeological Methods. In: Y. Rubin and S. Hubbard (Editors), *Hydrogeophysics*. Springer, Dordrecht, pp. 23-58.

Butler, J.J., Lanier, A.A., Healey, J.M., Sellwood, B.W., McCall, W. and Garnett, E. 2000. Direct-push hydraulic profiling in an unconsolidated alluvial aquifer, Lawrence. Kansas Geological Survey Open-file Report 2000-62.

Butler, J.J., Healey, J.M., McCall, G.W., Garnett, E.J. and Loheide, S.P., 2002. Hydraulic tests with direct-push equipment. *Ground Water*, 40(1): 25-36.

Butler, J.J. and Dietrich, P., 2004. New methods for high-resolution characterization of spatial variations in hydraulic conductivity, International Symposium on Hydrogeological Investigation and Remedial Technology, Jhongli, Taiwan, pp. 42-55.

Butler, J.J., Whittemore, D.O., Zhan, X.Y. and Healey, J.M., 2004. Analysis of Two Pumping Tests at the O'Rourke Bridge Site on the Arkansas River in Pawnee County, Kansas. Kansas Geological Survey Open-file Report 2004-32.

Butler, J.J., Whittemore, D.O. and Kluitenberg, G.J., 2005. Ground water assessment in association with salt cedar control; report on year one activities. Kansas Geological Survey Open-file Report 2005-19.

Butler, J.J., Dietrich, P., Wittig, V. and Christy, T., 2007a. Characterizing Hydraulic Conductivity with the Direct-Push Permeameter. *Ground Water* 45: 409-419.

Butler, J.J., Kluitenberg, G.J., Whittemore, D.O., Loheide, S.P., Jin, W., Billinger, M.A. and Zhan, X.Y., 2007b. A field investigation of phreatophyte-induced fluctuations in the water table. *Water Resources Research*, 43(2).doi:10.1029/2005WR004627.

Cameron, J.F., 1970. Neutron moisture gauges a guide-book on theory and practice, International Atomic Energy Agency, Wien.

Campbell, M.D., Starrett, M.S., Fowler, J.D. and Klein, J.J., 1990. Slug Test and Hydraulic Conductivity. *Ground Water Management*(4): 85-99.

Carman, P.C., 1937. Fluid flow through granular beds. *Transactions of the Institution of Chemical Engineers*(15): 150-166.

Chapius, R.P., 2004. Predicting the saturated hydraulic conductivity of sand and gravel using effective diameter and void ratio. *Canadian Geotechnical Journal*, 41: 787-795.

Chapius, R.P., Dallaire, V., Marcotte, D., Chouteau, m., Acevedp, N. and Gagnon, F. 2005. Evaluating the hydraulic conductivity at three different scales within an unconfined sand aquifer at Lachanaie, Quebec. *Canadian Geotechnical Journal*, 42: 1212-1220.

Cheong, J.Y., Hamm, S.Y., Kim, H.S., Ko, E.J., Yang, K. and Lee, J.H. 2008. Estimating hydraulic conductivity using grain-size analyses, aquifer tests, and

numerical modeling in a riverside alluvial system in South Korea. *Hydrogeology Journal*, 16(6): 1129-1143.

Chouker, F., 1970. *Methodische und theoretische Untersuchungen zur geophysikalischen Grundwassererkundung*. Freiburger Forschungshefte. VEB Deutscher Verlag für Grundstoffindustrie, Leipzig, Freiberg.

Christy, C.D., Christy, T.M. and Wittig, V., 1994. A Percussion Probing Tool for the Direct Sensing of Soil Conductivity. Geoprobe Systems Technical Paper No. 94-100.

Christy, T. and McCall, W., 2009. Hydraulic Conductivity Estimates Using the Hydraulic Profiling Tool, NovCare 2009; *Novel Methods for Subsurface Characterization and Monitoring: From Theory to Practice*. UFZ - Helmholtz Centre for Environmental Research, Leipzig, pp. 57.

Dandekar, A.Y., 2006. *Petroleum Reservoir Rock and Fluid Properties*. CRC Taylor & Francis, Boca Raton.

Davis, S.N. and De Wiest, R.J., 1966. *Hydrogeology*. John Wiley & Sons Inc., New York.

De Boer, R., 2005. *The Engineer and the Scandal*. Springer, Berlin.

Dekker, T.J. and Abriola, L.M., 2000. The influence of field-scale heterogeneity on the surfactant-enhanced remediation of entrapped nonaqueous phase liquids. *Journal of Contaminant Hydrology*, 42(2-4): 219-251.

De Ridder, N.A. and Wit, K.E., 1965. A Comparative study on the Hydraulic Conductivity of Unconsolidated Sediments. *Journal of Hydrology*, 3: 180-206.

Dietrich, P. et al., 2003. Field Comparison of Direct-Push Approaches for Determination of K-Profiles, AGU Fall Meeting, San Francisco.

Dietrich, P. and Leven, C., 2006. Direct Push-Technologies. In: R. Kirsch (Editor), *Groundwater Geophysics*. Springer, Berlin, pp. 321-340.

Dietrich, P., Butler, J.J. and Faiss, K., 2008. A rapid method for hydraulic profiling in unconsolidated formations. *Ground Water*, 46(2): 323-328.

DIN, 1984. DIN 38402-41:1984-05: *Deutsche Einheitsverfahren zur Wasser-, Abwasser- und Schlammuntersuchung; Allgemeine Angaben (Gruppe A); Ringversuche, Planung und Organisation (A 41)*.

DIN, 2002. *Geotechnische Erkundung und Untersuchung - Benennung, Beschreibung und Klassifizierung von Boden - Teil 1: Benennung und Beschreibung EN ISO 14688-1:2002*.

Douglas, B.J. and Olsen, R.S., 1981. Soil classification using electric cone penetrometer. *Cone Penetration and Experience*, ASCE National Convention. American Society of Engineers (ASCE), St. Louis, pp. 209-227.

Eggleston, J. and Rojstaczer, S., 1998. Identification of large-scale hydraulic conductivity trends and the influence of trends on contaminant transport. *Water Resources Research*, 34(9): 2155-2168.

Eissmann, L., 1994. Grundzüge der Quartärgeologie Mitteldeutschlands (Sachsen, Sachsen-Anhalt, Südbrandenburg, Thüringen). In: L. Eissmann and T. Litt (Editors), *Das Quartär Mitteldeutschlands*. Deutsche Quartärvereinigung e.V., Altenburg.

EPA, 1997a. Expedited Site Assessment Tools For underground Storage Tank Sites. A Guide for Regulators. U.S. Government Printing Office, Pittsburgh. EPA 510-B-97_001

EPA, 1997b. Field analytical and Site Characterization Technologies. Summary of Applications. U.S. EPA, Washington D.C. EPA 542-R-04-017

EPA, 2004. Site Characterization Technologies for DNAPL Investigations. EPA, Cincinnati. EPA 542-R-04-017

Evett, S.R. and Steiner, J.L., 1995. Precision of Neutron-Scattering and Capacitance Type Soil-Water Content Gauges from Field Calibration. *Soil Science Society of America Journal*, 59(4): 961-968.

Evett, S.R., Schwartz, R.C., Tolk, J.A. and Howell, T.A., 2009. Soil Profile Water Content Determination: Spatiotemporal Variability of Electromagnetic and Neutron Probe Sensors in Access Tubes. *Vadose Zone Journal*, 8(4): 926-941.

Gomezhernandez, J.J. and Gorelick, S.M., 1989. Effective Groundwater Model Parameter Values - Influence of Spatial Variability of Hydraulic Conductivity, Leakance, and Recharge. *Water Resources Research*, 25(3): 405-419.

Hazen, A., 1893. Some physical properties of sand and gravels, with special reference to their use in filtration. In: S.B.o.H.o. Massachusetts (Editor). *Annual Report*, pp. 541-556.

Hignett, C. and Evett, S.R., 2002. Neutron Thermalization. In: J.H. Dane and G.C. Topp (Editors), *Methods of Soil Analysis: Part 4 Physical Methods*. Soil Science Society of America, Madison, pp. 501-520.

Hilhorst, M.A., 1998. Dielectric Characterisation of Soil, Lanbouwuniversiteit Wageningen, 139 pp. Doctoral Thesis.

Hinsby, K., Bjerg, P.L., Andersen, L.J., Skov, B. and Clausen, E.V., 1992. A mini slug test method for determination of a local hydraulic conductivity of an unconfined sandy aquifer. *Journal of Hydrology*, 1-4(136): 87-106.

Hölting, B. and Coldewey, W.G., 2005. *Hydrogeologie - Einführung in die Allgemeine und Angewandte Hydrogeologie*, 6. Auflage. Elsevier, München.

Hütte, 1956. Band 3 Bautechnik. *Des Ingenieurs Taschenbuch*, 28. Verlag von Wilhelm Ernst und Sohn, Berlin.

Indelman, P., Moltyaner, G. and Dagan, G., 1999. Determining the hydraulic conductivity spatial structure at the Twin Lake site by grain-size distribution. *Ground Water*, 37(2): 223-227.

Istomina, V.S., 1957. Seepage Stability of the Soil (in Russian). Gosstrojizdat, Moscow.

Jefferies, M.G. and Davies, M.P., 1991. Soil classification by the cone penetration test: Discussion. *Canadian Geotechnical Journal*, 28(1): 173-176.

Johnson, A.I., 1967. Specific yield - Compilation of specific yields for various materials, United States Geological Survey Water-Supply Paper 1662-D.

Kamann, P.J., Ritzi, R.W., Dominic, D.F. and Conrad, C.M., 2007. Porosity and permeability in sediment mixtures. *Ground Water*, 45(4): 429-438.

Kasenow, M., 2002. Determination of hydraulic conductivity from Grain Size Analysis. Water Resources Publications, LLC, Littleton.

Kaubisch, M. and Fischer, M., 1985. Zur Berechnung des Filtrationskoeffizienten in Tagebaukippen. Teil 3: Ermittlung des Filtrationskoeffizienten für schluffige Feinsande aus Mischbodenkippen durch Korngrößenanalysen. *Neue Bergbautechnik*, 15: 142-143.

Kaubisch, M., 1986. Zur indirekten Ermittlung hydrogeologischer Kennwerte von Kippenkomplexen, dargestellt am Beispiel des Braunkohlebergbaus. Bergakademie Freiberg. Doctoral Thesis.

Kim, Y.S., Oh, M.H. and Park, J., 2007. Laboratory study on the dielectric properties of contaminated soil using CPT deployed probe. *Geosciences Journal*, 11(2): 121-130.

Knoth, W., 1995. Sachsen-Anhalt. In: L. Benda (Editor), *Das Quartär Deutschlands*. Gebrüder Bornträger, Berlin, pp. 148-170.

Köhler, H.P., 1965. Ein kombinierendes Verfahren zur Bestimmung des Durchlässigkeitsbeiwertes von Sand- und Kiesgemischen für Wasser aus Siebproben. *Bergbautechnik*, 15: 338-342.

Koltermann, C.E. and Gorelick, S.M., 1995. Fractional packing model for hydraulic conductivity derived from sediment mixtures. *Water Resources Research*, 31(12): 3283-3297.

Kozeny, J., 1953. *Hydraulik - Ihre Grundlagen und praktische Anwendung*. Springer, Wien.

Lal, R. and Shukla, M.K., 2004. *Principles of Soil Physics*. Marcel Dekker, Inc., New York.

Langguth, H.-R. and Voigt, R., 1980. *Hydrogeologische Methoden*. Springer-Verlag, Berlin.

Langmuir, D., 1997. *Aqueous environmental Geochemistry*. Prentice Hall, Upper Saddle River, 600 pp.

Liu, G.S., Butler, J.J., Bohling, G.C., Reboulet, E., Knobbe, S., and Hyndman, D.W. 2009. A new method for high-resolution characterization of hydraulic conductivity. *Water Resources Research*, 45. doi:10.1029/2009WR008319.

Lunne, T., Robertson, P.K. and Powell, J.J.M., 1997. *Cone Penetration Testing in Geotechnical Practice*. Spon Press, New York, 312 pp.

Mallet, C. and Pacquant, J., 1954. *Erdstaudämme*. VEB Verlag Technik, Berlin.

McCall, W., Nielsen, D.M., Farrington, S.P. and Christy, T.M., 2005. Use of Direct-Push Technologies in Environmental Site Characterization and Ground-Water Monitoring. In: D.M. Nielsen (Editor), *Practical Handbook of Environmental Site Characterization and Ground-Water Monitoring*. CRC Press Taylor and Francis Group, Boca Raton, pp. 345-471.

McCall, W., Christy, T.M., Christopherson, T., and Issacs, H. 2009. Application of Direct Push Methods to Investigate Uranium Distribution in an Alluvial Aquifer. *Ground Water Monitoring & Remediation*, 29(4): 65-76.

Meigh, A.C., 1987. *Cone Penetration Testing: methods and interpretation*. Butterworths, London, 144 pp.

Millero, F.J., 2001. *Physical Chemistry of Natural Waters*. Wiley, New York, 654 pp.

Mishra, S., Parker, J.C. and Singhal, N., 1989. Estimation of Soil Hydraulic-Properties and their Uncertainty from Particle-Size Distribution Data. *Journal of Hydrology*, 108(1-4): 1-18.

Papadopoulos, S.S., Bredehoeft, J.D. and Cooper, H.H., 1973. Analysis of Slug-Test Data. *Water Resources Research*, 9(4): 1087-1089.

Pitkin, S.E., Cherry, J.A., Ingleton, R.A. and Broholm, M., 1999. Field demonstrations using the Waterloo Ground Water Profiler. *Ground Water Monitoring and Remediation*, 19(2): 122-131.

Quinnan, J.A., Welty, N.R.H. and Killenbeck, E., 2010. Hydrostratigraphic and permeability profiling for groundwater remediation projects, 2nd Intl. Symposium on Cone Penetration Testing (CPT'10), Huntington Beach.

Robinson, D.A., Jones, S.B., Wraith, J.M., Or, D. and Friedman, S.P., 2003. A Review of Advances in Dielectric and Electrical Conductivity Measurement in Soils Using Time Domain Reflectometry. *Vadose Zone Journal*, 2(4): 444-475.

Robertson, P.K., 1990. Soil classification using the cone penetration test. *Canadian Geotechnical Journal*, 27(1): 151-158.

Robertson, P.K., 2009. Interpretation of cone penetration tests - a unified approach. *Canadian Geotechnical Journal*, 46(11): 1337-1355.

Robertson, P.K., Campanella, R.G., Gillespie, D. and Greig, J., 1986. Use of piezometer cone data, ASCE Specialty Conference In Situ '86: Use of In Situ Tests in Geotechnical Engineering. American Society of Engineers (ASCE), Blacksburg, pp. 1263-1280.

Robertson, P.K., Lunne, T. and Powell, J., 1996. Application of penetration tests for geo-environmental purposes. In: C. Craig (Editor), *Advances in site investigation practice*. Thomas Telford Publishing, London, pp. 407-420.

Robertson, P.K. and Wride, C.E., 1998. Evaluating cyclic liquefaction potential using the cone penetration test. *Canadian Geotechnical Journal*, 35(3): 442-459.

Rylov, A.A. and Sudoplatov, A.D., 1990. The calculation of specific electrical conductivity for sandy - clayed rocks and the usage of functional cross-plots for the decision of hydrogeological problems, *Scientific and technical achievements and advanced experience in the field of geology and mineral deposits research*, Moscow, pp. 27-41 (In Russian).

Schafmeister, M.-T., 2006. What grains can tell on Darcy velocity?, *International Symposium - Aquifers Systems Management*, Dijon, France.

Schmertmann, J.H., 1978. Guidelines for cone penetration test, performance and design. In: U.F.H. Administration (Editor), Washington D.C., pp. 145.

Schön, J.H. (Editor), 1996. *Physical Properties of Rocks: Fundamentals and Principles of Petrophysic. Handbook of Geophysical Exploration. Section I, Seismic Exploration*, 18. Paergamon, Oxford.

Schulmeister, M.K. et al., 2003. Direct-push electrical conductivity logging for high-resolution hydrostratigraphic characterization. *Ground Water Monitoring and Remediation*, 23(3): 52-62.

Seelheim, F., 1880. Methoden zur Bestimmung der Durchlässigkeit des Bodens. *Fresenius' Journal of Analytical Chemistry*, 19: 387-418.

Seeve, J., 2005. Methods and Procedures for Defining Aquifer Parameters. In: D.M. Nielsen (Editor), *Practical Handbook of Environmental Site Characterization and Ground-Water Monitoring*. CRC Press Taylor and Francis Group, Boca Raton, pp. 913-958.

Sellwood, S.M., Healey, J.M., Birk, S. and Butler, J.J., 2005. Direct-push hydrostratigraphic profiling: Coupling electrical logging and slug tests. *Ground Water*, 43(1): 19-29.

Serra, O., 1984. *Fundamentals of well-log interpretation*. Elsevier, Amsterdam.

Shepherd, R.G., 1989. Correlations of Permeability and Grain-Size. *Ground Water*, 27(5): 633-638.

Shevchin, V., Delago-Rodríguez, O., Mousatov, A. and A., R., 2006. Estimation of hydraulic conductivity on clay content in soil determined from resistivity data. *Geofisica Internacional*, 45(3): 195-207.

Shinn, J.D., Timian, D.A., Morey, R.M., Mitchell, G., Antle, C.L., and Hull, R. 1998. Development of a CPT deployed probe for in situ measurement of volumetric soil moisture content and electrical resistivity. *Field Analytical Chemistry and Technology*, 2(2): 103-109.

Song, J., Chen, X., Cheng, C., Wang, D., Lacey, S., and Xu, Z. 2009. Feasibility of grain-size analysis methods for determination of vertical hydraulic conductivity of streambeds. *J Hydrol*, 375: 428-437.

Sperry, J.M. and Peirce, J.J., 1995. A Model for Estimating the Hydraulic Conductivity of Granular Material Based on Grain Shape, Grain-Size, and Porosity. *Ground Water*, 33(6): 892-898.

Starr, J.L. and Paltineanu, I.C., 2002. Capacitance Devices. In: J.H. Dane and G.C. Topp (Editors), *Methods of Soil Analysis: Part 4 Physical Methods*. Soil Science Society of America, Madison, pp. 463-474.

Sudicky, E.A., 1986. A Natural Gradient Experiment on Solute Transport in a Sand Aquifer - Spatial Variability of Hydraulic Conductivity and its Role in the Dispersion Process. *Water Resources Research*, 22(13): 2069-2082.

Sudicky, E.A. and Huyakorn, P.S., 1991. Contaminant Migration in Imperfectly Known Heterogeneous Groundwater Systems. *Reviews of Geophysics*, 29: 240-253.

Szymczak, P., Wassiliew, M. and Behnke, A., 2009. Bedienungshinweise zum Programm für die Auswertung von Korngrößenanalysen im Fachinformationssystem Hydrogeologie Programm UK32. Sächsisches Landesamt für Umwelt, Landwirtschaft und Geologie, Dresden.

Terzaghi, C., 1925a. Principles of Soil Mechanics: III-Determination of Permeability of Clay. *Engineering News-Record*, 95: 832-836.

Terzaghi, K., 1925. *Erdbaumechanik auf bodenphysikalischer Grundlage*. F. Deuticke, Leipzig.

Todd, D.K. and Mays, L.W., 2005. *Groundwater Hydrology*. John Wiley & Sons, Inc., Hoboken.

Topp, G.C., Davis, J.L. and Annan, A.P., 1980. Electromagnetic Determination of Soil Water Content. Measurements in Coaxial Transmission Lines. *Water Resources Research*, 16(3): 574-582.

Topp, G.C. and Ferré, P.A., 2002. The Soil Solution Phase. In: J.H. Dane and G.C. Topp (Editors), *Methods of Soil Analysis: Part 4 Physical Methods*. Soil Science Society of America, Madison, pp. 417-1071.

Tronicke, J., Dietrich, P., Wahlig, U. and Appel, E., 2002. Integrating surface georadar and crosshole radar tomography: A validation experiment in braided stream deposits. *Geophysics*, 67(5): 1516-1523.

Uma, K.O., Egboka, B.C.E. and Onuoha, K.M., 1989. New Statistical Grain-Size Method for Evaluating the Hydraulic Conductivity of Sandy Aquifers. *J Hydrol*, 108: 343-366.

VandenBygaart, A.J. and Protz, R., 1998. The representative elementary area (REA) in studies of quantitative soil micromorphology. *Geoderma*, 89: 333-346.

van Genuchten, M.T., 1991. Recent Progress in Modelling Water Flow and Chemical Transport in the Unsaturated Zone, *Hydrological Interactions Between Atmosphere, Soil and Vegetation*. IAHS - International Association of Hydrological Sciences, Vienna, pp. 169-183.

Vera, J. et al., 2009. Soil water balance trial involving capacitance and neutron probe measurements. *Agricultural Water Management*, 96(6): 905-911.

Vuković, M. and Soro, A., 1992. Determination of Hydraulic Conductivity of Porous Media from Grain-Size Composition. *Water Resources Publications*, LLC, Littleton.

Weight, W.D., 2008. *Hydrogeology Field Manual*. McGraw-Hill books, New York.

Weiß, H., Teutsch, G., Fritz, P., Daus, B., Dahmke, A., Grathwohl, P., Trabitzzsch, R., Feist, B., Ruske, R., Böhme, O. and Schirmer, M. 2001. Sanierungsforschung in regional kontaminierten Aquiferen (SAFIRA) - 1. Information zum Forschungsschwerpunkt am Standort Bitterfeld. *Grundwasser*, 6: 113-122.

Woodbury, A., Render, F. and Ulrych, T., 1995. Practical Probabilistic Groundwater Modeling. *Ground Water*, 33(4): 532-538.

Zheng, C.M. and Gorelick, S.M., 2003. Analysis of solute transport in flow fields influenced by preferential flowpaths at the decimeter scale. *Ground Water*, 41(2): 142-155.

Zlotnik, V.A. and McGuire, V.L., 1998. Multi-level slug tests in highly permeable formations: 1. Modification of the Springer-Gelhar (SG) model. *Journal of Hydrology*(204): 271-282.

Acknowledgment

I would like to thank Prof. Dr. Grathwohl and Dr. Peter Dietrich for the supervision of this thesis.

Thereby I owe special thanks to Dr. Peter Dietrich for his support of my work during the last three years, his valuable scientific advice, and his guidance during the last months.

For his support and the many discussions of the field data during his time at the UFZ and beyond I would like to thank Dr. Carsten Leven.

This thesis is based on extensive field data that was collected during numerous field days in Bitterfeld and two field campaigns in the US. For their great support, their commitment during the field work, and their help I would like to thank Steffen Graupner, Gerard Kluitenberg, Simon Kögler, Helko Kotas, Katrin Matthes, Ed Reboulet, Uwe Schneidewind, Andreas Schossland, and Ludwig Zschornack. Also I would like to thank the colleagues at the Bitterfeld test site for their technical support and help.

And I thank Anna for always being there.

Appendix

Appendix A

Appendix A: Grain size diameter determined based from grain size analyses of soil samples. Depth is given in m below ground surface, all grain size diameters are given in mm. For chapter 2, grain size distribution from cores S1, S2, and S4 were used in data analyses; for chapter 5 grain size distributions from all samples were included

Core	Sample	depth from	depth to	d_{10}	d_{20}	d_{30}	d_{50}	d_{60}	d_e
S1L2	G	2.88	3.02	0.0152	0.0764	0.126	0.2731	0.4164	0.0017
S1L2	H	3.02	3.05	0.0698	0.1074	0.145	0.2766	0.4185	0.0032
S1L2	I	3.05	3.40	0.0107	0.0639	0.153	0.3907	0.5259	0.0015
S1L2	J	3.40	3.60	0.0152	0.1051	0.2051	0.4619	0.5902	0.0017
S1L3	A	3.60	3.73	0.0143	0.0846	0.1373	0.2777	0.3737	0.0014
S1L3	B	3.73	3.97	0.0916	0.1933	0.2908	0.4841	0.5807	0.0040
S1L3	C	3.97	4.10	0.0017	0.0149	0.0433	0.1333	0.1934	0.0009
S1L3	D	4.10	4.27	0.0019	0.0198	0.0515	0.1488	0.208	0.0010
S1L3	E	4.35	4.45	0.0014	0.0093	0.0233	0.0659	0.1245	0.0007
S1L3	F	5.00	5.10	0.0014	0.0088	0.0218	0.0614	0.1193	0.0007
S1L3	G	5.15	5.30	0.0444	0.0889	0.1205	0.1836	0.2478	0.0019
S1L3	H	5.30	5.31	0.1094	0.2127	0.2657	0.3716	0.4245	0.0048
S1L3	I	5.31	5.35	0.0823	0.1609	0.2956	0.7525	1.8663	0.0038
S1L3	J	5.35	5.39	0.0179	0.0608	0.0972	0.1691	0.2244	0.0016
S1L3	K	5.39	5.46	0.0666	0.1187	0.1663	0.3832	0.5104	0.0030
S1L3	L	5.46	5.54	0.1851	0.4854	1.0522	3.1283	4.3819	0.0066
S1L3	M	5.54	5.60	0.0882	0.1443	0.2346	0.4905	0.6185	0.0045
S1L4	A	6.02	6.55	0.0845	0.1491	0.2468	0.4597	0.5661	0.0029
S1L4	B	6.55	6.96	0.0367	0.0853	0.1154	0.1756	0.2267	0.0019
S1L4	C	6.96	7.16	0.0387	0.0909	0.1307	0.2246	0.3193	0.0020
S1L4	D	7.16	7.18	0.0052	0.0339	0.0707	0.156	0.1987	0.0010
S1L4	E	7.18	7.48	0.0666	0.1068	0.147	0.2659	0.3627	0.0022
S1L4	F	7.48	7.60	0.0991	0.2092	0.2863	0.4404	0.5175	0.0045
S1L5	A	7.60	7.72	0.0648	0.1477	0.2402	0.415	0.5024	0.0027
S1L5	B	7.72	7.76	0.1437	0.3103	0.4678	1.5159	2.9356	0.0062
S1L5	C	7.76	7.89	0.0745	0.1503	0.2372	0.3956	0.4748	0.0024
S1L5	D	7.89	7.95	0.0017	0.0213	0.0536	0.211	0.3679	0.0009
S1L5	E	7.95	8.04	0.0054	0.0348	0.0792	0.3173	0.495	0.0011

Appendix

Core	Sample	depth from	depth to	d_{10}	d_{20}	d_{30}	d_{50}	d_{60}	d_e
S1L5	F	8.04	8.08	0.0275	0.1674	0.4826	4.4304	8.2161	0.0019
S1L5	G	8.08	8.30	0.0066	0.0525	0.2279	0.7629	1.7853	0.0014
S1L5	H	8.30	8.83	0.0009	0.0018	0.0106	0.0448	0.0822	0.0005
S1L5	I	8.83	9.02	0.0007	0.0015	0.0039	0.0228	0.0447	0.0004
S1L5	J	9.02	9.45	0.2157	0.3361	0.4566	0.9885	1.6287	0.0072
S1L5	K	9.45	9.49	0.266	0.3881	0.4814	1.3694	2.2496	0.0096
S1L5	L	9.49	9.60	0.2468	0.332	0.4171	0.5874	0.8965	0.0075
S1L6	A	9.95	10.30	0.1013	0.2274	0.3577	0.6183	1.4241	0.0048
S1L6	B	10.30	10.40	0.1331	0.2997	0.4632	1.8505	3.1825	0.0057
S1L6	C	10.40	10.50	0.243	0.4471	0.9379	4.2622	5.9892	0.0102
S1L6	D	10.50	11.00	0.1644	0.2614	0.3354	0.4835	0.5575	0.0054
S1L6	E	11.00	11.05	0.5028	1.3632	2.2295	3.5796	4.2546	0.0110
S1L6	F	11.05	11.20	0.2145	0.295	0.3755	0.5366	0.6171	0.0060
S1L6	G	11.20	11.30	0.2024	0.2619	0.3213	0.4403	0.4998	0.0058
S1L6	H	11.35	11.40	0.1126	0.222	0.2908	0.4284	0.4972	0.0047
S1L6	I	11.54	11.6	0.2352	0.5897	1.1706	2.9807	4.4895	0.0075
S2L2	E	2.68	2.75	0.1066	0.2829	0.5591	2.86	4.4826	0.0043
S2L2	F	3.05	3.70	0.1003	0.1771	0.2985	0.5545	1.3691	0.0038
S2L3	A	3.80	4.00	0.0876	0.1718	0.2655	0.4473	0.5382	0.0045
S2L3	B	4.00	4.16	0.1003	0.2186	0.362	0.9173	3.1246	0.0049
S2L3	C	4.16	4.76	0.0063	0.0514	0.1281	0.32	0.4388	0.0013
S2L3	D	4.76	5.02	0.0947	0.1869	0.2931	0.507	0.614	0.0047
S2L3	E	5.02	5.22	0.0969	0.158	0.2415	0.404	0.4853	0.0039
S2L3	F	5.22	5.31	0.0577	0.0969	0.1329	0.2167	0.3358	0.0027
S2L3	G	5.31	5.32	0.0941	0.1526	0.2566	0.5395	0.9588	0.0055
S2L3	H	5.32	5.47	0.0586	0.1035	0.1456	0.287	0.4095	0.0023
S2L3	I	5.47	5.70	0.0939	0.1608	0.2767	0.5506	0.9965	0.0039
S2L4	A	5.80	6.18	0.0698	0.1297	0.2103	0.4384	0.5524	0.0032
S2L4	B	6.18	6.62	0.0674	0.1299	0.1915	0.3738	0.4663	0.0026
S2L4	C	6.62	6.70	0.0017	0.0178	0.0492	0.1338	0.1808	0.0009
S2L4	D	6.70	6.82	0.063	0.1264	0.1884	0.3635	0.4523	0.0024
S2L4	E	6.82	6.85	0.0059	0.0414	0.103	0.3124	0.427	0.0012
S2L4	F	6.85	7.30	0.1069	0.1796	0.2477	0.3685	0.4289	0.0040
S2L4	G	7.30	7.70	0.1892	0.3135	0.4329	0.9121	1.7179	0.0067
S2L5	A	7.75	8.04	0.0794	0.134	0.1859	0.367	0.4602	0.0033
S2L5	B	8.04	8.15	0.1681	0.277	0.3635	0.5366	0.6231	0.0033
S2L5	C	8.15	8.30	0.0014	0.0113	0.032	0.1444	0.2845	0.0007
S2L5	D	8.30	8.47	0.0374	0.2087	0.333	0.5815	1.0064	0.0019
S2L5	E	8.47	8.70	0.0011	0.0044	0.0197	0.0915	0.2131	0.0006

Appendix

Core	Sample	depth from	depth to	d_{10}	d_{20}	d_{30}	d_{50}	d_{60}	d_e
S2L5	F	8.70	8.82	0.0007	0.0015	0.0047	0.0357	0.0594	0.0004
S2L5	G	8.82	9.00	0.164	0.365	0.538	1.6948	3.4162	0.0035
S2L5	H	9.00	9.08	0.0009	0.0018	0.0106	0.055	0.2263	0.0005
S2L5	I	9.08	9.70	0.2898	0.4096	0.4981	1.246	1.777	0.0088
S2L6	A	9.90	10.10	0.0786	0.1387	0.1985	0.4102	0.5164	0.0033
S2L6	B	10.10	10.22	0.2054	0.3126	0.4198	0.6536	1.2441	0.0041
S2L6	C	10.22	10.32	0.1718	0.3199	0.4577	1.1312	1.7995	0.0055
S2L6	D	10.32	10.48	0.1367	0.2683	0.3688	0.5697	0.8223	0.0041
S2L6	E	10.48	10.75	0.2461	0.4109	0.5643	2.1392	3.5307	0.0045
S2L6	F	10.85	11.20	0.5134	1.054	1.5977	4.2958	6.1178	0.0162
S2L6	G	11.20	11.70	0.3442	0.5957	2.2314	6.0879	9.725	0.0082
S3L2	A	2.72	3.01	0.0266	0.1201	0.21	0.3644	0.4416	0.0020
S3L2	B	3.01	3.12	0.0958	0.2089	0.2827	0.4305	0.5044	0.0038
S3L2	C	3.12	3.62	0.2619	0.4248	0.5804	2.2716	3.7804	0.0067
S3L3	A	3.82	3.97	0.2585	0.4305	0.5986	2.6947	3.8925	0.0093
S3L3	B	3.97	4.82	0.0104	0.0543	0.1239	0.4038	0.6076	0.0015
S3L3	C	4.82	4.87	0.0775	0.1243	0.1645	0.3484	0.4559	0.0029
S3L3	D	4.87	5.22	0.0719	0.1188	0.1589	0.3138	0.4034	0.0025
S3L3	E	5.22	5.25	0.1179	0.2656	0.4383	1.5332	2.8537	0.0052
S3L3	F	5.25	5.28	0.0688	0.11	0.1513	0.3059	0.435	0.0024
S3L3	H	5.33	5.56	0.0725	0.1254	0.1738	0.3519	0.4475	0.0023
S3L3	I	5.56	5.62	0.2473	0.4502	0.7652	1.9939	3.0696	0.0063
S3L4	A	6.11	6.34	0.0469	0.1077	0.1594	0.3939	0.5396	0.0022
S3L4	B	6.34	6.51	0.0765	0.1263	0.1708	0.3282	0.4125	0.0025
S3L4	C	6.51	6.62	0.0265	0.0772	0.111	0.1787	0.2494	0.0017
S3L4	D	6.62	6.68	0.0018	0.0259	0.0463	0.1451	0.2169	0.0010
S3L4	E	6.68	6.78	0.0299	0.0832	0.1143	0.1764	0.2311	0.0017
S3L4	F	6.78	6.84	0.0056	0.0346	0.0711	0.195	0.3628	0.0012
S3L4	G	6.84	6.95	0.0684	0.1282	0.1862	0.3879	0.4922	0.0024
S3L4	H	6.95	7.07	0.0654	0.0873	0.1093	0.1531	0.175	0.0019
S3L4	I	7.07	7.21	0.1694	0.2767	0.368	0.5506	0.6934	0.0046
S3L4	J	7.21	7.30	0.0825	0.1139	0.1453	0.2267	0.3296	0.0032
S3L4	K	7.30	7.62	0.111	0.1761	0.2527	0.3951	0.4663	0.0039
S3L5	A	7.72	7.97	0.2415	0.4301	0.6174	0.1781	3.183	0.0052
S3L5	B	7.97	8.24	0.1049	0.2	0.353	0.8666	2.2186	0.0045
S3L5	C	8.24	8.56	0.0831	0.1489	0.2534	0.542	1.0867	0.0030
S3L5	D	8.56	8.84	0.075	0.1193	0.157	0.3703	0.5146	0.0027
S3L5	E	8.84	9.23	0.0066	0.0437	0.082	0.1609	0.2021	0.0012
S3L5	F	9.23	9.62	0.0953	0.1602	0.2454	0.4133	0.4973	0.0034

Appendix

Core	Sample	depth from	depth to	d_{10}	d_{20}	d_{30}	d_{50}	d_{60}	d_e
S3L6	A	10.22	10.44	0.1148	0.189	0.2499	0.3632	0.4198	0.0068
S3L6	B	10.44	10.82	0.2707	0.3925	0.4848	0.903	1.1629	0.0085
S3L6	C	10.82	11.16	0.3112	0.4369	0.6461	1.2908	1.6132	0.0143
S3L6	D	11.16	11.30	0.5355	1.406	2.2435	3.5252	4.166	0.0285
S3L6	G	11.30	11.62	0.3393	0.7878	1.6181	5.199	7.7405	0.0150
S4L2	B	2.93	3.25	0.1763	0.2951	0.4031	0.6192	1.315	0.0062
S4L2	C	3.25	3.66	0.1934	0.2979	0.3988	0.6007	1.134	0.0114
S4L2	D	3.66	3.83	0.2636	0.4019	0.5247	1.4341	2.0903	0.0088
S4L3	A	4.03	4.18	0.2	0.3468	0.4863	1.7405	2.9714	0.0060
S4L3	B	4.18	4.30	0.2438	0.3532	0.4626	0.8972	1.4656	0.0090
S4L3	C	4.30	4.87	0.0012	0.0061	0.0183	0.0604	0.1393	0.0006
S4L3	D	4.87	5.11	0.104	0.2357	0.4141	1.3663	2.546	0.0054
S4L3	E	5.11	5.15	0.035	0.0747	0.096	0.1385	0.1598	0.0021
S4L3	F	5.15	5.23	0.1644	0.3152	0.4558	1.1667	1.8729	0.0063
S4L3	G	5.23	5.26	0.0446	0.0819	0.1076	0.1588	0.1844	0.0024
S4L4	A	6.05	6.15	0.176	0.3005	0.4122	0.6639	1.3421	0.0045
S4L4	B	6.15	6.45	0.1165	0.2498	0.3682	0.6051	1.2859	0.0059
S4L4	C	6.45	6.58	0.1034	0.1699	0.2558	0.4247	0.5092	0.0047
S4L4	E	7.21	7.43	0.0087	0.0522	0.0901	0.1624	0.1986	0.0013
S4L4	F	7.43	7.71	0.1009	0.2079	0.2685	0.3898	0.4505	0.0041
S4L4	G	7.71	7.73	0.0738	0.0955	0.1172	0.1605	0.1822	0.0028
S4L4	H	7.73	7.83	0.1352	0.238	0.307	0.445	0.514	0.0063
S4L5	A	7.87	7.99	0.0687	0.1065	0.1444	0.2614	0.3773	0.0031
S4L5	B	7.99	8.11	0.0838	0.1755	0.2596	0.4142	0.4916	0.0033
S4L5	C	8.11	8.19	0.0923	0.1453	0.2372	0.5129	1.0494	0.0047
S4L5	D	8.19	8.23	0.0136	0.0528	0.0836	0.1391	0.1669	0.0015
S4L5	E	8.23	8.84	0.0669	0.1233	0.1768	0.3851	0.498	0.0026
S4L5	F	8.84	9.41	0.1786	0.296	0.4027	0.6161	1.4141	0.0051
S4L5	G	9.41	9.66	0.3407	0.6024	1.3265	4.0407	5.8627	0.0114
S4L5	H	9.66	9.83	0.0061	0.0482	0.2058	0.5932	1.774	0.0013
S4L6	A	9.88	9.98	0.0822	0.1355	0.1864	0.3497	0.4334	0.0033
S4L6	B	9.98	10.23	0.1106	0.2328	0.3387	0.5506	0.9905	0.0050
S4L6	C	10.23	10.57	0.1182	0.2591	0.3666	0.5816	0.9838	0.0038
S4L6	D	10.57	11.04	0.2754	0.4768	1.0359	3.858	5.6276	0.0086
S4L6	E	11.07	11.83	0.24	0.3331	0.4262	0.6123	1.4006	0.0087

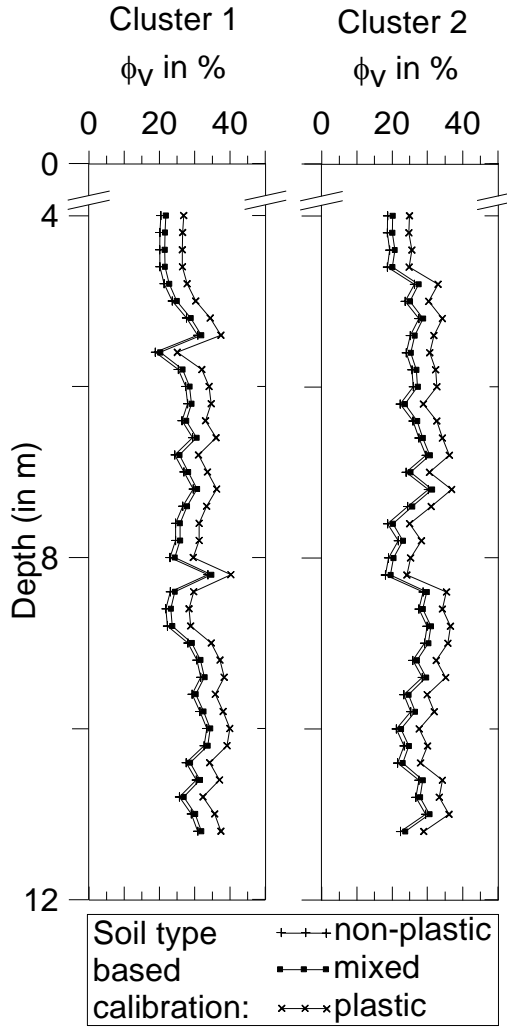
Appendix B

Appendix B: Grain size diameter for the slug test interval with d in mm. Grain size distribution of samples within individual slug test intervals were averaged according to their abundance and grain size diameters were derived. SC is Sampling Cluster, and CL is core loss observed on samples within the slug test interval. Where no grain size diameter is given, no material was retained.

depth from	depth to	SC	CL	K_{DPST}	d_{10}	d_{20}	d_{30}	d_{50}	d_{60}	d_e
5.16	5.73	1	0.13	9.24E-05	0.0645	0.1149	0.1598	0.3728	0.5047	0.0027
5.71	6.28	1		2.58E-04						
6.93	7.5	1		1.14E-04	0.0512	0.0989	0.1392	0.248	0.3459	0.0021
7.53	8.10	1		3.07E-06	0.0257	0.1183	0.2119	0.4274	0.5352	0.0019
8.15	8.72	1		5.49E-05	0.0011	0.0037	0.0168	0.0766	0.2185	0.0006
8.73	9.30	1		1.12E-03	0.0015	0.0128	0.0427	0.3292	0.4927	0.0008
9.41	9.98	1		1.18E-03						
5.34	5.91	2	0.10	1.19E-04	0.0762	0.1363	0.1957	0.4461	0.5729	0.0031
5.93	6.50	2		5.48E-05	0.0688	0.1338	0.1985	0.3994	0.5001	0.0028
6.49	7.06	2		1.31E-04	0.045	0.1152	0.1786	0.3379	0.4891	0.0021
7.08	7.65	2		1.65E-04	0.164	0.2702	0.3559	0.5272	0.6129	0.0051
7.63	8.20	2	0.05	8.12E-06	0.0654	0.1379	0.2298	0.4284	0.5277	0.0026
8.48	9.05	2		6.55E-04	0.0013	0.0099	0.0341	0.2846	0.5196	0.0007
8.83	9.40	2		9.15E-04	0.2628	0.3993	0.5358	1.3809	1.9541	0.0058
9.41	9.98	2	0.20	9.66E-04	0.2186	0.3352	0.4517	0.9064	1.4943	0.0066
10.22	10.79	2	0.04	1.35E-03	0.2027	0.3366	0.4706	1.1713	1.8396	0.0046
10.96	11.53	2		1.67E-03	0.3541	0.875	1.7823	5.3048	8.2512	0.0101
11.46	12.03	2		1.33E-03						
8.38	8.95	4		1.27E-04	0.0735	0.1305	0.2078	0.4312	0.5429	0.0029
10.33	10.90	4		2.31E-04	0.2015	0.3546	0.4904	1.6086	2.9982	0.0056
4.87	5.44	4	0.18	1.95E-04	0.0889	0.1478	0.2614	0.6501	1.6575	0.0044
5.97	6.54	4	0.08	7.70E-05	0.1135	0.2415	0.3506	0.5689	0.9867	0.0054
7.8	8.37	4	0.04	3.07E-05	0.0694	0.1229	0.1728	0.3636	0.4685	0.0030
10.93	11.50	4	0.03	1.35E-03	0.2433	0.349	0.4546	0.958	1.9228	0.0087
9.73	10.30	4	0.05	1.16E-03	0.1019	0.199	0.2988	0.4983	0.5981	0.0042
5.43	6.00	4		1.41E-04						
6.88	7.45	4		1.34E-04						

Appendix C

Appendix C: Neutron probe soil water content measurements in dependency of the applied soil type based calibration at sampling cluster 1 and sampling cluster 2 in Bitterfeld.



Curriculum vitae

Thomas Vienken

Geboren: 03. August 1979

Bildungsgang

1999	Abitur am Norbert-Gymnasium Knechtsteden
1999-2007	Studium Geologie-Paläontologie an der Universität zu Köln. Diplomnote: sehr gut (1.21) Diplomarbeit: Auswirkungen des menschlichen Siedlungsbaus und der Nutzung oberflächennaher Geothermie auf die Grundwassertemperatur
August 2003 bis Januar 2004	Auslandssemester: SOEST - School of Ocean and Earth Science and Technology, University of Hawaii at Manoa
Seit August 2007	Doktorand am Helmholtz-Zentrum für Umweltforschung GmbH - UFZ, Department Monitoring- und Erkundungstechnologien, Betreuer: Dr. Peter Dietrich
Seit Mai 2010	Doktorand im Promotionsfach Geologie, Eberhard Karls Universität Tübingen, Hauptbetreuer: Prof. Dr. Grathwohl